

DEVELOPMENT OF Pt-CeO₂/C AND Pt-Rh-CeO₂/C
CATALYSTS FOR ETHANOL ELECTRO-OXIDATION
IN DIRECT ETHANOL FUEL CELL

DISSERTATION

by

HARIYANTO
84 030 000 21



Submitted to the Postgraduate Program, Faculty of Engineering
of University of Indonesia in Partial Fulfillment of
the Requirements for the Degree of
DOCTOR
Promotion, on January 07, 2008

D
00906

Postgraduate Program of Engineering Study
Faculty of Engineering
University of Indonesia
2007/2008

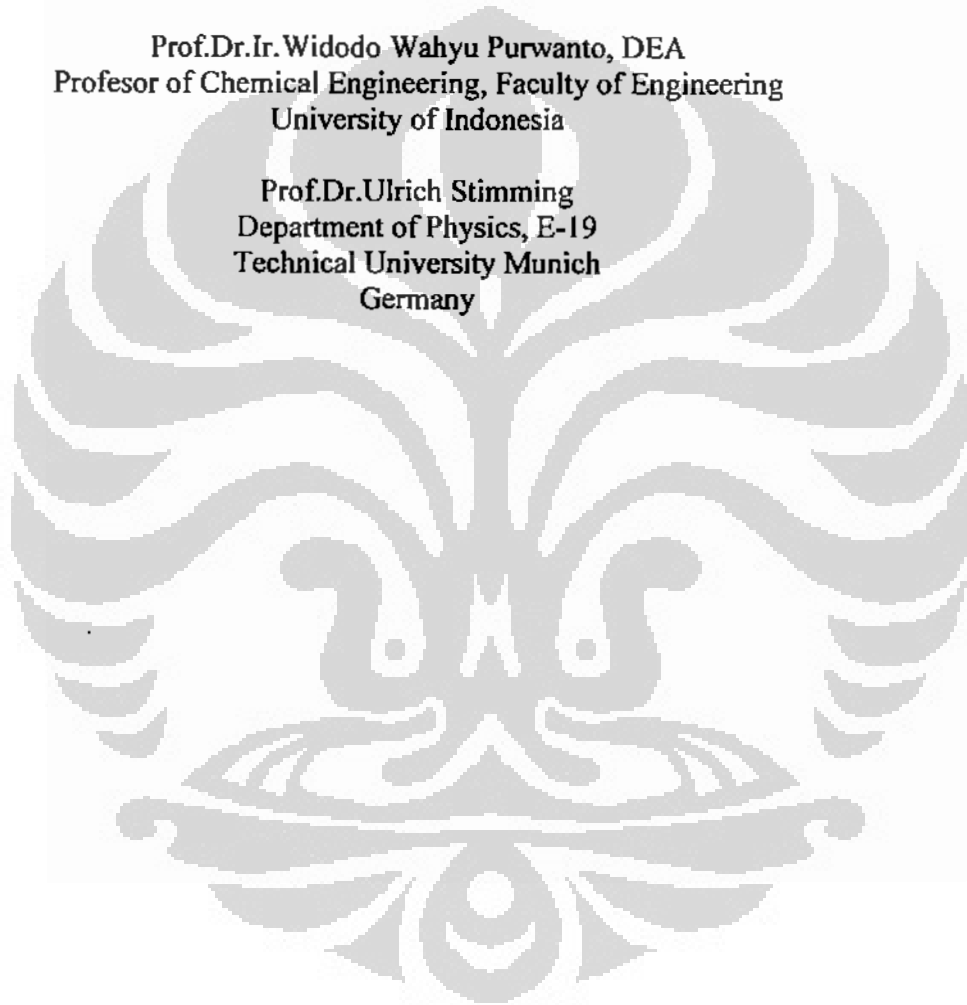
Promoter:

Prof. Dr.Ir.Roekmijati W. Soemantojo, Msi
Profesor of Chemical Engineering, Faculty of Engineering
University of Indonesia

Co-Promoters:

Prof.Dr.Ir. Widodo Wahyu Purwanto, DEA
Profesor of Chemical Engineering, Faculty of Engineering
University of Indonesia

Prof.Dr.Ulrich Stimming
Department of Physics, E-19
Technical University Munich
Germany



Dissertation Committee

1. Prof. Dr.Ir.Roekmijati W. Soemantojo, Msi
Department of Chemical Engineering, Faculty of Engineering, University of Indonesia
2. Prof.Dr.Ir.Widodo Wahyu Purwanto, DEA
Department of Chemical Engineering, Faculty of Engineering, University of Indonesia
3. Prof.Dr.Ulrich Stimming
Department of Physics, E-19, Technical University Munich, Germany
4. Prof. Dr. M. Nasikin, M.Eng
Department of Chemical Engineering, Faculty of Engineering, University of Indonesia
5. Prof. riset. Dr.Petrus Panaka
Agency for the Assessment and Application of Technology
6. Dr.Ir. Slamet, MT
Department of Chemical Engineering, Faculty of Engineering, University of Indonesia
7. Ir. Mahmud Sudibandriyo, Ph.D.
Department of Chemical Engineering, Faculty of Engineering, University of Indonesia

STATEMENT of ORIGINALITY

I herewith declare:

The Dissertation entitled:

DEVELOPMENT OF Pt-CeO₂/C AND Pt-Rh-CeO₂/C CATALYSTS FOR ETHANOL ELECTRO-OXIDATION IN DIRECT ETHANOL FUEL CELL

Which is submitted to the Postgraduate Program, Faculty of Engineering of University of Indonesia in partial fulfillment of the requirements for the Degree of **DOCTOR**, as I know is not as a duplication or copy of dissertation which had published at University of Indonesia or in other Universities/Institutions, except the parts which the sources of information was declared.

Depok, January 08, 2008



HARIYANTO
84 030 000 21

PAGE OF APPROVAL

Dissertation with the title:

Development of Pt-CeO₂/C and Pt-Rh-CeO₂/C Catalysts for Ethanol
Electro-oxidation in Direct Ethanol Fuel Cell

Name : Hariyanto
Regr. Number : 84 030 00 021
Study Program: Engineering

Submitted to the Postgraduate Program, Faculty of Engineering of University of
Indonesia in Partial Fulfillment of the Requirements for the Degree of **DOCTOR**

This Dissertation has approved in final promotion on January 7, 2008

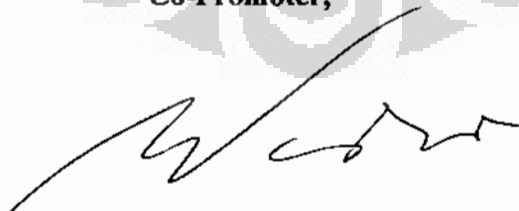
Depok, January 2008

Promoter:



Prof. Dr. Ir. Roekmijati W. Soemantojo, Msi
NIP 130 220 443

Co-Promoter,



Prof. Dr. Ir. Widodo W. Purwanto, DEA
NIP 131 627 864

PAGE OF APPROVAL

Dissertation with the title:

Development of PtCeO₂/C and PtRhCeO₂/C Catalysts for Ethanol
Electro-oxidation in Direct Ethanol Fuel Cell

Name : Hariyanto
Regr. Number : 84 030 00 021
Study Program: Engineering

Submitted to the Postgraduate Program, Faculty of Engineering, The University of
Indonesia in Partial Fulfillment of the Requirements for the Degree of **DOCTOR**

Munich, January 2008

Co Promoter


(Prof. Dr. Ulrich Sommering)

ACKNOWLEDGEMENT

Firstly, I would like to thank my promoter Prof.Dr.Ir. Roekmijati W. Soemantojo,MSi and my co-promoter Prof.Dr.Ir. Widodo Wahyu Purwanto, DEA for their support, guidance and encouragement during the work and writing dissertation.

I want to express my special gratitude to Prof. Dr.Ulrich Stimming for all facilities which was provided to me and supervising my work during research experiment at Department of Physics, E-19, Technical University Munich, Germany.

I would like to thank the members of my dissertation committee for their acceptance of this task and their helpful comments and suggestions in preparing this dissertation: Prof. Dr.Ir.M. Nasikin, M.Eng, Ir. Mahmud Sudibandriyo, Ph.D, Dr.Ir. Slamet, MT, Dr.Petrus Panaka, APU

Many thank Rector of University of Indonesia, Dean of Faculty of Engineering, Head of Department of Chemical Engineering and Head of Balai Besar Teknologi Energi-BPPT for gave me an opportunity to pursue the doctoral degree at University of Indonesia.

I am grateful for the experience of being a part of the Department of Chemical Engineering, University of Indonesia. I want to thank in general all fellows, members of the Department.

Many thank Deutscher Akademischer Austauschdiensts (DAAD) for grant me sandwich program scholarship. Financial support from Program Pascasarjana Rintisan Gelar RISTEK also gratefully acknowledged.

I thank Petra Belle and Sigfried Schrier for TEM and SEM-EDX measurements and discussion and also Dr. Christina Tealdy from University of Pavia, Italy for XRD measurement and discussion.

Special thank to Vineet Rao who as a good friend, was always willing to help and give his best suggestions.

I also would like to thank all people at Interfaces and Energy Conversion Group, E-19, Technical University Munich for for giving me their friendship, as deep and as rich as friendship can be, during the time I living in Munich.

The last, and surely the most, I want to thank my family, for their love. I thank my wife Rina and my children: Anita Fitriana, Hilmy Zweinanda and Hafiz Ramadhan for being with me through the good times and bad, and also my parents for their pray, not just this last time, but so many times in my life. I devote this book to them.

<p><u>Hariyanto</u> 840 300 0021 Postgraduate Program Engineering Science University of Indonesia</p>	<p><u>Promotor</u> Prof. Dr. Ir. Roekmijati W. Soemantojo, MSi <u>Co Promotor</u> Prof. Dr. Ir. Widodo W. Purwanto, DEA Prof. Dr. Ulrich Stimming</p>
<p>Development of PtCeO₂/C and PtRhCeO₂/C Catalysts for Ethanol Electro-oxidation in Direct Ethanol Fuel Cell</p>	
<p>Abstract</p> <p>Direct oxidation fuel cells (DOFCs) have recently attracted major attention, as an alternative to hydrogen fuel cells, mainly due to easier fuel storage and handling. The organic liquids used for DOFCs are much simpler to handle than gaseous hydrogen and also in many cases do not require any new distribution infrastructure. Ethanol is one of the fuel candidates for direct oxidation fuel cell (DOFC). The advantages of ethanol are due to non toxicity, renewability and high energy density. Unfortunately, utilization of ethanol as fuel in direct ethanol fuel cell (DEFC) is still covered by main problem which is slow kinetic reaction due to difficult to break C-C bond in ethanol. In order to solve this main problem in ethanol electro-oxidation reaction (EOR) the research work is aimed to develop and investigate an anode catalyst base on carbon supported platinum catalyst for ethanol electro-oxidation in direct ethanol fuel cell (DEFC) which capable to promote in breaking C-C bond toward total oxidation reaction of ethanol.</p> <p>First specific objective of the research is to study the effect of Rhodium on carbon supported Pt catalysts to the activity and selectivity of ethanol electro-oxidation reaction. The second specific objective is to study the effect of CeO₂ on carbon supported Pt catalysts to the activity and selectivity of ethanol electro-oxidation reaction. Moreover, the third specific objective of the research work is to study the effect of Rh and CeO₂ addition on carbon supported Pt catalysts to the activity and selectivity of ethanol electro-oxidation reaction.</p> <p>The research methodology was comprised of activities: catalyst syntheses, physical characterization, electrochemical characterization, membrane electrode assembly (MEA), in-situ differential mass spectrometry and fuel cell test in single cell setup. CeO₂ nano-size particle material was prepared by two step conventional precipitation (in-house CeO₂) and for comparison purpose; we also used commercial CeO₂ purchased from Johnson Mattews. Preparation of catalysts (Pt-CeO₂/C, Pt-Rh/C and Pt-Rh-CeO₂/C) was carried out by colloidal method using ethylene glycol reductant agent. All of catalysts synthesized with 20 weight percent of Pt loading. New developed catalysts then characterized by SEM-EDX to analyze the morphology of catalysts, X-ray diffraction (XRD) to analyze the crystallography, and transmission electron microscopy (TEM) to investigate the particle size and particle dispersion.</p> <p>Physical characterizations result indicated that in-house CeO₂ was a crystallite as</p>	

CeO₂ commercial was with the particle size diameter of about 9 nm, meanwhile the particle size diameter of commercial CeO₂ about 19 nm. Particle size diameter of Pt-CeO₂/C and Pt-Rh-CeO₂/C catalysts was about 2-3.5 nm and well dispersed with light agglomeration. Energy dispersive of X-Ray (EDX) analysis shows that all of element in the catalyst was detected.

Electrochemical characterization was carried out by normal cyclic voltammetry, chronoamperometry, and cyclic voltammetry in present of ethanol either in acid or alkaline medium. Electrochemical characterization is to investigate the activity of the catalyst correlated to the Faradaic current which obtained in half cell/model electrode. In-situ differential electrochemical mass spectrometry (DEMS) was conducted to further investigate the activity and selectivity of ethanol electro-oxidation over PtCeO₂/C and PtRhCeO₂/C in real fuel cell setup.

New developed catalysts of PtCeO₂/C and PtRhCeO₂/C which was synthesized by colloidal method improved the activity and selectivity to CO₂ product in ethanol electro-oxidation toward total oxidation reaction in direct ethanol fuel cell. Whereas, effect addition of rhodium in the catalyst was to improve capability in C-C bond breaking, while effect addition of CeO₂ in the catalyst was to donor oxygen onto Pt surface to break C-C bond and to promote CO_{ads} intermediate to the CO₂ product on the surface of platinum.

Addition of rhodium to the carbon supported Pt catalyst improved in C-C bond breaking in ethanol electro-oxidation. However, the result of C-C bond breaking was not converted to CO₂ product totally, due to strongly adsorption of CO intermediate product on surface of PtRh. Therefore, it was only slightly increase of the activity and selectivity of ethanol electro-oxidation reaction (EOR) over PtRh/C compared to commercial Pt/C reference catalyst.

Addition of CeO₂ to the carbon supported catalyst improved the activity of catalysts in C-C bond breaking and improved the selectivity by promoted the oxidation of CO intermediate product to CO₂ on Pt surface. The ceria effect was associated to the capabilities of ceria to provide oxygen on Pt surface that finally could improve activity and selectivity of the catalyst in ethanol oxidation reaction.

Addition of Rh and CeO₂ to the carbon supported catalyst improved the activity of catalysts in C-C bond breaking and improved the selectivity for CO₂ formation. The improvements of activity and selectivity of the catalyst is due to a synergistic effect. In the real fuel cell, improvement of an activity in electrochemical cell measurement was also obtained by in-situ differential electrochemical mass spectrometry. Increase in activity over ceria modified catalyst also led to increase in selectivity for CO₂ formation. Increasing in activity was indicated by increment of Faradaic current and the increasing selectivity of the catalysts to the CO₂ formation was indicated by increment of the CO₂ current efficiency. Both

increasing of the activity and selectivity were occurred at low potential less than 0.6 V vs. RHE

Increasing activity of ethanol oxidation over ceria modified Pt-based catalysts in comparison to reference catalyst (20% Pt/C) at potential 0.6 V and temperature 90°C are: 20% PtCeO₂/C (in-house CeO₂): 5.99%, 20% PtCeO₂/C (commercial CeO₂): 3.89%, 20% PtRhCeO₂/C (in-house CeO₂): 19.6%, 20% PtRhCeO₂/C (Commercial CeO₂): 26.3%.

The product of the ethanol oxidation reaction over Pt/C, PtCeO₂/C, PtRh/C and PtRhCeO₂/C which was investigated by in-situ DEMS were CO₂, acetaldehyde, methane, ethane. Meanwhile, acetic acid was not detected by DEMS due to low volatility. CO₂ current efficiency (CCE) was represented the selectivity to CO₂ formation of ethanol oxidation. Increasing CCE over ceria modified Pt-based catalysts in comparison to reference catalyst (20% Pt/C) at potential 0.6 V and temperature 90°C are: 20% PtCeO₂/C (in-house CeO₂): 20%, 20% PtCeO₂/C (commercial CeO₂): 19 %, 20% PtRhCeO₂/C (in-house CeO₂): 27%, 20% PtRhCeO₂/C (Commercial CeO₂): 24%.

Keywords: Ethanol electro-oxidation, Pt-CeO₂/C, Pt-Rh-CeO₂/C, activity, selectivity, CO₂, Faradaic current

<p><u>Hariyanto</u> 840 300 0021 Program Pascasarjana Bidang Ilmu Teknik Universitas Indonesia</p>	<p><u>Promotor</u> Prof. Dr. Ir. Roekmijati W. Soemantojo, MSi <u>Co Promotor</u> Prof. Dr. Ir. Widodo W. Purwanto, DEA Prof. Dr. Ulrich Stimming</p>
<p>Pengembangan katalis PtCeO₂/C dan PtRhCeO₂/C untuk Elektro- oksidasi Ethanol pada <i>Direct Ethanol Fuel Cell</i></p>	
<p>Abstrak</p>	
<p><i>Direct oxidation fuel cells (DOFCs)</i> telah banyak menarik perhatian sebagai alternative pengganti dari <i>hydrogen-fuel cell</i> dikarenakan lebih mudah penanganan dan transportasi bahan bakarnya. Penggunaan bahan bakar cair pada DOFC akan lebih sederhana dibandingkan <i>hydrogen</i> dan tidak memerlukan infrastruktur baru pada transportasi bahan bakarnya. Ethanol adalah salah satu kandidat bahan bakar untuk DOFC yang mempunyai kelebihan diantaranya : tidak beracun, sebagai bahan bakar terbarukan, dan mempunyai kerapatan energi yang tinggi. Akan tetapi penggunaan ethanol pada <i>direct ethanol fuel cell (DEFC)</i> dihadapkan pada permasalahan utama yaitu kesulitan untuk memutus ikatan C-C pada ethanol dimana reaksi oksidasi akan terjadi secara parsial sehingga energi listrik yang dihasilkan tidak maksimal . Untuk memecahkan masalah tersebut maka penelitian ini bertujuan untuk mengembangkan katalis anoda berbasis platina berpenyangga karbon untuk oksidasi ethanol yang mampu memutus ikatan C-C menuju reaksi oksidasi total.</p>	
<p>Tujuan khusus yang pertama pada penelitian ini adalah studi pengaruh penambahan rhodium pada katalis platina berpenyangga karbon terhadap aktivitas dan selektivitas katalis untuk oksidasi ethanol. Tujuan khusus kedua adalah studi pengaruh penambahan ceria pada katalis platina berpenyangga karbon terhadap aktivitas dan selektivitas katalis untuk oksidasi ethanol. Sedangkan tujuan khusus ketiga adalah studi pengaruh penambahan rhodium dan ceria bersama-sama pada katalis platina berpenyangga karbon terhadap aktivitas dan selektivitas katalis untuk oksidasi ethanol.</p>	
<p>Metoda penelitian terdiri dari beberapa aktivitas yaitu: sintesis katalis, karakterisasi fisik katalis, karakterisasi elektrokimia, <i>perakitan membrane electrode assembly (MEA)</i>, pengukuran on-line dengan teknik <i>differential electrochemical mass spectrometry (DEMS)</i> dan uji kinerja fuel cell susunan tunggal. Ceria disintesis menggunakan teknik precipitasi konvensional dengan dua tahap. Sebagai pembanding pada penelitian ini juga digunakan ceria komersial dari Alfa Aesar. Preparasi katalis (Pt-CeO₂/C, Pt-Rh/C and Pt-Rh-CeO₂/C) dilakukan dengan teknik koloid menggunakan ethylene glycol sebagai reduktan. Semua katalis di preparasi dengan target 20% berat platinum. Katalis yang telah di preparasi kemudian di karakterisasi dengan SEM-EDX untuk</p>	

menganalisa morfologi permukaan katalis, dengan XRD untuk menganalisa kristalinitas dan struktur katalis, dan transmission elektron mikroskopy (TEM) untuk mengukur diameter partikel dan distribusinya. Dari hasil karakterisasi fisik diketahui bahwa ceria yang disintesa adalah berbentuk kristal sama dengan ceria komersial dengan diameter kristal 9 nm, sedangkan diameter ceria komersial adalah 19 nm.

Ukuran diameter partikel katalis Pt-CeO₂/C and Pt-Rh-CeO₂/C adalah sekitar 2-3.5 nm dan terdistribusi merata dengan sedikit agglomerasi. Dari hasil EDX diketahui bahwa semua elemen katalis terdeteksi.

Karakterisasi elektrokimia dilakukan dengan normal cyclic voltammetry, chronoamperometry, and cyclic voltammetry pada media asam dan basa. Karakterisasi elektrokimia dilakukan untuk menginvestigasi aktivitas katalis yang dinyatakan dengan arus faraday yang dihasilkan pada uji setengah sel. Uji DEMS dilakukan untuk investigasi aktivitas katalis dan selektivitas pembentukan CO₂ yang telah dirakit dalam susunan fuel cell.

Katalis PtCeO₂/C dan PtRhCeO₂/C yang disintesis dengan metoda koloid meningkatkan aktivitas dan selektivitas terhadap pembentukan CO₂ pada elektro-oksidasi ethanol yang mengarah kepada reaksi oksidasi total pada pengujian di *direct ethanol fuel cell* (DEFC).

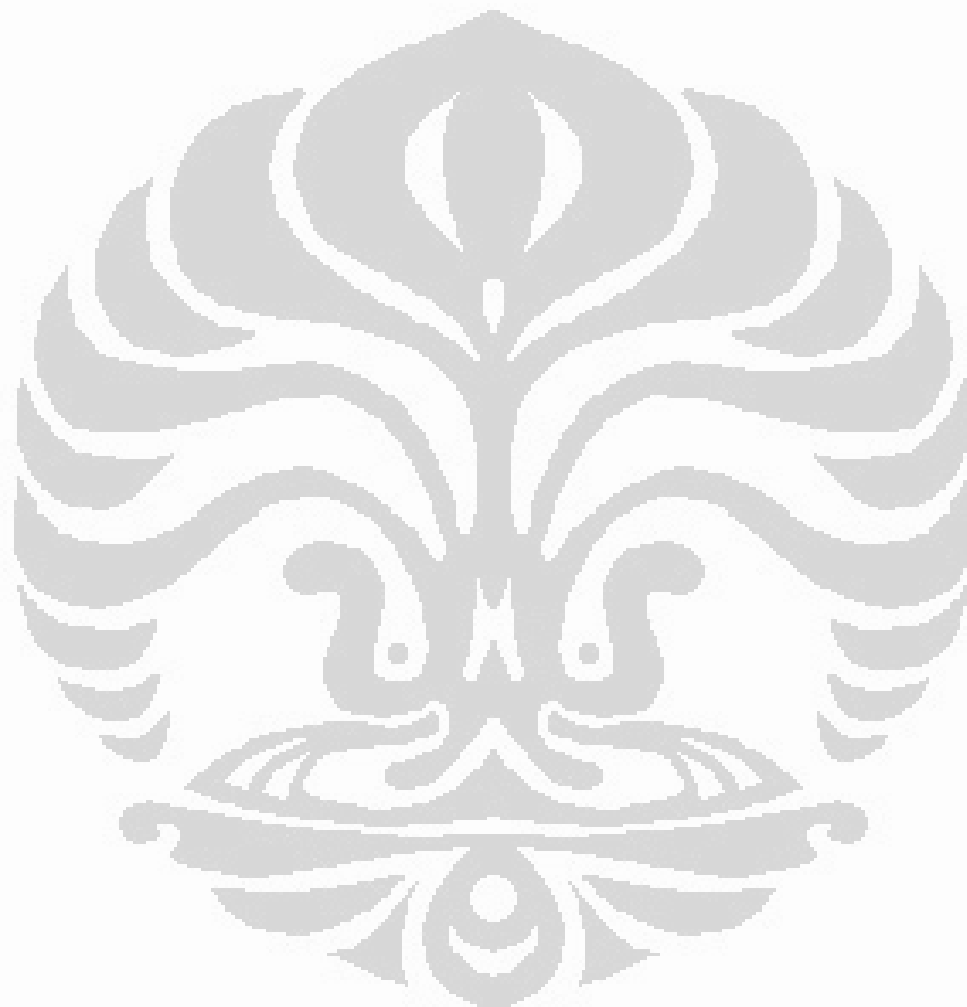
Penambahan rhodium (Rh) pada katalis Pt/C meningkatkan kemampuan untuk memutus ikatan C-C pada ethanol. Akan tetapi hasil pemutusan ikatan C-C tersebut tidak semua di konversi menjadi CO₂ di sebabkan adsorpsi CO pada permukaan Rh yang kuat, sehingga peningkatan aktivitas dan selektivitas katalis tersebut tidak terlalu besar.

Penambahan CeO₂ pada katalis Pt/C meningkatkan kemampuan katalis untuk memutus ikatan C-C pada elektro-oksidasi ethanol, sekaligus meningkatkan kemampuan katalis untuk mengoksidasi lanjut CO *intermediate product* menjadi CO₂. Peningkatan aktivitas dan selektivitas katalis tersebut disebabkan fungsi CeO₂ sebagai pendonor oksigen kepada permukaan platina, sehingga dengan adanya oksigen yang cukup pada permukaan platina meningkatkan kemampuan memutus ikatan C-C dan meningkatkan kemampuan mengkonversi CO menjadi CO₂. Penambahan Rh dan CeO₂ secara bersama-sama meningkatkan aktivitas dan selektivitas katalis pada reaksi elektro-oksidasi ethanol. Peningkatan tersebut lebih besar dibandingkan jika hanya di tambah rhodium saja ataupun hanya ditambahkan CeO₂ saja. Penambahan keduanya tersebut akan bersinergi sehingga meningkatkan aktivitas dan selektivitas katalis PtRhCeO₂/C. Peningkatan aktivitas katalis yang disintesis (in-house) terhadap katalis referensi Pt/C pada potential 0,6 V dan suhu operasi 90°C adalah : 20% PtCeO₂/C (in-house CeO₂): 5.99%, 20% PtCeO₂/C (commercial CeO₂): 3.89%, 20% PtRhCeO₂/C (in-house CeO₂): 19.6%, 20% PtRhCeO₂/C (Commercial CeO₂): 26.3%.

Peningkatan selektivitas katalis yang di sintesis (in-house) untuk pembentukan

CO₂ terhadap katalis referensi Pt/C pada potensial 0,6 V suhu operasi 90°C adalah: 20% PtCeO₂/C (in-house CeO₂): 20%, 20% PtCeO₂/C (commercial CeO₂): 19 %, 20% PtRhCeO₂/C (in-house CeO₂): 27%, 20% PtRhCeO₂/C (Commercial CeO₂): 24%.

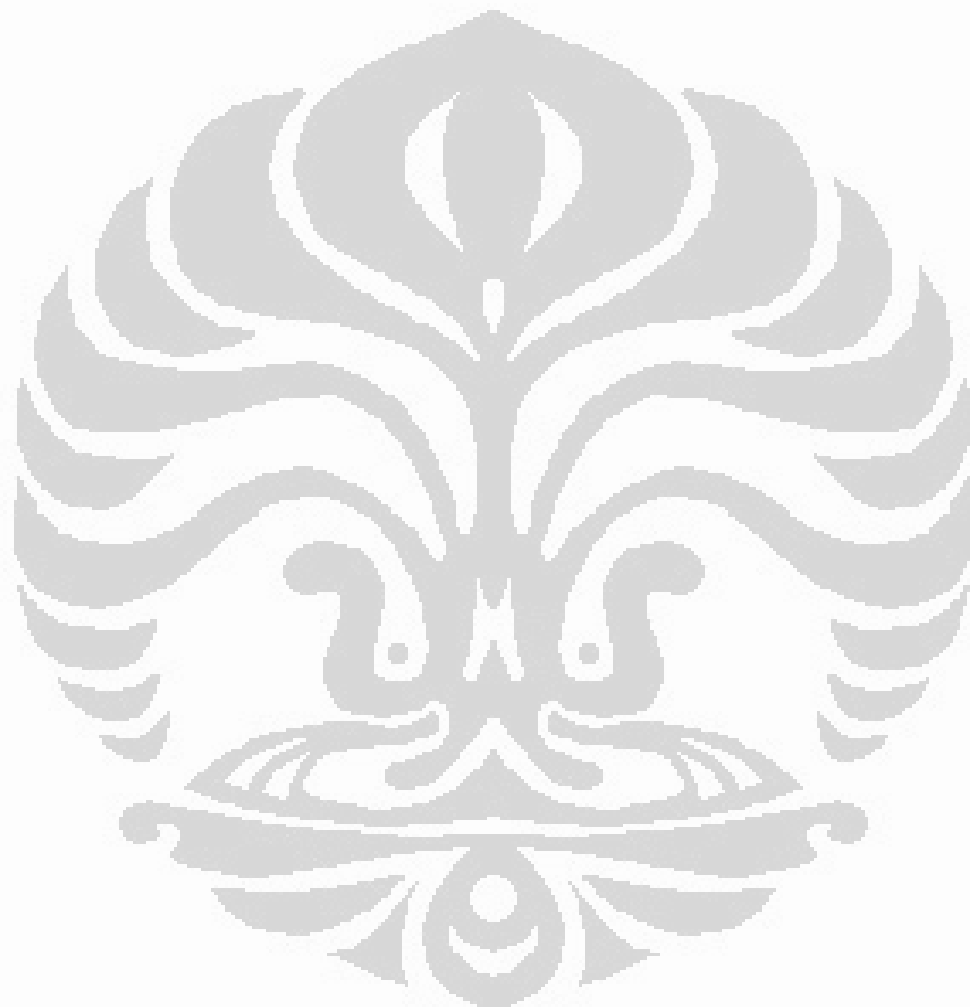
Kata kunci: Elektro-oksidasi ethanol, Pt-CeO₂/C, Pt-Rh-CeO₂/C, aktivitas, selektivitas, CO₂, arus Faraday



TABEL OF CONTENT

	Page
STATEMENT of ORIGINALITY	i
PAGE OF APPROVAL	ii
PAGE OF APPROVAL	iii
ACKNOWLEDGEMENT	iv
1 INTRODUCTION	1
1.1 Background	1
1.2 Problem definition	4
1.3 Hypothesis	4
1.4 Research Objectives	5
1.5 Outlines of the Dissertation	5
2 LITERATURE REVIEW	7
2.1 Fuel cell history and concept	7
2.2 Thermodynamic of direct ethanol fuel cells	13
2.3 Ethanol electro-oxidation reaction (EOR)	15
2.4 Catalyst synthesis	18
2.5 Catalyst Characterization	20
2.6 Electrochemical Measurement	21
2.7 Introduction to Differential Electrochemical Mass spectrometry (DEMS)	24
3 EXPERIMENTAL METHOD	26
3.1 Material and Chemicals	26
3.2 Catalyst preparation	27
3.3 Physical Characterisation	32
3.4 Half cell electrochemical measurements	33
3.5 Differential electrochemical mass spectrometry (DEMS) measurement of fuel cell	35
3.6 Single cell performance test	43
4 RESULT AND DISCUSSION	44
4.1 Physical characterization of catalysts	44
4.2 Electrochemical characterization of catalyst	51
4.3 Electrochemical activity and selectivity of the catalyst in fuel cell setup: Potentiodynamics measurements	64
4.4 Electrochemical activity and selectivity of the catalyst in fuel cell setup: Potentiostatics measurements	71
4.5 Effect of Rh metal catalyst and CeO ₂ modifier on Pt based catalyst	77
4.6 The Role of Rh and CeO ₂ in the reaction mechanism of ethanol electro-oxidation in direct ethanol fuel cell	79

4.7	Polarization curve of single cell testing on Pt/C, PtCeO ₂ /C (A), PtRhCeO ₂ /C (A) catalysts	80
5	CONCLUSIONS	82
	REFERENCES	85



LIST OF FIGURES

	Page
Figure 1.1 Chart of variety of fuel cells application	2
Figure 2.1 schematic diagram of hydrogen oxygen fuel cells	8
Figure 2.2 Maximum H ₂ fuel cell efficiency in comparison to the Carnot limit [14]	10
Figure 2.3 Schematic diagram of direct ethanol fuel cells	13
Figure 2.4 ethanol oxidation reaction over Pt or PtSn/C catalysts	16
Figure 2.5 chemical synthesis of supported metal nano particle	19
Figure 2.6 cyclic voltammogram of polycrystalline platinum in alkaline (KOH)	23
Figure 3.2 Catalyst synthesis by ethylene glycol reduction method.	29
Figure 3.3. diagram of preparation of nano-size particle of CeO ₂ [32]	30
Figure 3.4 flow diagram of catalyst preparation [17]	31
Figure 3.5. Schematic representation of electrode in electrochemical cell	34
Figure 3.6. Electrochemical cell setup (a) and Potentiostat (b)	35
Figure 3.7 Schematic diagram of DEMS setup	36
Figure 3.8 Picture of differential electrochemical mass spectrometry (DEMS) setup	37
Figure 3.9 Schematic diagram of MS setup	38
Figure 3.10. (a) MEA of DEFC and (b) catalyst spraying device	39
Figure 3.11. Faradaic current as function of time from H ₂ interference	41
Figure 3.12 (a) m/z 44 ion current (CO ₂) and (b) current as function of time on CO potentiostatic for calibration	42
Figure 3.13 Performance test of single cell	43
Figure 4.1 X-Ray Diffraction pattern of in-house CeO ₂ (A) and Commercial CeO ₂ (B)	45
Figure 4.2 X-Ray diffraction pattern of PtCeO ₂ /C and PtRhCeO ₂ /C using in-house CeO ₂ , weight ratio Pt to CeO ₂ , 2:1	46
Figure 4.3 X-Ray Diffraction pattern of PtCeO ₂ /C and Pt ₇ -Rh ₃ -CeO ₂ /C with commercial CeO ₂ , weight ratio Pt to CeO ₂ , 2:1	47
Figure 4.4 Pictures of (a) SEM & EDX of PtCeO ₂ /C (A) & (b) SEM & EDX of Pt- CeO ₂ /C (B) catalysts	49
Figure 4.5 Pictures of (a) SEM & EDX of PtRhCeO ₂ /C (in-house CeO ₂) & (b) SEM & EDX of Pt-RhCeO ₂ /C (Commercial CeO ₂) catalysts	50
Figure 4.6 TEM image of (a) in-house-CeO ₂ (HRTEM) (b) 20%Pt-CeO ₂ /C (A) catalyst	51
Figure 4.7 Cyclic Voltammogram of PtCeO ₂ /C varying with the composition Pt to CeO ₂ at 30°C, scanrate 10 mV/s, 0.5 H ₂ SO ₄	52
Figure 4.8 Chronoamperometry of PtCeO ₂ /C [A] varying with Pt to CeO ₂ composition, at 0.6 V vs RHE, scanrate 10 mV/s at 30°C.	54
Figure 4.9 Ethanol electro-oxidation on PtCeO ₂ /C at 30°C, scanrate 10 mV/s, 0.5 H ₂ SO ₄ and 1 M ethanol	55
Figure 4.10 CV of PtRh/C catalyst in acid medium (0.5 M H ₂ SO ₄) at 30°C, scanrate 50 mV/s	56

Figure 4.11 Cronoamperometry of PtRh /C catalysts varied with composition ratio Pt to Rh (1:1, 4:1, 7:3) in acid medium + 1 M ethanol at temperature 30°C, scanrate 10 mV/s.	57
Figure 4.12 Ethanol electro-oxidation over PtRh/C catalysts varied with the composition Pt to Rh, 1:1, 4:1 and 7:3 atomic weight %, at temperature 30°C, scanrate 10 mV/s	58
Figure 4.13 Cyclic Voltammogram of PtCeO ₂ /C (A&B) and PtRhCeO ₂ /C (A&B) at 30 °C scanrate 50 mV/s, 0.5 H ₂ SO ₄	59
Figure 4.14 CO stripping Voltammetry of synthesized catalysts, at temperature 30 °C and scanrate 10 mV/s, in 0.5 M H ₂ SO ₄	60
Figure 4.15 Arrhenius plot over catalysts of (a) 20% PtRhCeO ₂ /C (A), (b) 20% PtCeO ₂ /C (A), (c) 20% Pt/C, at V= 0.6 V vs RHE, and at temperature range between 30°C-60°C.	61
Figure 4.16 electro-oxidation of ethanol in acid medium (0.5 M H ₂ SO ₄ + 1 M Ethanol), at 30°C , scanrate 10 mV/s	62
Figure 4.17 Cyclic Voltammetry of different catalysts in alkaline medium (0.1 M NaOH), at 30 °C, with scanrate 50 mV/s.	63
Figure 4.18 Electro-oxidation of ethanol in alkaline medium (0.1 N NaOH)+ 1 M ethanol , at 30°C scanrate 10 mV/s,	64
Figure 4.19. CV and MSCV of 20% Pt/C (Alfa Aesar-JM) catalyst at temperature 90°C, ethanol flowrate 5 ml/min, with scanrate 5 mV/s (a) CV (b) MSCV for m/z = 29 (c) MSCV for m/z = 30 (d) MSCV for m/z = 22 and (e) mSCV for m/z = 15	65
Figure 4.20 CV and MSCV of 20% Pt-Rh/C catalyst at temperature 90°C, ethanol flowrate 5 ml/min, with scanrate 5 mV/s(a) CV (b) MSCV for m/z = 29 (c) MSCV for m/z = 30 (d) MSCV for m/z = 22 and (e) mSCV for m/z = 15	66
Figure 4.21. CV and MSCV of 20% Pt-CeO ₂ /C (A) catalyst at temperature 90°C, ethanol flowrate 5 ml/min, with scanrate 5 mV/s(a) CV (b) MSCV for m/z = 29 (c) MSCV for m/z = 30 (d) MSCV for m/z = 22 and (e) mSCV for m/z = 15	67
Figure 4.22. CV and MSCV of 20% Pt-Rh-CeO ₂ /C (A) at temperature 90°C, ethanol flowrate 5 ml/min, with scanrate 5 mV/s(a) CV (b) MSCV for m/z = 29 (c) MSCV for m/z = 30 (d) MSCV for m/z = 22 and (e) MSCV for m/z = 15	68
Figure 4.23.CV and MSCV of 20% PtCeO ₂ /C (B) at temperature 90°C, ethanol flowrate 5 ml/min, with scanrate 5 mV/s(a) CV (b) MSCV for m/z = 29 (c) MSCV for m/z = 30 (d) MSCV for m/z = 22 and (e) mSCV for m/z = 15	69
Figure 4.24. CV and MSCV of PtRhCeO ₂ /C (B), at temperature 90°C, ethanol flowrate 5 ml/min, with scanrate 5 mV/s(a) CV (b) MSCV for m/z = 29 (c) MSCV for m/z = 30 (d) MSCV for m/z = 22 and (e) mSCV for m/z = 15	70
Figure 4.25. Faradaic current vs. potential for different catalysts at temperature 90°C, scanrate 5 mV/s, ethanol flowrate 5 ml/min.	73

- Figure 4.26. CO₂ current efficiency vs potential for different catalysts at temperature 90°C, scanrate 5 mV/s, ethanol flowrate 5 ml/min 73
- Figure 4.27. CO₂ current efficiency vs Pt loading for different catalysts at potential 0.6 V , temperature 90°C, scanrate 5 mV/s, ethanol flowrate 5 ml/min 75
- Figure 4.28. CO₂ current efficiency vs CO stripping charge for different catalysts at potential 0.6 V , temperature 90°C, scanrate 5 mV/s, ethanol flowrate 5 ml/min. denoted A means using in-house CeO₂, denoted B means using commercial CeO₂. 76
- Figure 4.29 The schematic representation of ethanol electro-oxidation over PtRhCeO₂/C catalyst 79
- Figure 4.30 Polarization curves and power density curves of direct ethanol fuel cell (1 M ethanol, cell temperature 90°C, p anode and cathode 1 bar, 0.8 mgcm⁻² of 20% Pt/C and PtCeO₂/C, 0.9 mgcm⁻² of 20% PtRhCeO₂/C and 2.5 mg.cm⁻² of cathode catalyst (40% Pt/C (E TEK)). 81

LIST OF TABLES

	Page
Table 2-1. Different fuel cells that have been realized and are currently in use and development [13]	11
Table 2-2 state of the art of catalyst development for DEFC	17
Table 4-1 mean crystallite size estimation (XRD) compared to TEM measurement result	48
Table 4-2 Electrochemical Active Surface area (EAS) of synthesized catalysts	60
Table 4-3. CCE for different catalysts at potential 0.6 V	74
Table 4-4. CO Stripping charge of synthesized and reference catalysts in membrane electrode assembly (MEA)	76

ABBREVIATIONS

AFC	Alkaline Fuel Cell
Ads	Adsorption
Catalyst (A)	Catalyst modified with in-house CeO ₂
Catalyst (B)	Catalyst modified with commercial CeO ₂
Commercial Ceria	Ceria purchased from Alfa Aesar_Johnson Mattew
CCE	CO ₂ Current Efficiency
CV	Cyclic Voltammetry
CE	Counter Electrode
DAFC	Direct Alcohol Fuel Cell
DEMS	Differential Electrochemical Mass Spectrometry
DEFC	Direct Ethanol Fuel Cell
DMFC	Direct Methanol Fuel Cell
DOFC	Direct Oxidation Fuel Cell
EAS	Electrochemical Active Surface Area (cm ²)
EOR	Ethanol Oxidation Reaction
FTIR	Fourier Transform Infrared
HRTEM	High Resolution Transmission Electron Microscopy
In-house Ceria	Ceria synthesized in this research work
MSCV	Mass Spectrometric Cyclic Voltammetry
MS	Mass spectrometer
m/z	Mass ion current
MCFC	Molten Carbonate Fuel Cell
MEA	Membrane Electrode Assembly
OCP	Open Circuit Potential
PAFC	Phosphoric Acid Fuel Cell
PEMFC	Proton Exchange Membrane Fuel Cell
RHE	Reversible Hydrogen Electrode
RE	Reference Electrode
SEM	Scanning Electron Microscopy
SOFC	Solid Oxide Fuel Cell
SHE	Standard Hydrogen Electrode
TEM	Transmission Electron Microscopy
WE	Working Electrode
XRD	X-ray Diffraction
EDX	Energy Dispersive X-Ray

SYMBOLS

C	Carbon
d_{XRD}	Mean crystallite size (nm)
d_{TEM}	Mean diameter particle size (nm)
E_a	Activation Energy (kJ/mole)
Hg_2SO_4	Mercury Sulfate
Hg	Mercury
HgO	Mercury Oxide
I_F	Faradaic Current (A)
I_{MS}	Steady state ion current $m/z = 22$
K_F	Calibration constant
λ	Wave Length for X-Ray (0.154184 nm)
Q_{CO}	CO Stripping charge (mC)
η_{th}	Theoretical Efficiency (%)
ΔG_R	Gibb Free Energy
ΔH_R	Reaction Enthalpy
Pt	Platinum
Rh	Rhodium
Ru	Ruthenium
Re	Rhenium
Sn	Tin
β	The width of the peak at the half height
K	Constant (0,94)
λ	Wave length of X-Ray (0.154184 nm)
θ	The Bragg angle
E_{emf}	Electromotive force (V)
We	Energy density (kWh/kg)

1 INTRODUCTION

1.1 Background

In the last decade, fuel cells become an important issue as an energy conversion device. It was because of fuel cells have several important advantages over conventional electrical energy generation such as internal combustion engine. First, they are more efficient at converting fuel sources to end-use energy. Fuel cells are projected to achieve overall efficiencies of around 70%-80%, when utilizing the waste heat. Second, because combustion is not involved, no combustion by-products, such as nitrogen oxide (NO_x), sulfur oxide (SO_x), or particulates, are produced. Third, fuel cells are very simple. It was because of their ability to be built to a certain size and then have their power output quickly and easily increased by adding more stacks of fuel cells or its capacity, when demand for electricity increases.

A variety of fuel cells are in different stages of development. They can be classified by use of diverse categories, depending on the combination of type of fuel and oxidant, whether the fuel is processed outside (external reforming) or inside (internal reforming) the fuel cell, the type of electrolyte, the temperature of operation, whether the reactants are fed to the cell by internal or external manifolds, etc. The most common classification of fuel cells is by the type of electrolyte used in the cells and includes 1) proton exchange membrane fuel cell (PEMFC), 2) alkaline fuel cell (AFC), 3) phosphoric acid fuel cell (PAFC), 4) molten carbonate fuel cell (MCFC), and 5) solid oxide fuel cell (SOFC). These fuel cells are listed in the order of approximate operating temperature, ranging from $\sim 80^\circ\text{C}$ for PEMFC, $\sim 100^\circ\text{C}$ for AFC, $\sim 200^\circ\text{C}$ for PAFC, $\sim 650^\circ\text{C}$ for MCFC, $\sim 800^\circ\text{C}$ - 1000°C for SOFC.

There are very wide ranges of applications of fuel cells from systems of a few watts up to megawatts. Each type of fuel cells normally has a specific appropriate application as shown in Fig.1.1

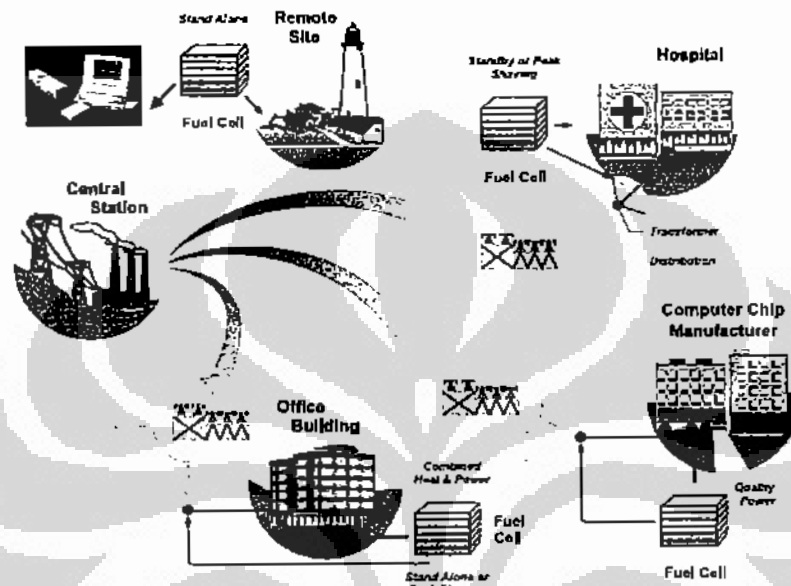


Figure 1.1 Chart of variety of fuel cells application

PEMFC is one type of fuel cells that intensively developed among the types of fuel cells in the last decade. People believed that PEMFC have big opportunities for portable power and good opportunity to replace batteries in the future. Many improvements effort activities have been carried out by doing a development of a new efficient material for PEMFC till optimization of PEMFC operation parameters. First generation of PEMFC used hydrogen as a fuel. However, due to the problem in handling of gas hydrogen, people try to looking for an alternative fuel for PEMFC. Alcohol was the next choice as fuel in PEMFC, because of their easily handling (liquid), high energy density and can be directly fed to fuel cell without any reformer device in Direct alcohol fuel cell (DAFC). Methanol was the most common alcohol that used in DAFC. However, there is a problem that methanol is toxic for human. Based on these aspects of DMFC, there are several other fuel materials, which are

investigated as a fuel for direct oxidation fuel cell (DOFC). Ethanol is one of alcohols fuel which has a good expectation for direct ethanol fuel cell (DEFC) application [1–8]. It is well known that ethanol is not toxic for human and is easily produced from biomass. This means that carbon dioxide (CO_2) emitted from direct type fuel cell using ethanol as a fuel can be recycled by planting. This CO_2 recycling leads to decreasing or keeping constant the amount of CO_2 emitted into the air.

Development DEFC is aimed for portable application and powered vehicles. For vehicles application, there are some problems in utilization gaseous fuel i.e hydrogen or hydrogen rich gas, due to hydrogen storage which is bulky and required external fuel reformer. Another problem in gaseous fuel utilization in transportation is due to lack of an infrastructure of fuel gas distribution. By using liquid alcohols fuel i.e ethanol, it could overcome the main problems of fuel cell application in transportation sector.

Another interesting application of direct ethanol fuel cell is for small portable power which aimed to replace batteries such as application for laptop, hand phone, video camera etc. In this portable application, DEFC directed to has a longer life time than the conventional batteries.

Indonesia is one of the tropical countries has abundant potential resources for ethanol production. To accelerate ethanol production, government of republic Indonesia has a target of about 2.7 billions liter per year in 2010 which the main consumption is for bio-ethanol/gasohol fuel [43]. It is a good opportunities to develop such way alternative technology to utilize an abundant ethanol fuel in Indonesia through development of new energy conversion technology.

In the case of ethanol utilization as the fuel in a direct ethanol fuel cell (DEFC), the problem is more complicated than methanol because ethanol contains two atoms of carbon, and a good electro-catalyst towards complete oxidation of ethanol to CO_2 must activate the C–C bond breaking (while avoiding the poisoning of the catalytic surface by CO species as occurs with methanol oxidation). To achieve this catalyst performance, it is necessary to modify the existing anode catalysts. So far, platinum is one of the best anode catalysts for DEFC. However, platinum itself is known to be

rapidly poisoned on its surface by strongly adsorbed species coming from the dissociative adsorption of the organic molecule.

This present work reports a study on ethanol utilization in direct ethanol fuel cell. The experimental study was emphasized on application such a new developed catalysts PtCeO₂/C and PtRhCeO₂/C catalyst for ethanol electro-oxidation in direct ethanol fuel cell. The activity and selectivity of the catalysts was investigated through systematic study.

1.2 Problem definition

So far development of direct ethanol fuel cell isn't as fast as direct methanol fuel cells (DMFC). The most common problem which covered of the DEFC was due to the sluggish reaction kinetics at electro-oxidation of ethanol. Platinum is considered to be the only stable and active catalyst for the electro-oxidation of ethanol in a strong acid environment as Nafion®. Unfortunately, the dissociative chemisorptions of ethanol leads to the formation of poisoning species like CO, which strongly adsorbed on platinum surface and block the electro-active sites of the catalyst. On the other hand, most of catalysts (binary or ternary Pt-based catalysts) which have been developing in DEFC up to now are leading to partial oxidation of ethanol which produced acetaldehyde, acetic acid and small amount of carbon dioxide.

1.3 Hypothesis

Platinum catalyst capable to break C-C bond in ethanol electro-oxidation . However, C-C bond breaking taken place at high potential (≥ 0.6 V) and Pt surface easily poisoned by CO intermediate product.

Rhodium (Rh) is a good metal catalyst for C-C bond dissociation. By addition of Rh to carbon supported Pt catalyst will improve activity of the catalyst in C-C bond breaking in ethanol electro-oxidation

CeO₂ is a good oxygen donor or oxygen storage capacity (OSC). By addition of CeO₂ to carbon supported Pt catalyst will improve activity and selectivity for CO₂ formation in ethanol electro-oxidation

It is expected that by addition of second metal catalyst of Rh and CeO₂ will play synergistic role in improving the activity of the anode catalyst toward total ethanol oxidation reaction (EOR) in direct ethanol fuel cell (DEFC)

1.4 Research Objectives

The main objective of this research work is to develop and investigate an anode catalyst base on carbon supported platinum catalyst for ethanol electro-oxidation in direct ethanol fuel cell (DEFC) which capable to promote C-C bond breaking toward total oxidation reaction of ethanol.

The specific research objectives comprise of as follows:

- To study the effect of Rh modifier on carbon supported Pt catalysts to the activity and selectivity to CO₂ product in the ethanol electro-oxidation reaction
- To study the effect CeO₂ modifier on carbon supported Pt catalysts to the activity and selectivity to CO₂ product in the ethanol electro-oxidation reaction.
- To study the effect Rh and CeO₂ modifier on carbon supported Pt catalysts to the activity and selectivity to CO₂ product in the ethanol electro-oxidation reaction.

1.5 Outlines of the Dissertation

This Dissertation was written in 5 chapters. The content of each chapter was explained in brief as follows:

Chapter 1. Introduction: is consisting of an introduction to the background, problem definition, hypothesis and objectives of the research work.

Chapter 2. Literature review: is consisting of basics theory and state of the art of this research topics area.

Chapter 3. Experimental methods: expressed the detailed experiment methods which consist of the material for the experiment, technique for catalyst preparation, physical characterization, electrochemical characterization, on-line differential electrochemical mass spectrometry and single cell fuel cell testing.

Chapter 4. Result and Discussion: concern the result of two main catalysts performance result, they were; Pt-CeO₂/C and Pt-Rh-CeO₂/C catalysts. The performance test result concerned to the activity and selectivity of the catalyst.

Chapter 5. Conclusion: conclude the result of the research work and outlook for the future work.

2 LITERATURE REVIEW

In this chapter, literature review was composed from the historical of fuel cell technology, type of fuel cell, and thermodynamics till state of the art of direct ethanol fuel cell development.

2.1 Fuel cell history and concept

In 1800, British scientists William Nicholson and Anthony Carlisle had described the process of using electricity to decompose water into hydrogen and oxygen. William Robert Grove, however took this idea one step further or, more accurately, one step in reverse in 1838. Grove discovered that by arranging two platinum electrodes with one end of each immersed in a container of sulfuric acid and the other ends separately sealed in containers of oxygen and hydrogen, a constant current would flow between the electrodes. The sealed containers held water as well as the gases, and he noted that the water level rose in both tubes as the current flowed. By combining several sets of these electrodes in a series circuit, he created what he called a "gas battery"- the first fuel cell [11].

Francis Thomas Bacon (1904 -1992) began researching alkali electrolyte fuel cells in the late 1930s. In 1939, he built a cell that used nickel gauze electrodes and operated under pressure as high as 3000 Psi. During World War II, Bacon worked on developing a fuel cell that could be used in Royal Navy submarines, and in 1958 demonstrated an alkali cell using a stack of 10-inch diameter electrodes for Britain's National Research Development Corporation.

The fuel cell concept is quite similar to the working principle of a battery; both consist of an anode and a cathode electronically separated by the electrolyte. In the anodic compartment of the fuel cell (or battery) an oxidation reaction takes place, while the electrons produced are used for the reduction process taking place at the cathode. Spatially separating both processes - oxidation at the anode and reduction at the cathode - ions can still diffuse through the electrolyte, whereas the electrons have to make their way via the external wire thereby closing the electric circuit. In dependence of the ions produced at the anode, an appropriate electrolyte has to be chosen in order to allow adequate ion diffusion. A marked difference between fuel cells and batteries is the continuous fuel supply in the fuel cell, while batteries have to be recharged after consumption of their reaction depots.

The reaction process in a low-temperature polymer electrolyte membrane fuel cell (PEMFC) using pure hydrogen as anode feed gas is shown in Fig. 2-1.

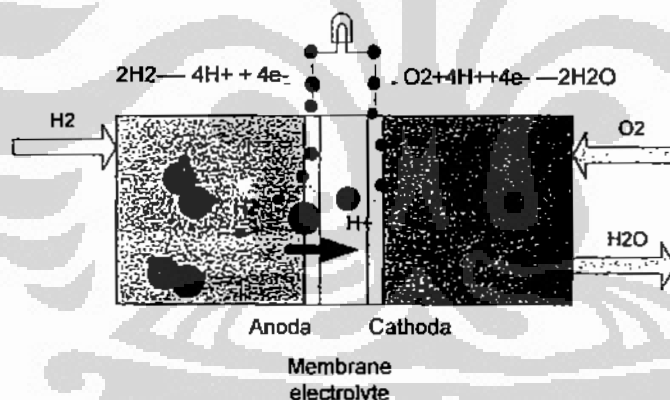
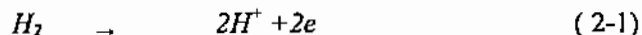


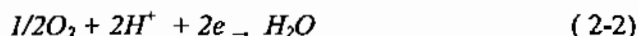
Figure 2.1 schematic diagram of hydrogen oxygen fuel cells

As long as pure hydrogen and oxygen are supplied, the only reaction product is pure water (equations 2-1 - 2-3). Hence, no harmful air pollutants are present in the exhaust gas, and the whole reaction is a convincing example for a true zero emission

Anode Reaction:



Cathode Reaction:



Cell Reaction:



Fuel cells: Efficiency compared with Carnot-process

Besides their pollution-free operation, fuel cells offer still another advantage compared with conventional combustion engines working on the basis of the well-known *Carnot*-process: a higher efficiency [14]. The theoretical efficiency η_{th} of an electrochemical process is defined as the ratio of the *Gibbs* free energy ΔG_R and the reaction enthalpy ΔH_R .

Theoretical efficiency of a fuel cell:

$$\eta_{th,FC} = \Delta G_R / \Delta H_R \quad (2-4)$$

The theoretical thermodynamic derivation of Carnot Cycle shows that even under ideal conditions, a heat engine cannot convert all the heat energy supplied to it into mechanical energy; some of the heat energy is rejected. In an internal combustion engine, the engine accepts heat from a source at a high temperature (T_1), converts part of the energy into mechanical work and rejects the remainder to a heat sink at a low temperature (T_2). The greater the temperature difference between source and sink, the greater the efficiency,

Theoretical efficiency of a combustion engine:

$$\eta_{th,Carnot} = (T_1 - T_2) / T_1 \quad (2-5)$$

Fuel cells: Types and applications

Generally, fuel cell was classified into five different types. Working temperature of those fuel cells was varied from 60°C up to 1000 °C. Alkaline fuel cell (AFC), the proton exchange membrane fuel cell (PEMFC) and the phosphoric acid fuel cell (PAFC) are generally summarized as low-temperature fuel cells. The molten carbonate fuel cell (MCFC) and the solid oxide fuel cell (SOFC) belong to the group of high-temperature fuel cells working at temperatures above 600 °C. A summary of these, their working temperatures, electrode reactions and electrolytes can be found in Table 2.1.

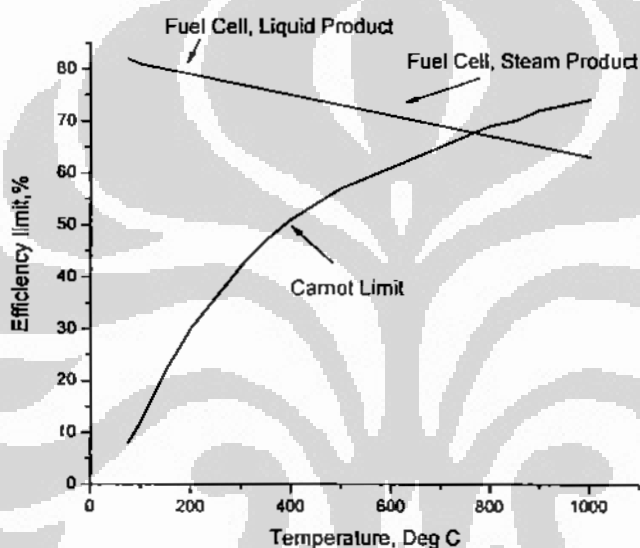


Figure 2.2 Maximum H₂ fuel cell efficiency in comparison to the Carnot limit [14]

Alkaline Fuel Cell (AFC): The electrolyte in this fuel cell is normally 35-50 wt% KOH for lower temperature (<120°C) operation. The electrolyte is retained in a matrix (usually asbestos), and a wide range of electrocatalysts can be used (e.g., Ni, Ag, metal oxides, spinels, and noble metals). The fuel supply is limited to non-reactive constituents except for hydrogen. CO is a poison, and CO₂ will react with the KOH to form K₂CO₃, thus altering the electrolyte. Even the small amount of CO₂ in air must be considered with the alkaline cell.[13,30]

Phosphoric Acid Fuel Cell (PAFC): Phosphoric acid concentrated to 100% is used for the electrolyte in this fuel cell, which operates at 150 to 220°C. At lower temperatures, phosphoric acid is a poor ionic conductor, and CO poisoning of the Pt electrocatalyst in the anode becomes severe. The relative stability of concentrated phosphoric acid is high compared to other common acids; consequently the PAFC is capable of operating at the high end of the acid temperature range (100 to 220°C). In addition, the use of concentrated acid (100%) minimizes the water vapor pressure so water management in the cell is not difficult. The matrix universally used to retain the acid is silicon carbide and the electrocatalyst in both the anode and cathode is Pt [13].

Table 2-1. Different fuel cells that have been realized and are currently in use and development [13]

	AFC	PAFC	PEMFC	DMFC	MCFC	SOFC
Operating Temp.(C)	<100	160-220	60-120	60-120	600-800	800-1000
Electrolyte Charge Carrier	OH ⁻	H ⁺	H ⁺	H ⁺	CO ₃ ²⁻	O ₂ ²⁻
Power Range	5-150 kW	50 kW-11MW	5-250 kW	5 kW	100 kW-2MW	100 kW-250 kW
Anode Reaction	$H_2 + 2OH^- \rightarrow 2H_2O + 2e^-$	$H_2 \rightarrow 2H^+ + 2e^-$	$H_2 \rightarrow 2H^+ + 2e^-$	$CH_3OH + H_2O \rightarrow CO_2 + 6H^+ + 6e^-$	$H_2 + CO_3^{2-} \rightarrow CO_2 + H_2O + 2e^-$	$H_2 + O_2 \rightarrow H_2O + 2e^-$
Cathode Reaction	$\frac{1}{2}O_2 + 2H^+ + 2e^- \rightarrow H_2O$	$\frac{1}{2}O_2 + 2H^+ + 2e^- \rightarrow H_2O$	$\frac{1}{2}O_2 + 2H^+ + 2e^- \rightarrow H_2O$	$\frac{3}{2}O_2 + 6H^+ + 6e^- \rightarrow 3H_2O$	$\frac{1}{2}O_2 + CO_2 + 2e^- \rightarrow CO_3^{2-}$	$\frac{1}{2}O_2 + 2e^- \rightarrow O^{2-}$
Application	Space, Military	Combined heat and power for stationary power systems	Transportation, and Energy storage systems		Combined heat and power for stationary and mobile systems	

Notes: AFC: Alkaline Fuel Cell, PAFC: Phosphoric acid fuel cell, PEMFC : Proton exchange membrane fuel cell, DMFC: Direct methanol fuel cell, MCFC : Molten carbonate fuel cell, SOFC: Solid oxide fuel cell

Development of Pt-Rh-CeO₂/C and Pt-CeO₂/C catalysts for ethanol electro-oxidation in direct ethanol fuel cell

Proton-exchange membrane (PEM) fuel cells are the most common type of fuel cells for light-duty transportation use, because they can vary their output quickly (such as for startup) and fit well with smaller applications. The advantages of PEMs are that they react quickly to changes in electrical demand, will not leak or corrode, and use inexpensive manufacturing materials (plastic membrane).

Direct methanol fuel cells (DMFC) use methanol instead of hydrogen and are being considered for use in the transportation industry. DMFCs differ from the other types of fuel cells in that hydrogen is obtained from the liquid methanol, eliminating the need for a fuel reformer [13,30]

Molten carbonate fuel cells (MCFCs) operate at high temperatures which mean that they can achieve higher efficiencies and have a greater flexibility to use more types of fuels. Fuel-to-electricity efficiencies approach 60%, or upwards of 80% with cogeneration [13,30].

Solid oxide fuel cells (SOFCs) also operate at higher temperatures and have demonstrated very good performance in combined-cycle applications. SOFCs are a promising option for high-powered applications, such as industrial uses or central electricity-generating stations.[13,30].

Direct oxidation of alcohols

Fuel cells employing alcohols directly as fuel - direct alcohol fuel cells (DAFC) - are attractive as power sources for mobile stationary and portable application. Direct oxidation of methanol in direct methanol fuel cell (DMFC) has been investigated over many years. However, methanol has some disadvantages, for example: it is relatively toxic, low a boiling point and it is not primary fuel. Therefore other alcohols, particularly those coming from biomass resources, are being considered as alternative fuels. Ethanol is a promising substitute for methanol as fuel in DAFC due to its higher energy density and non-toxic properties [1]. Another advantage of ethanol is due to it is renewable fuel that can be produced in large quantities from agriculture product.

Working principle of direct ethanol fuel cells are shown in Fig.2-3. Liquid ethanol fed into anode compartment, then ethanol will electro-oxidize with aid of the catalyst. Proton moves to the cathode side through the electrolyte membrane, on the other hand electron transport from anode to cathode through external circuit. Finally, oxidant will react with electron and proton to produce water at cathode side.

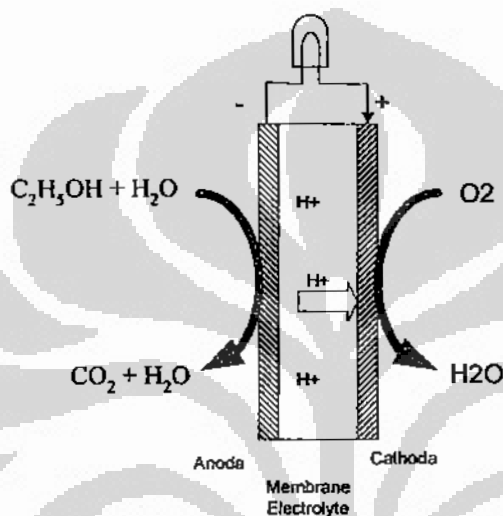


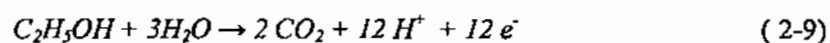
Figure 2.3 Schematic diagram of direct ethanol fuel cells

The reactions take place in direct ethanol fuel cell obeys the following reaction:



2.2 Thermodynamic of direct ethanol fuel cells

The complete oxidation of ethanol involves 12 electrons per molecule, as following:



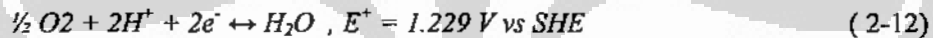
The reversible anode potential under standard condition can be calculated from the thermodynamic data. For ethanol electro-oxidation that followed the reaction (2-9), a Gibbs energy change calculated from standard energy of formation ΔG^f of reactans :

$$\begin{aligned}\Delta G &= 2 \Delta G_{CO_2}^f - \Delta G_{C_2H_5OH}^f - 3 \Delta G_{H_2O}^f & (2-10) \\ \Delta G &= -2 \times 394.4 + 174.8 + 3 \times 237.1 \\ &= 97.3 \text{ kJ mol}^{-1}\end{aligned}$$

This gives the anode potential:

$$E^- = \frac{\Delta G^-}{12F} = 0.084V \text{ vs SHE} \quad (2-11)$$

for the cathode reaction:



So that standard electromotive force is:

$$E_{emf} = E^+ - E^- = 1.229 - 0.084 V = 1.145 V \quad (2-13)$$

Corresponding to Gibbs energy change $\Delta G = -1326.7 \text{ kJ/mol}$ and for the overall combustion reaction:



this gives an energy density:

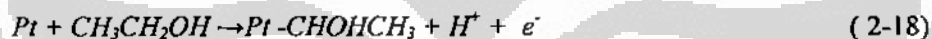
$$We = \frac{-\Delta G}{3600M} = 8.01 \text{ kWh kg}^{-1} \quad (2-15)$$

where $M = 46.07 \text{ g}$ is the molecular weight of ethanol. The enthalpy change $\Delta H = -1367.9 \text{ kJ mol}^{-1}$ allows calculation of a reversible energy efficiency at equilibrium potential :

$$\varepsilon_r = \frac{\Delta G}{\Delta H} = \frac{1326.7}{1367.9} = 0.970 \quad (2-16)$$

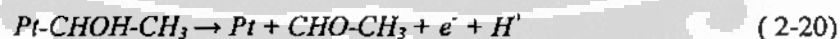
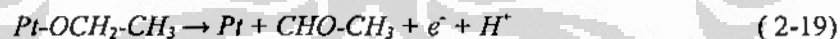
2.3 Ethanol electro-oxidation reaction (EOR)

Ethanol oxidation has been extensively studied at platinum electrodes [1-3]. Iwasita et al., reported that ethanol can be O- or C-adsorbed on platinum single crystal [4] :

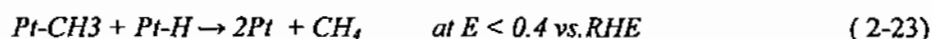
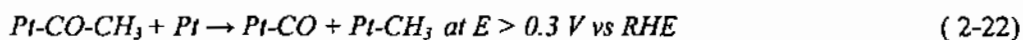
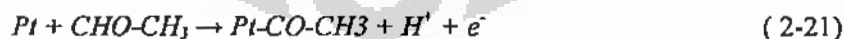


Those reactions above represent the initial step of adsorption and oxidation reaction of ethanol.

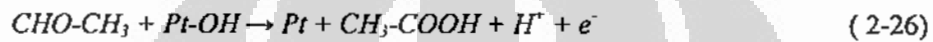
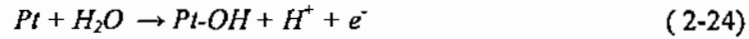
The next reaction was led to formation of acetaldehyde as confirmed by Lamy et al., that observed at low potential by infrared spectroscopy [5].



The acetaldehyde formed then adsorbed on Pt surface and further reaction as follows:



This formation was observed by Iwasita et al.[4], by spectroscopy technique at potential lower than 0.4 V. Since dissociative adsorption of water was occurred at potential higher than 0.6 V vs. RHE, this Pt-OH could promote the next reaction of Pt-CO as following:



Furthermore, base on result from Iwasita et al.[4,6], and Leger et al.[7], mechanism of ethanol oxidation reaction over Pt and PtSn catalyst was summarized as following reaction mechanism:

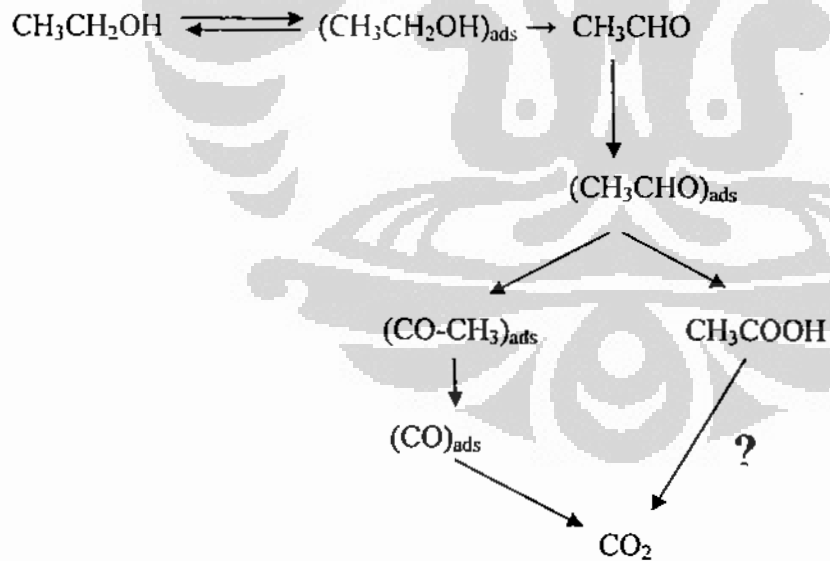


Figure 2.4 ethanol oxidation reaction over Pt or PtSn/C catalysts

Catalyst for ethanol electro-oxidation in direct ethanol fuel cell

There are some catalysts that already employed for ethanol electro-oxidation in direct ethanol fuel cell, such as: Pt, PtSn, PtRe, PtRu, etc., either carbon supported or unsupported. Iwasita et al [4,6,8] had studied the reaction mechanism of ethanol electrooxidation over single crystal of Pt catalyst and PtRu catalysts using infrared spectroscopy and differential electrochemical mass spectrometry (DEMS) technique. Lamy et al.[1,5,7], had investigated intensively the binary and ternary catalysts base on Pt catalyst in direct ethanol fuel cell (DEFC). They concluded that PtSn catalyst was the best catalyst for ethanol electro-oxidation so far. The recent status of DEFC development is summarized in the Table 2.2.

Today the state of the art catalyst for ethanol oxidation is based on Pt and PtSn combinations. Although there are many studies devoted to the activity and selectivity of ethanol oxidation on several catalysts, a systematic approach to investigate ethanol oxidation, under fuel cell relevant conditions is still missing. So, in this work activity and selectivity of ethanol oxidation on new developed anode catalysts (PtCeO₂/C and PtRhCeO₂/C) under technically relevant conditions (90 °C, 1 M methanol, membrane electrode assembly (MEA)) was studied and discussed in connection with literature results (Chapter 4).

Table 2-2 state of the art of catalyst development for DEFC

Investigator	Catalyst	Technique	Conditions & Results	Ref
Lamy et al.	PtSn, PtRe, Pt, PtRu	Infrared reflectance spectroscopy, cyclic voltammetry (CV), single cell testing	1.5 mg/cm ² Pt loading of anode catalyst, 2.0 mg/cm ² platinum loading of cathode catalyst. Pt ₅ Sn ₁ was the best catalyst for EOR. Result : power density : 20 mW/cm ² at temperature cell 90°C, 1 M ethanol	[1,5,7]
Iwasita et al.	Pt single crystal, PtRu	FTIR, half-cell measurement	Electrolyte 1 M ethanol + 0.1 HClO ₄ . at T= 25 deg C. Result :on Pt single crystal scission of C-C bond taken place only to limited extent. Pt Ru catalyst selective product to acetic acid, maximum of CO ₂ product was about 5 %	[6,8]

Development of Pt-Rh-CeO₂/C and Pt-CeO₂/C catalysts for ethanol electro-oxidation in direct ethanol fuel cell

Qin Xin et al.	PtSn	Half-cell measurement, single cell measurement	1.5 mg/cm ² Pt loading of anode catalyst, 1.0 mg/cm ² platinum loading of cathode catalyst. Result : power density : 20 mW/cm ² (Pt:Sn, 2:1 at. weight ratio)	[9]
Fujiwara et al.,	PtRu	Differential electrochemical mass spectrometry (DEMS) connected to electrochemical cell	Electrolyte 1 M CD ₃ CH ₂ OH + 1M HClO ₄ , at 25 deg C, Result : optimum selectivity to CO ₂ formation over Pt _{0.67} Ru _{0.33} at 5°C and Pt _{0.85} Ru _{0.15} at 25 and 40°C.	[3]
Behm et al.	Pt, PtRu, PtSn	DEMS of fuel cell connected to electrochemical cell	Electrolyte: 1 M ethanol + 0.5 M H ₂ SO ₄ , at T: 60 deg C Results : DEMS measurements reveal that in both potentiodynamic and potentiostatic measurements the addition of Ru or Sn in the binary Pt catalysts lowers the onset potential for ethanol electro-oxidation and the onset for CO _{ad} oxidation, but does not increase the selectivity for complete oxidation to CO ₂ under present reaction conditions	[10]
Nart, et al.,	PtRh	DEMS connected to electrochemical cell, FTIR	Electrolyte: 0.1 M ethanol + 0.1 M HClO ₄ at 25 deg C Results : FTIR : detected products : Acetic acid, acetaldehyde, CO ₂ DEMS : Pt ₇₃ Rh ₂₇ was the best composition for selectivity to CO ₂ product	[12]

2.4 Catalyst synthesis

The synthesis of metal nanoparticles has developed into a large field with diverse interests and applications. The preparation procedures can be broadly divided into physical or chemical methods. The physical methods mainly proceed with atomisation of metals in a vacuum by thermal evaporation or sputtering. Through the physical methods, It is normally more difficult to get uniform size nanoparticles especially when high loading is needed. For loading mixed metal catalysts into high surface area porous supports, e.g. Vulcan 72 carbon, physical method generated nanoparticles cannot penetrate far into the inner regions of the carbon powder.

A large variety of chemical methods have been reported for the syntheses of metal nanoparticles, such as : impregnation method, protected colloidal and unprotected colloidal methods and microemulsion method. For applications as electrocatalysts, the final state requires the nanoparticles to be supported on a conducting substrate. The steps in the synthesis can be simplified and are generalized schematically in Fig. 2.5. The starting point of the synthesis is a metal precursor either in an ionic or a molecular state. Chemical changes are initiated to convert the precursor to metal atoms, which then merge to form nanoparticles. In the presence of a confining support or a protection agent, particle growth is confined. Supported and size-controlled nanoparticles are then formed

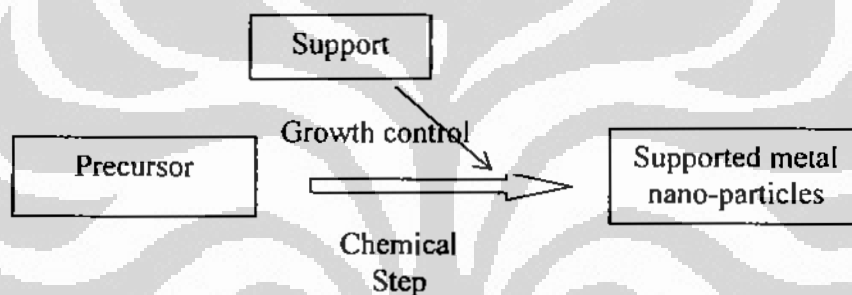


Figure 2.5 chemical synthesis of supported metal nano particle

Among of the chemical syntheses methods, colloidal method is recently widely used for synthesizing metal nanoparticles with size contro. In the presence of a protective agent, such as surfactant molecules, the metal precursor is chemically reduced or reacted to form metal nanoparticles. A narrow size distribution is achieved as the colloidal metal nanoparticles are stabilized either by steric hindrance or by electrostatic charges. Colloidal metals can form in the organic medium (organosols) or aqueous medium (hydrosols). In the case of adsorbed ions or charged colloids, protection from merging into larger particles is provided by the electrostatic repulsion of like charges. On the other hand, steric stabilization can be provided by coating the metal core with organic chain molecules. Examples of common protecting ligands

include NR_4^+ , PPh_3 , PVP, and PVA. Though the colloidal method can provide a narrow size distribution of metal nanoparticles, the major drawback is the presence of the protecting agent, which may also hinder the catalytic function of the nanoparticles. The organic protecting shell can be removed by washing in an appropriate solvent or by decomposition at elevated temperature in an inert atmosphere. Before the removal of the protecting agent, adsorption into a protecting micro porous catalyst support is necessary to prevent agglomeration into larger metal particles. It would be preferable to use the alternative route of preparing colloidal nanometals without the use of protecting agents. This can be achieved for certain metals by appropriate combination of precursor, solvents, reducing agent and electrolyte. In the recent work of Wang et al.[18], the use of sodium hydroxide dissolved in ethyl glycol as solvent appears to be suitable for preparation of a number of metal nanoparticles, especially for platinum, without the use of a protecting agent. The electrocatalytic performance of supported platinum nanoparticles prepared with this method has been reported recently [30]. Dissolution or precipitation of the colloidal metal nanoparticles requires careful control of process parameters, e.g. pH and water concentration. Bock and MacDougall [17] were prepared the PtRu catalyst using ethylene glycol reduction method. The colloidal metal nanoparticles may be protected by glycol, which serves as both a solvent and the protecting agent. The glycol can be removed by electro-oxidation during usage as an anode. The glycol colloidal process is very attractive for large-scale synthesis of metal nanoparticles. In this research work catalysts were synthesized by colloidal methods (ethylene glycol reduction methods) due to a simple in preparation, but it is able to control the particle size and distribution.

2.5 Catalyst Characterization

Crystallography of catalyst

X-ray diffraction (XRD) is mostly used for bulk structure analysis, yet it has one feature which makes suitable for size determination, if the concentration of the active

component is large enough. Quantitatively, the average particle size is estimated by using Scherrer equation [40]:

$$d = \frac{K \cdot \lambda}{\beta \cdot \cos \theta} \quad (2-27)$$

Where:

d = the average crystallite size

β = the width of the peak at the half height (peak height is calculated from a baseline).

K = Constant (0,94)

λ = wave length of X-Ray (0.154184 nm)

θ = the Bragg angle

Morphology of catalyst

Shape and size are two important features of morphology. Information of this nature is necessary for complete knowledge of all catalytic components.

Instrumentation for this purpose includes various types of electron microscopy such as scanning electron microscopy (SEM) and transmission electron microscopy (TEM)

Particle size of catalyst

The most important of powder catalyst property is particle size. The most common of instrumentation for this purpose is transmission electron spectroscopy. The particle size of powder catalyst also can be estimated by Scherrer equation from the XRD pattern result.

2.6 Electrochemical Measurement

Electrochemical measurement was carried out in half cell setup/model electrode comprise of some techniques such as: normal cyclic voltmmetry (CV), CO stripping voltammetry, and CV in presence of ethanol to test the activity of the catalysts.

2.6.1 Cyclic Voltammetry

In principle, all electrochemical techniques purpose at the investigation of electrode processes to achieve a more detailed understanding of the reaction rate, the reaction mechanism, possible reaction intermediates and adsorption processes.

As part of this work, cyclic voltammetry (CV) was applied to study the electrocatalytic activity of the catalysts in question. The main advantage of this technique is, that a rough idea of the specific features of an electrochemical system can be obtained in very short time, in contrast to several other, more time consuming procedures. It is particularly suited to detect typical surface reactions and the formation of oxide layers on noble metal catalysts as well as the electrochemical conversion of adsorbates. With the abrupt change of one of the electrode parameters, e.g. current, potential or concentration, a predefined system will need a distinct time to react to the new situation and to gain its new stationary state. Hence, the slower the parameter change takes place, the more one will expect stationary conditions.

Exemplary, quasi stationary conditions will be anticipated, if a moderate potential course, linear or sinusoidal in time, is imposed on the electrode. However, as these methods might work with rapid potential changes as well, they are characterized as transient methods at present. In cyclic voltammetry, a potential is forced upon the working electrode, that changes triangular with time, and the resulting current response is recorded.

2.6.2 CV in electrolyte in absence of ethanol

In Fig. 4, a base voltammogram of a bulk platinum electrode in aqueous solution is shown. If there are no species in the aqueous solution, which are redox-active in the potential region between the turn-round potentials, the observed current-potential behavior will correspond to the formation and dissolution of chemisorbed hydride and oxide layers on the electrode surface.

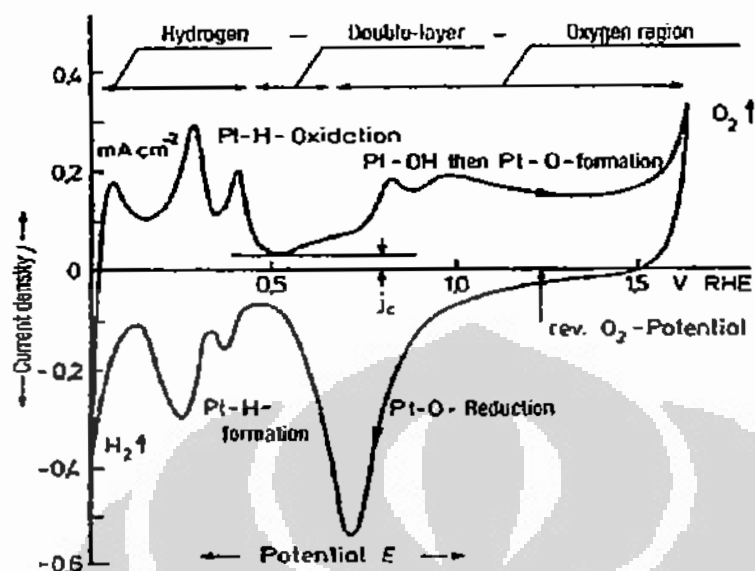
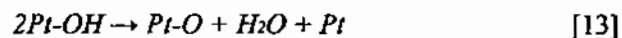


Figure 2.6 cyclic voltammogram of polycrystalline platinum in alkaline (KOH)

In the following, the respective electrode processes causing the specific shape of the voltammogram will be described in detail. For the discussion, all potentials will be given versus the reversible hydrogen electrode (RHE, $\text{Pt}/\text{H}_2/\text{H}_2\text{aq} +, a\text{H} + \text{variable}, E_{\text{R}} = -0.059 \text{ pH}$). Starting in positive direction (forward sweep), between 450 and 550 mV vs RHE only minor currents were recorded that are needed for the charging of the electrolytic double layer. At approximately 550 mV vs RHE, the formation of oxygen adsorption layer begins.

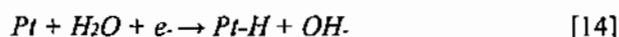


At more positive potentials of about 800 mV vs RHE, another oxygen adsorbate species is formed, until at ca. 1600 mV vs RHE oxygen evolution sets in.



In negative direction (reverse scan), the oxygen adsorbate layers were reduced with an over potential of several 100 mV first, followed by a comparatively small double layer region at around 500 mV.

Adsorption of hydrogen starts at approximately 350 mV vs RHE.



Reaching the hydrogen potential, hydrogen evolution occurs, indicated by a strong increase in the cathodic current. As the sweep direction is reversed again, molecular as well as adsorbed hydrogen is oxidized with increasing potential.

The cyclic voltammogram explained above was measured at a polycrystalline electrode.

2.6.3 CO stripping voltammetry

Carbon monoxide is considered to be a kind of “test molecule” in electrocatalysis. CO stripping voltammetry has a threefold function. First, CO stripping charge can be used for estimation of real surface area. Second, commencement, peak potential and shape of CO stripping wave are surface sensitive [16]. Third, since CO is considered as an intermediate in ethanol oxidation, higher activity in CO oxidation can be correlated to higher activity towards ethanol oxidation.

Basically the CO adsorption method is the same as the hydrogen adsorption method *i.e.* a probe molecule is adsorbed at the surface (at potential where CO oxidation does not occur), removed from the surface in a potential sweep and then the charge under the oxidation peak is calculated. This method should have some advantages over the hydrogen adsorption method due to its more general applicability.

2.7 Introduction to Differential Electrochemical Mass spectrometry (DEMS)

Online observation of mass signals from the volatile reaction products offers useful additional information on the reaction-taking place at an electrochemical interface. Mass spectroscopy is especially useful for studying fuel cells reactions in simple

laboratory cells and also fuel cell systems, at ambient conditions and also at elevated temperature and pressure.

DEMS represent one of the equipments, which are very assist to test performance of catalysts for the application of fuel cell. Because for many electrochemical study, examination of cyclic voltammetry not yet adequate enough, due to its limitation to interpret product of electro-oxidation reaction. By conducting examination use DEMS will assist in analyzing product, which is volatile.

In order to produce a mass signal cyclic voltammogram (MSCV), it is necessary to obtain differential signals as a function of time and herewith as a function of potential like in the current / potential CV. The sensitivity in the form of ion current per mA of electrochemical current must be high and in a linear relation, and as a second condition, the total gas volume has to be emptied in a time near 10^2 s or less. Therefore turbo molecular pumps are needed.

Online mass spectroscopy as described above can be applied in all cyclic voltammogram studies, galvanostatic or potentiostatic experiments wherever volatile species are involved. Additional information can be derived by comparing of CV and MSCV.

3 EXPERIMENTAL METHOD

In the following section, the synthesis of the CeO₂ nano-size particle and synthesis of different catalysts will be described. Structural characterization of the supported catalyst powders was performed by a number of methods such as X-ray diffraction (XRD), energy dispersive of X-ray (EDX), scanning electron microscopy (SEM) and transmission electron microscopy (TEM).

The electrocatalytic activity of the catalysts was measured by cyclic voltammetry in electrochemical cell setup under various conditions.

The catalysts coated onto carbon paper gas diffusion layer (GDL) by printing catalyst ink which controlled by CNC. Electrode and electrolyte membrane then to be assembled in membrane electrode assembly (MEA) by hot pressing. The prepared MEA, then arranged in single cell of fuel cell by using bipolar plate with single serpentine flow field.

Differential electrochemical mass spectrometry (DEMS) measurement setup was consist of fuel cell which is coupled to mass spectrometer and connected to the potentiostat and controlled by computer. Single cell performance testing was carried out by varying cell potential to obtain the certain current output. The overall step of experiment was shown in Fig.3.1

3.1 Material and Chemicals

The starting materials used were: cerium nitrate hexahydrate (Ce(NO₃)₃·6H₂O, anal., Alfa-Johnson Matthew), hydrogen peroxide (30% H₂O₂, p.a., Merck) and ammonium hydroxide (NH₄OH, 25 vol% p.a., Merck).

$\text{H}_2\text{PtCl}_6 \cdot 6\text{H}_2\text{O}$ (Johnson Matthew) and $\text{RhCl}_3 \cdot 3\text{H}_2\text{O}$ (Johnson Matthew) were used as precursors of PtRh catalysts. Material of carbon support was Vulcan-XC-72 from Cabot Co.

In all experiments, 0.5 M sulfuric acid prepared from concentrated sulfuric acid (Merck suprapur), 0.1 sodium hydroxide (Merck suprapur) and water from a Milli-Q system (18 M Ω cm) was used as electrolyte. One molar ethanol in 0.5M sulfuric acid solution was prepared, using ethanol (LiChrosolv, 99,99 %) from Merck. High purity Ar (Linde Gas, 4.8) and CO (Linde Gas, N 4.7) were employed for electrolyte purging and CO saturation.

3.2 Catalyst preparation

In the following section, the synthesis of the different catalyst systems will be described. First, we synthesize ceria (CeO_2) nanoparticle with the two step preparation method [3]. Ceria is added as promoter in the following synthesizes catalysts. In the next sections, the catalysts which is synthesize by using in house ceria is denoted as *catalyst A*, and the catalyst which is synthesize by using commercial ceria is denoted as *catalyst B*. For example *PtCeO₂/C (A)*, this mean using in-house ceria and *PtCeO₂/C (B)* means using commercial ceria from Alfa Aesar-Johnson Matthews.

FLOW DIAGRAM OF RESEARCH EXPERIMENT

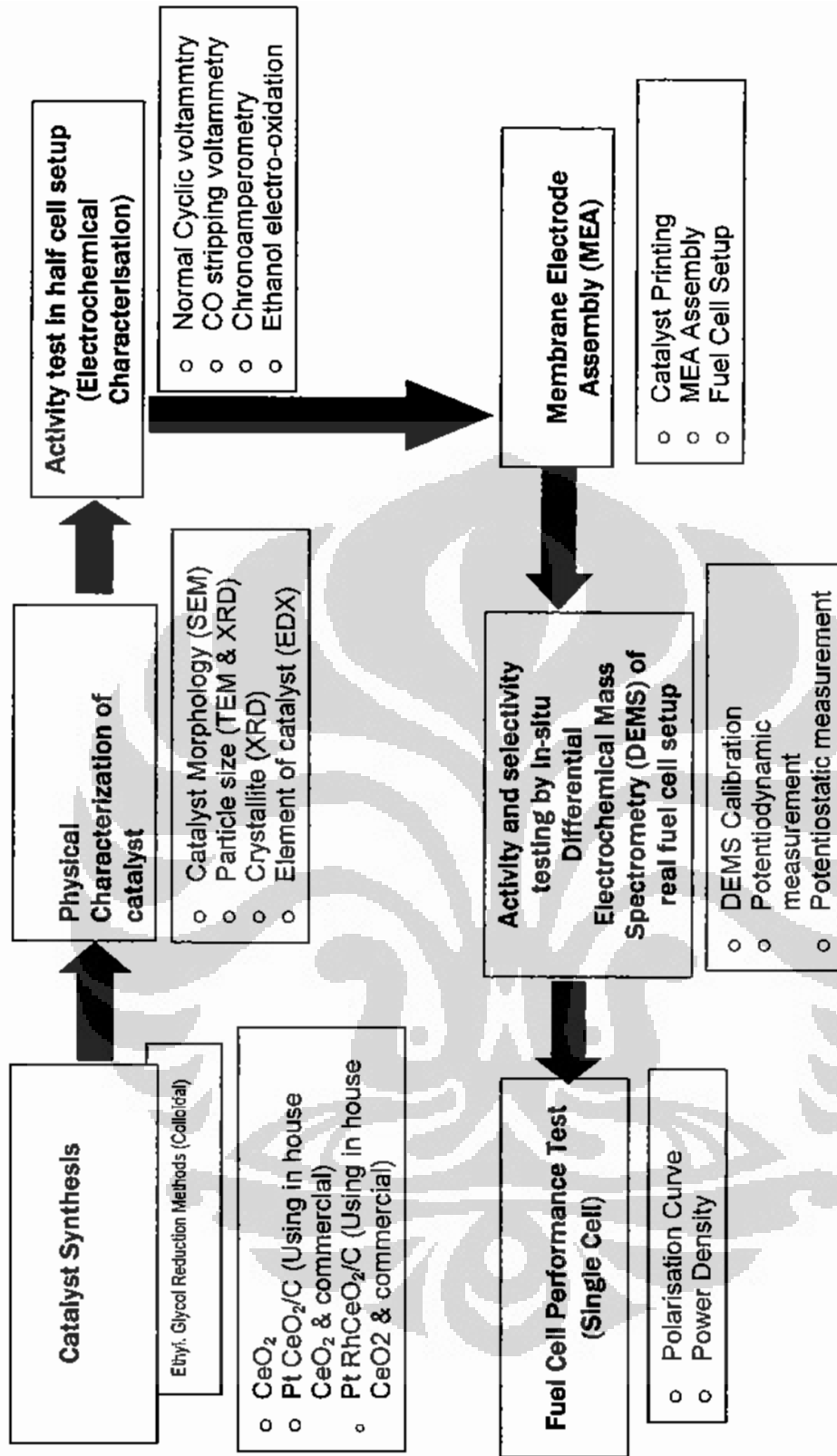


Figure 3.1. Flow diagram of research experiment

Development of Pt-Rh-CeO₂/C and Pt-CeO₂/C catalysts for ethanol electro-oxidation in direct ethanol fuel cell

In this study, catalyst synthesis are carried out by ethylene glycol reduction method. All of the catalysts synthesis are targeted with the platinum loading 20% (weight percentage) to the total catalyst. The composition of Pt to Ceria is varied with 1:1; 2:1 and 3:1. As a reference catalyst is used commercial catalyst of 20% Pt/C Alfa Aesar-Johnson Matthews. In this study we also used ceria commercial (Alfa Aesar-Johnson Matthews) for comparison with in house ceria. Fig.3.2 shows the reduction process by ethylene glycol in thermo oil bath.

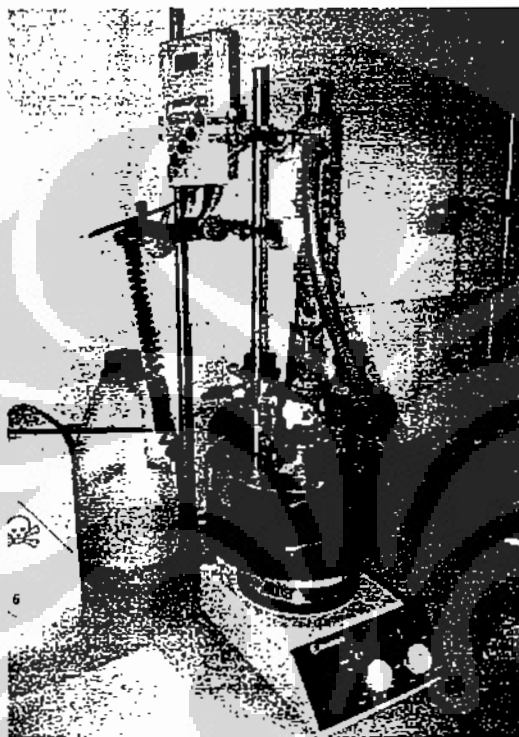


Figure 3.2 Catalyst synthesis by ethylene glycol reduction method.

3.2.1 Cerium oxide (CeO_2) preparation

Separate solutions of 0.1 mol Ce(III) nitrate in water and of 30 vol% hydrogen peroxide were cooled to 5°C and then mixed together under constant stirring. After 8-10 min the solution turned first yellow then orange-yellow, but remained transparent. Ammonium hydroxide solution was then added to increase the pH value to 10. The solution then refluxed at 90°C in oil bath for 2 hours. Precipitation therefore occurred in two stages. The solution was decanted and the precipitate was washed and dried at $80 \pm 5^\circ\text{C}$, then calcined at 500°C under air for 3 h. The step of the CeO_2 preparation was simplified in Fig.3.3

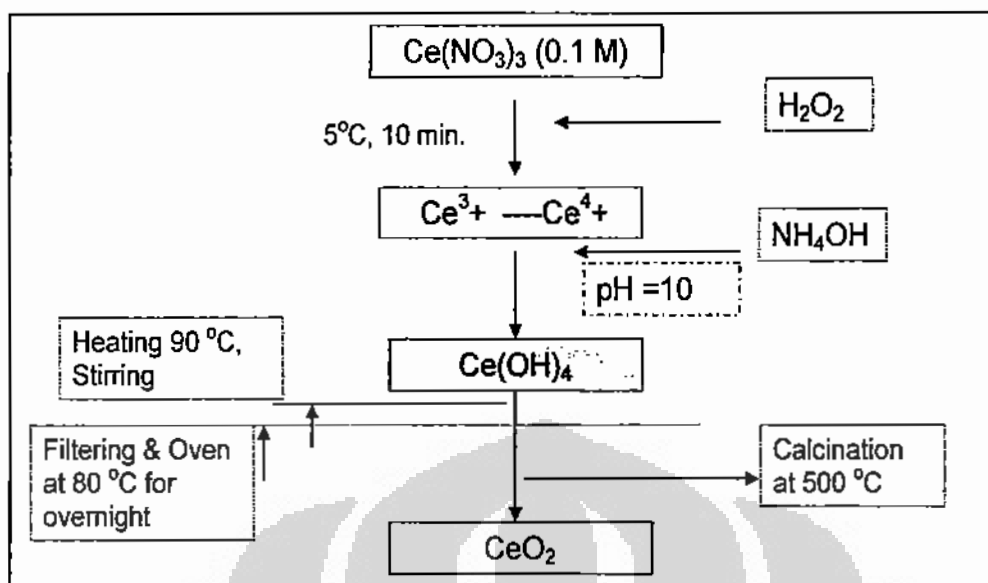
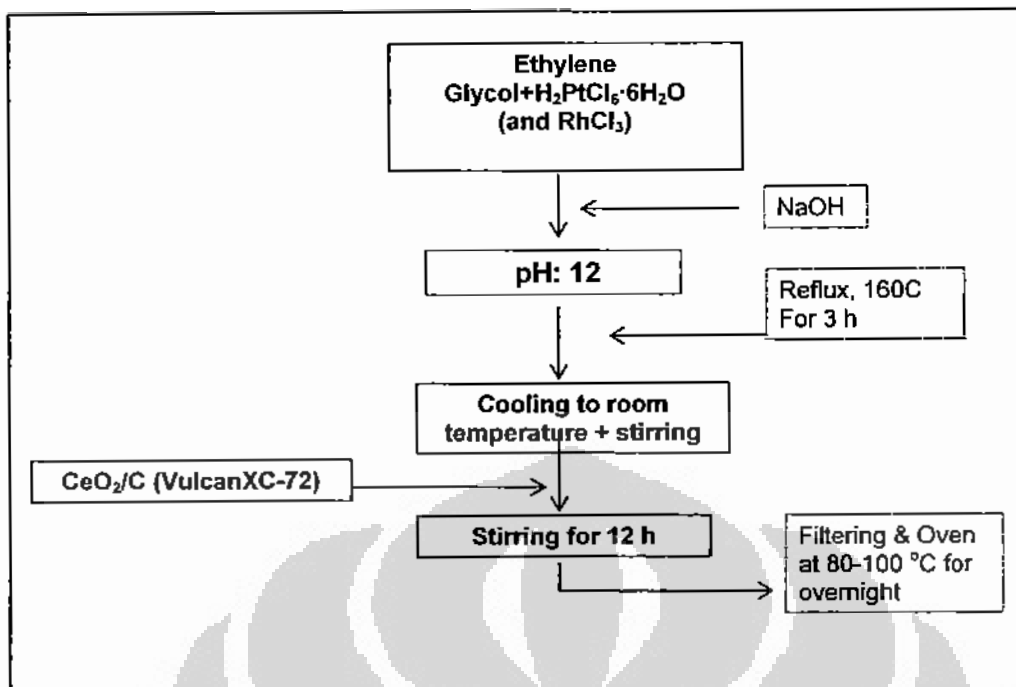


Figure 3.3. diagram of preparation of nano-size particle of CeO₂ [32]

3.2.2 Pt-CeO₂/C Preparation

The needed amount of H₂PtCl₆·6H₂O was added into ethylene glycol solution and stirred for half an hour. Prior to the synthesis of colloidal solution, all of ethylene glycol was dried using molecular sieve. Then the pH value of the solution was justified to 12 with sodium hydroxide (0.5 M) and the solution was heated under reflux to 160 °C in oil bath, and kept at this temperature for 2 h to obtain brown-black sol. The solution then cooled until room temperature and the calculated amount of CeO₂ and carbon Vulcan XC-72 was added to the sol and stirred for another 12 h. The obtained black product was then filtered and extensively washed with distilled water, and dried at 80°C for overnight. The composition Pt to CeO₂ was varied in weight percentage. The step of preparation of catalysts was illustrated in Fig.3.3



3.2.3 Pt-Rh/C Preparation

PtRh/C electrocatalyst was prepared by using H₂PtCl₆·6H₂O and RhCl₃ as metal precursors with co-reduction procedure. The methods of preparation these catalysts were similar with the procedure to prepare the catalyst as described above. Composition of Pt to Rh was 7:3 at.wt.% ratio and composition Pt to CeO₂ was 2:1 wt.% ratio.

3.2.4 Pt-Rh-CeO₂/C Preparation

PtRhCeO₂/C electrocatalyst was prepared by using H₂PtCl₆·6H₂O and RhCl₃ as metal precursors with co-reduction procedure. Then the pH value of the solution was adjusted to 12 with sodium hydroxide (0.5 M) and the solution was heated under reflux to 160 °C in oil bath, and kept at this temperature for 2 h to obtain brown-black sol. The solution of PtRh then cooled until room temperature and the calculated amount of CeO₂ and carbon Vulcan XC-72 was added to the sol and stirred for another 12 h. The obtained black product was then filtered and extensively washed with distilled water, and dried at 80 °C for overnight. The composition of Pt to CeO₂ was varied in weight percent.

3.3 Physical Characterisation

Physical characterisation of prepared catalysts was carried in order to study a structure, particle size and morphology of the catalysts by using the technique such as : X-ray diffraction, scanning electron microscopy (SEM) , EDX and transmission electron microscopy (TEM)

3.3.1 X-Ray Diffraction

Principle

XRD is mainly used to identify the crystallographic phase that are present in the catalyst. metal clusters of the approximate size of the wavelength of X-ray, are the most interesting to catalysis. As the particle get small compared to the X-ray wavelength, their diffraction get increasingly diffuse. This line broadening is exploited for determination of metal particle size.

Procedure

Measurement is done used instrumentation of Bruker D8 Advance diffractometer equipped with a Cu anticathode, adjustable divergence slit, graphite monochromator on the diffracted beam and proportional detector.

Data acquired at 2θ range from 20 to 65°, scan step of 0.02° and fixed counting time of 6 s for each step.

3.3.2 Scanning Electron Microscopy

Principle

Scanning electron microscopy (SEM) scans over a sample surface with a probe of electrons (5-50 kV). Electrons (and photons), backscattered or emitted produce an image on a cathode ray tube, scanned synchronously with the beam.

Magnification of 20-50,000 are possible with a resolution of about 5 nm [14]. The SEM is a powerful tool for study of overall topography. Sample preparation is not demanding, so that practical catalysts are easily handled.

Procedure

SEM measurement was done by used instrumentation with Hitachi S-4000
Methods of acquisition is amount of catalysts powder was prepared on the carbon
tape sample holder 200 kV voltage, magnification till 15000 X.

3.3.3 Energy Dispersive X-Ray (EDX)

Principle

EDX equipment sensor was coupled with SEM. Prior to the measurements, the
sensor was cooled with the liquid nitrogen

Procedure

Method of acquisition was amount of catalysts powder was prepared on the
carbon tape sample holder 200 kV voltage, magnification till 15000 X. Whilst,
EDX measurement is conducted by using Windshell software and data stored in
ASCII format.

3.3.4 Transmission Electron Microscopy (TEM)

Principle

In Transmission electron microscopy (TEM), 100 kV or higher electrons are
transmitted through a thin spectrum and the scattered electrons magnified with
electromagnetic optics. Image are projected onto fluorescent screen or video
detector with magnification up to 1000,000 at better than 0.5 nm resolution under
ideal condition.

Procedure

TEM measurement was carried out at TU-Muenchen with the instrumentation of
JEOL JEM 2000 EX. Sample preparation on holey carbon Cu-grids, TEM
operating at 120 kV ,bright field, dry preparation on grid data storage with 150 kX
magnification.

3.4 Half cell electrochemical measurements

All electrochemical measurements were performed in electrochemical cell as shown in the following schematic diagram:

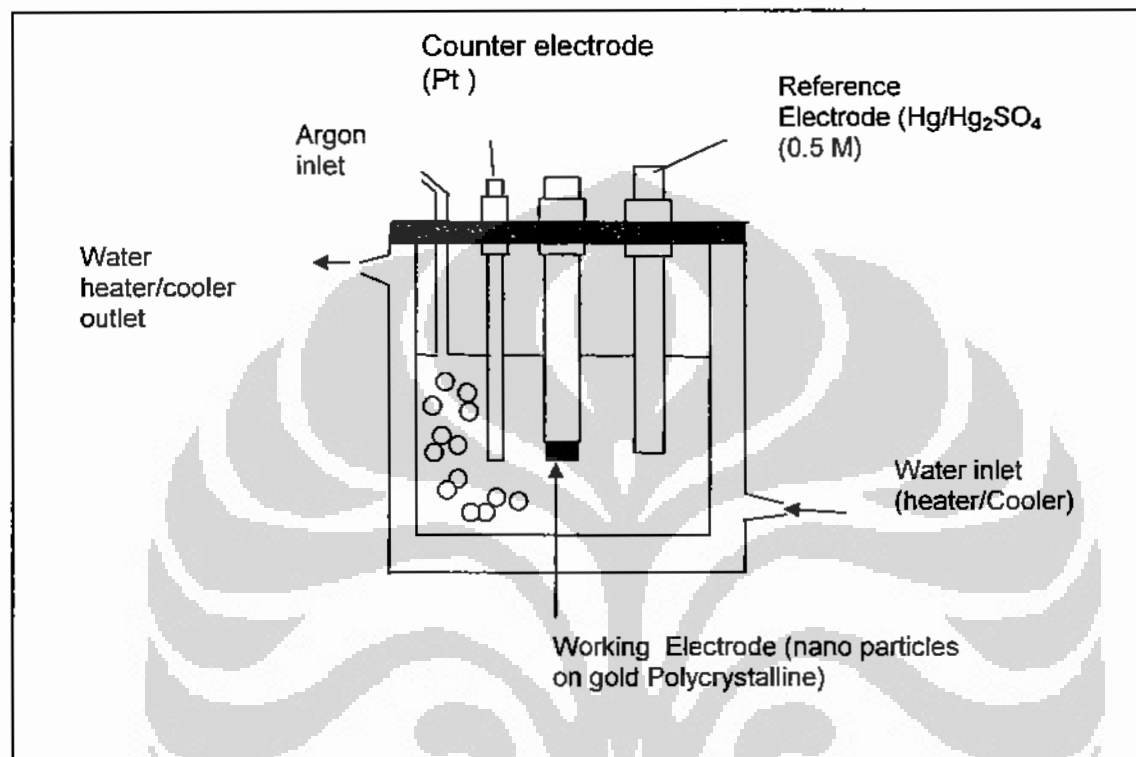


Figure 3.5. Schematic representation of electrode in electrochemical cell

The cell consists of three electrode: working electrode (WE), counter electrode (CE) and reference electrode (RE) . Working electrode was made from polycrystalline gold with smooth surface and nanoparticle of catalyst was deposited on it. The reference electrode compartment is connected to the counter electrode and working electrode compartment by a luggin capillary. In this study RE used was Hg/HgSO₄ (0.5 M) for acidic medium and Hg/HgO (NaOH 0.1 M) for alkaline medium.

This electrochemical cell was connected to the potentiostat to apply potential and current to the WE. Working principle of the potentiostat was that it observes the potential difference between the WE and RE, and pumps current through the CE, such that the potential difference between the WE and RE remains constant at some predefined value set by the user. This value can be anything depending on

the nature of the experiment in concern. If the potential of the working electrode was cycled between some upper and lower limit with a defined potential scan rate, and corresponding current was measured, then such an experiment is called cyclic voltammetry. This technique is most frequently in electrochemical experiments. During the experiment, the cell temperature was controlled by Julabo thermostat.

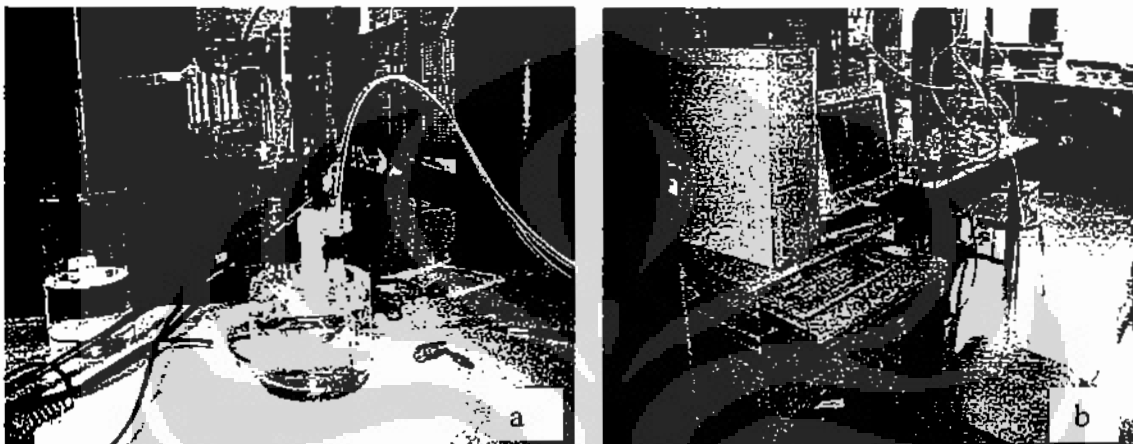


Figure 3.6. Electrochemical cell setup (a) and Potentiostat (b)

3.5 Differential electrochemical mass spectrometry (DEMS) measurement of fuel cell

DEMS measurement was aimed to measure the activity and selectivity to CO_2 formation in ethanol electro-oxidation. The main equipment in this setup is consisting of fuel cell, potentiostat, mass spectrometer and computer.

3.5.1 Description of DEMS Setup

The DEMS setup that consisted of two differentially pumped chambers, a Balzers QMS 200 mass spectrometer, AGEF potentiostat and computerized data acquisition system. The DEMS sensor was located at the outlet channel of anode compartment, it consist of a cylindrical detection volume with a diameter of 7 mm and a height of 2 mm through which anode outlet flow passes. This volume is separated from the vacuum system of the mass spectrometer by a Microporous Teflon membrane (Schleicher & Schuell, TE30) with a pore size of 0.02

micrometer and a thickness of 110 micrometer. The membrane is supported by a Teflon disc of 2 mm in diameter, with holes.

The fuel cell consisted of two stainless steel plates with integrated serpentine medium distribution channels. Six threaded studs and nuts held the two plates together. The fuel cell can be operated in both modes half-cell and full cell. Generally during the investigation of anode it is used as a half-cell.

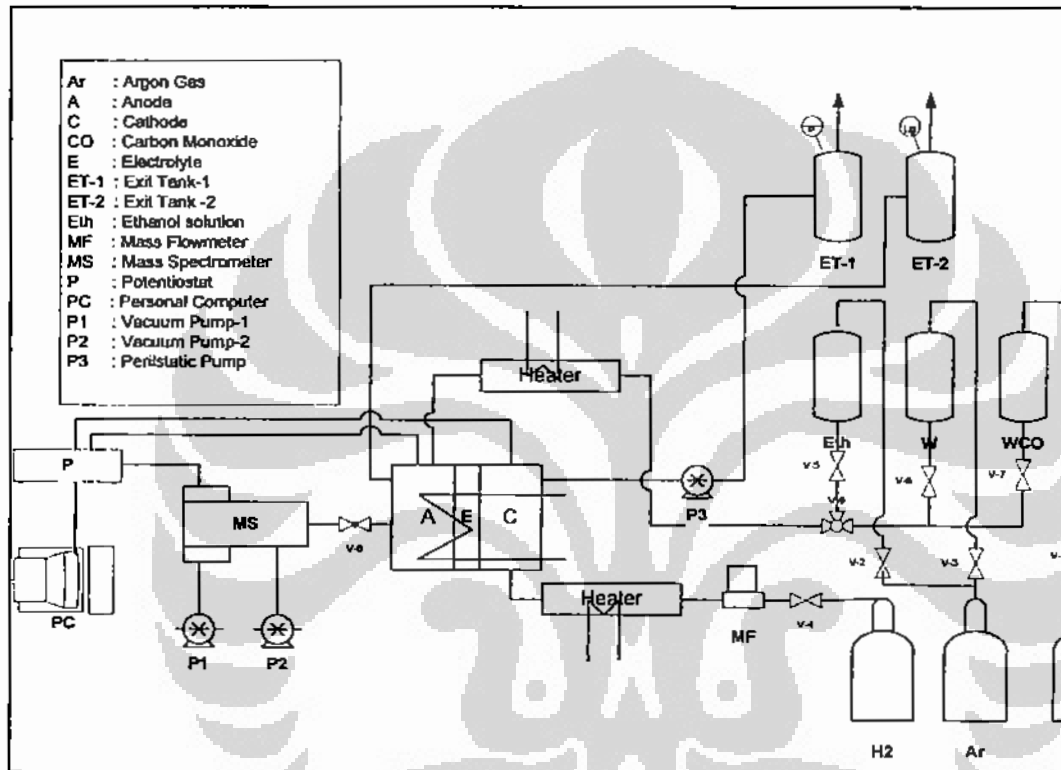


Figure 3.7 Schematic diagram of DEMS setup

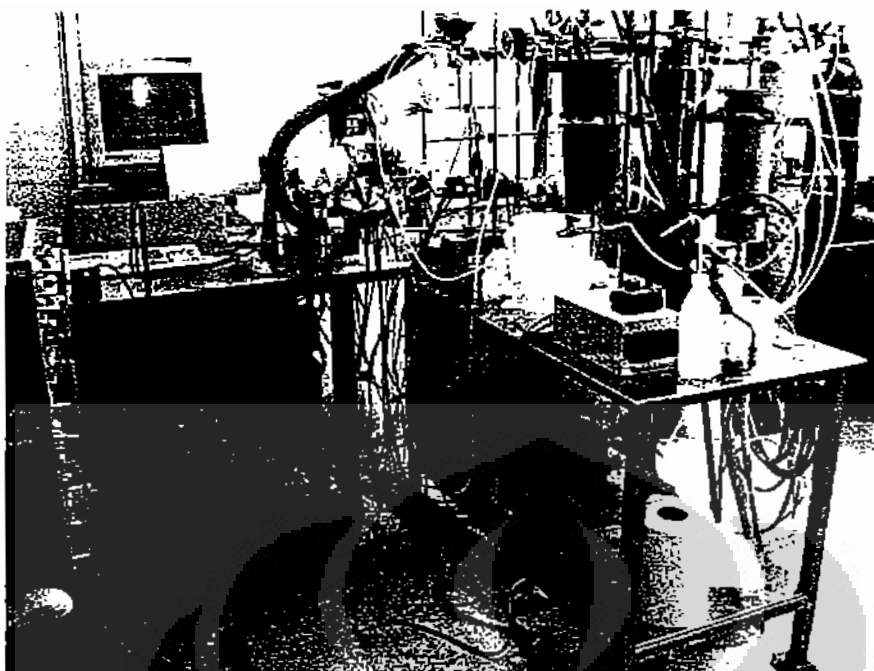


Figure 3.8 Picture of differential electrochemical mass spectrometry (DEMS) setup

Cathode with Pt loading ($2.5\text{mg}/\text{cm}^2$) and continuous hydrogen flow works as counter and reference both. Potential of the cathode is assumed to be same as of the reversible hydrogen electrode (RHE). All potential are reported in reference to this.

The anode flow system comprised of a tank filled with ethanol solution and a tank filled with water. These tanks are connected via heated tubes with the three-way valve at the fuel cell inlet. The ethanol solution and the Millipore water are deaerated with argon gas for 40 minutes. A dosing pump between the cell outlet and exit tank controls the flow of ethanol solution and water through the cell. To avoid the gas bubble formation due to the large gas production and low solubility of CO_2 at elevated temperature, the anode flow system is pressurized at 3 bars overpressure. The cathode overpressure is kept at 1 bar to limit the crossover of H_2 to anode side. The permeation of alcohol to the cathode side does not affect the potential of the cathode (which is reference electrode also).

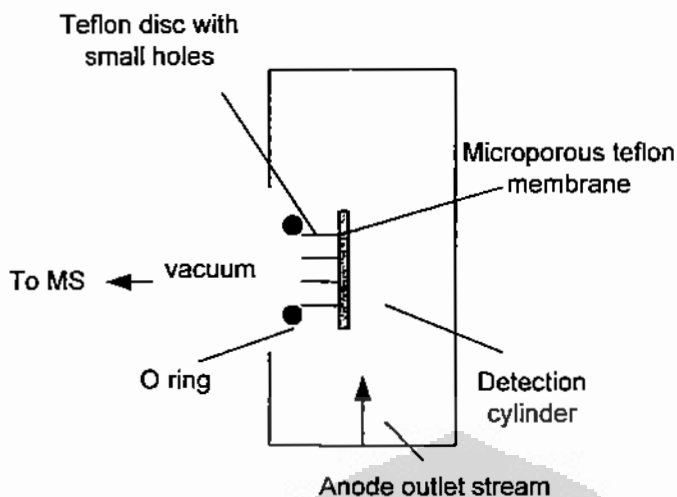


Figure 3.9 Schematic diagram of MS setup

Connection of fuel cell to mass spectrometer (MS) was presented in Fig.3.9. Porous Teflon membrane was used as window between cell and MS. After the connection of the cell to the MS, a large part of the species produced or consumed at the interface is entering the MS through the pores of the membrane, a part of the species being ionized in the ion source of the MS.

3.5.2 Preparation for DEMS measurement

Electrolyte materials, which are used in this experiment, was Nafion® 117, carbon paper was product from Toray TGPH 060 not wet proofing. The described cleaning procedure of the membrane is repeated separately with 1 M sulfuric acid, 10% hydrogen peroxide and then in 1 M sulfuric acid. The membrane samples were then boiled in deionized water for one hour, before being stored in deionized water at room temperature for future use. Ethanol (Li Chrosolv) is obtained from Merck. Carbon support materials used were Carbon Vulcan XC-72 from Cabot Co. Prior to experiment, water and ethanol solution are deaerated with high purity Argon. Whereas CO saturated water is prepared by bubbled water with CO for 40 minutes. CO stripping is carried out at temperature 50°C and all of DEMS experiment is carried out at temperature 90°C.

This DEMS measurement is carried out in the fuel cell setup with cell dimension 1.2 cm² Experiment carried out by potentiodynamics and potentiostatics with scan rate 5 mV/s and ethanol flow rate 5 ml/min.

3.5.3 Membrane Electrode Assembly (MEA)

The membrane electrode assembly (MEA) was prepared by following procedure: catalyst ink was prepared by mixing the required amount of catalyst powder with 20 % Nafion® solution (Du Pont) to give 30% wt. of Nafion®, and then diluted with a mixture of millipore™ water and 2-propanol. The resulting ink then placed in an ultrasonic bath until the catalyst powder had fully dispersed. This ink then sprayed onto a piece of carbon paper which was kept at 110°C throughout the process, in order to assist the binding of the catalyst to the backing layer. The spraying machine consisted of motorised X-Y table controlled by a CNC automation controller as shown in Fig.3.10 (b). The catalysts inks (anode and cathode catalysts) were sprayed onto carbon paper with 5 cm² area. For installation in fuel cell setup for DEMS measurement purpose, these catalysts layer on carbon paper cut by dimension of 1.1 cm x 1.1 cm. The catalyst layer on carbon paper then sandwiched with porous carbon paper to make the membrane electrode assembly (MEA) by pressing at 1 kNcm⁻², and 140°C for 5 minutes as shown in Fig.3.10 (a). The catalysts for anode were Pt/C (Alfa Aesar- JM) as reference, Pt-CeO₂/C (A), Pt-CeO₂/C (B), Pt-Rh-CeO₂/C (A&B). All of catalysts have designed with Pt weight percentage 20%. Meanwhile, catalyst employed for cathode was 40% Pt/C (ETEK Inc.). The loading of catalyst (platinum loading) for anode side was targeted 0.8 mg/cm² and for cathode side was 2.5 mg/cm².

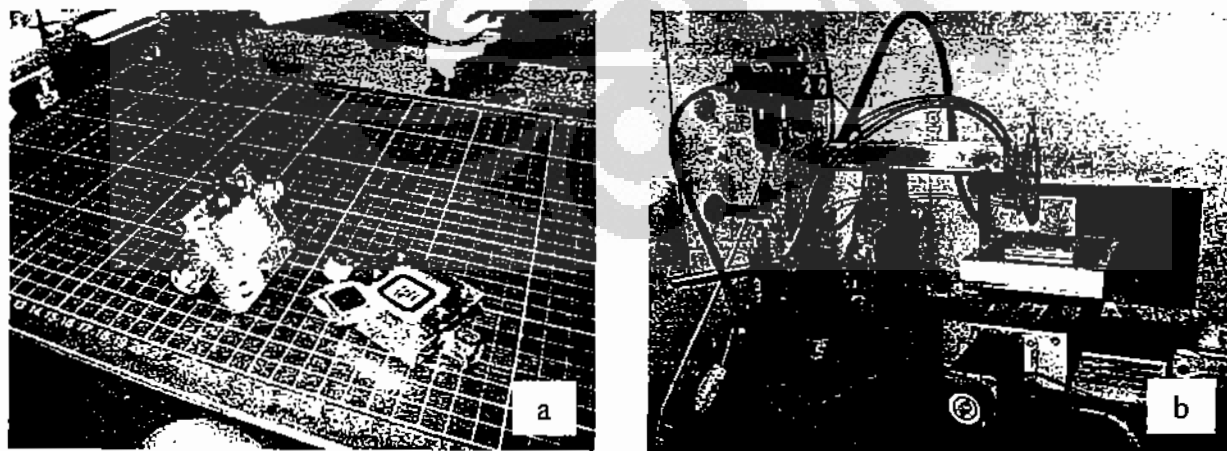


Figure 3.10. (a) MEA of DEFC and (b) catalyst spraying device

3.5.4 Calibration of DEMS System

The main products of ethanol electro-oxidation are carbon dioxide, acetaldehyde and acetic acid. From those three products, they were only carbon dioxide and acetaldehyde that can be monitored by DEMS measurement because its high volatility. The main problem in DEMS measurement is because the mass number of both CO_2 and CH_3CHO is the same at 44. To monitor both together is not possible at $m/z = 44$. To solve this problem, Fujiwara et al.[4], used deuterated ethanol ($\text{CD}_3\text{CH}_2\text{OH}$) for determining reaction products that had same mass number. Due to the high cost of this material, extensive utilization is limited. To avoid interference between CO_2^+ and CH_3CHO^+ ion current (both at $m/z = 44$), which are the major ethanol electrooxidation products, carbon dioxide and acetaldehyde was monitored at $m/z = 22$ and $m/z = 29$ respectively; AS reported by Wang et al [5].

The calibration of DEMS for CO_2 is performed with H_2 oxidation current interference and potentiostatic bulk CO oxidation.

3.5.5 H_2 Oxidation Current Interference from cathode to anode

Measurement of H_2 oxidation for DEMS calibration is aimed to take into account of H_2 that diffuse from cathode to anode. This H_2 diffusion could increase the faradaic current around 0.25 mA-1 mA. This increasing current if didn't take into account will affect an error in calculation of faradaic current in DEMS measurement. Typical H_2 interference measurement result can be shown in Fig.3.11

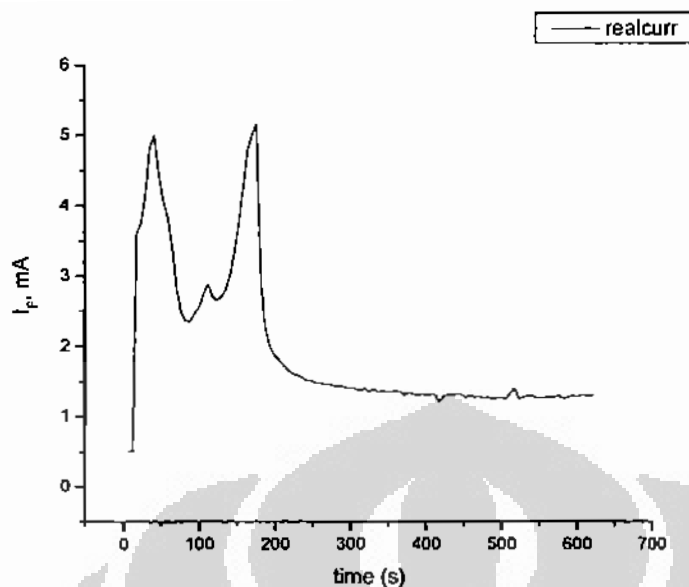


Figure 3.11. Faradaic current as function of time from H₂ interference

3.5.6 Potentiostatic bulk CO oxidation for calibration

Calibration of DEMS for CO₂ is done by potentiostatic bulk CO oxidation. The result of typical Potentiostatic bulk CO oxidation is shown in Fig.3.12. This Faradaic current and ion mass signal for CO₂ is used for calibration of DEMS for CO₂

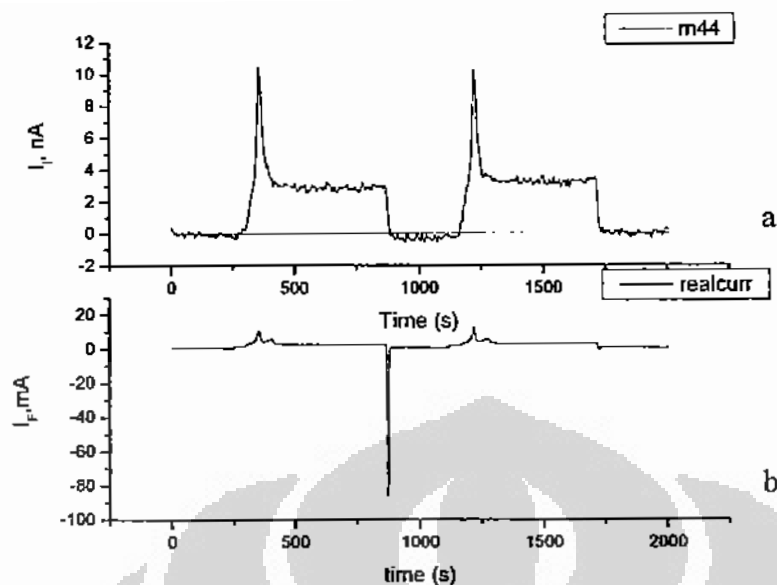


Figure 3.12 (a) m/z 44 ion current (CO_2) and (b) current as function of time on CO potentiostatic for calibration

The calibration constant is calculated using the formula:

$$K_F^* = 2 \cdot I_{MS} / I_F \quad (1)$$

where I_{MS} is the steady state ion current for $m/z = 22$, and I_F is the corresponding Faradaic current.

In order to measure the current efficiency of CO_2 formation during ethanol oxidation, we performed a potentiostatic oxidation of ethanol at various potentials. Calibration constants were obtained for all temperatures separately. Then the CO_2 current efficiency can be calculated using the formula:

$$(\text{CO}_2 \text{ current efficiency}) = 6 \cdot I_{MS} / I_F K_F^* \quad (2)$$

Where I_{MS} is the steady state ion current for $m/z = 22$ for ethanol oxidation, and I_F is the corresponding Faradic current.

3.6 Single cell performance test

Although cyclic voltammetry is useful enough to check the activity of an electrocatalyst, in this research work was necessary to observe the performance of the catalysts in the complete fuel cell arrangement. It was because of the working conditions such as temperature, pressure and fuel flowrate are crucial to determine the real performance of the system. Single cell performance test is conducted by testing at open circuit potential (OCP) and continued by varied with the load (current). As anode catalysts are used prepared catalysts: 20% PtCeO₂/C, 20% PtRhCeO₂/C and 20% Pt/C (Alfa Aesar-JM) as reference. Meanwhile, 40% Pt/C (EOTEK) is used as cathode catalyst. The fuel cell which is used for single cell testing was same cell for DEMS measurement, with stainless steel bipolar plate and cell area of about 1.2 cm². Performance test carried out at operating temperature: 90 °C, ethanol solution flowrate: 5 ml/min, O₂ flowrate : 30 sccm and both anode and cathode pressure were 1 bar. Apparatus setup of single cell was shown in Fig.3.13.



Figure 3.13 Performance test of single cell

4 RESULT AND DISCUSSION

The result of experiments will be presented and discussed in the following section. The discussion was emphasized on the beneficial effect on ethanol electro-oxidation when adding of Rhodium (Rh) and cerium oxide/ceria (CeO_2) to the Pt catalyst.

4.1 Physical characterization of catalysts

Physical characterization of catalysts was conducted in order to investigate the structure of catalysts, morphology of catalysts and particle size of catalysts.

4.1.1 Structure of catalysts

Fig 4.1 show X-ray diffraction pattern (XRD) of in-house ceria (denoted A) which was prepared by precipitation method and calcined at temperature of about 500°C . For comparison purpose, we also characterized the commercial ceria which was purchased from Alfa Aesar-Johnson Matthews (denoted B). The characteristic peaks of both ceria were located at 2θ : 28.5° , 33.1° , 47.5° , 56.3° and 59.01° . These patterns are corresponding to $\{111\}$, $\{200\}$, $\{220\}$, $\{311\}$ and $\{222\}$ planes, respectively. These patterns match well with the peaks of cubic fluorite CeO_2 crystal structure in JCPDS database. The picture shows that in-house ceria pattern was broader than the pattern of ceria commercial and from XRD patterns also can be seen that in-house ceria was in the form of crystallite, same as commercial ceria. This means that either in-house or commercial ceria can act as oxygen storage capacity (OSC) in the catalyst. The mean crystallite size of both kinds of ceria was estimated by Scherer formula and was listed in Table 4.1. Both of XRD patterns of CeO_2 , in-house and commercial were shown that the dominant lattice fringes were from $\{111\}$ plane. TEM analysis in the present study shows that there were also some amorphous ceria clusters in the nano-particles of CeO_2 . However

these fine ceria clusters might be very sensitive to the reducing atmosphere and structural changes might occur.

It is well known that there were three low-index planes in the ceria fluorite cubic structure, namely the very stable and neutral {111} plane, the less stable {110} plane, and the higher-energy {001} plane [33]. Thus a stable Ce^{4+}/Ce^{3+} cycle can be maintained to generate better catalytic performance during reaction.

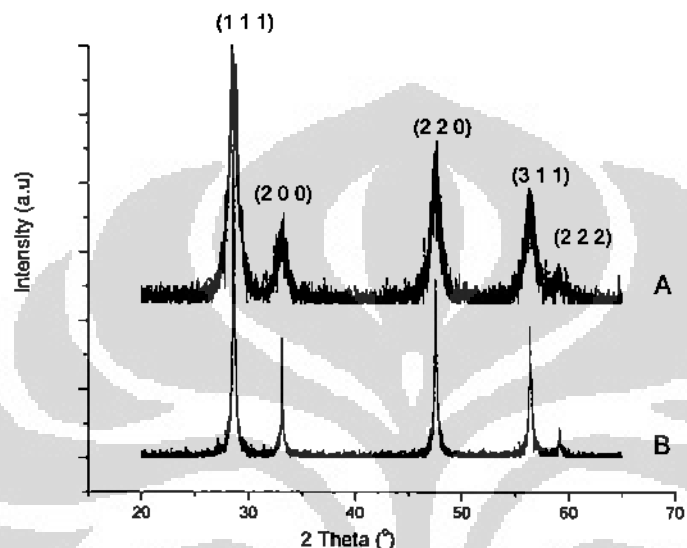


Figure 4.1 X-Ray Diffraction pattern of in-house CeO_2 (A) and Commercial CeO_2 (B)

Fig. 4.2 shows the X-Ray diffraction pattern of $PtCeO_2/C$ (CeO_2 (A)) and $PtRhCeO_2/C$ (CeO_2 (A)) catalysts. First peak at $2\theta \approx 23^\circ$ originates from the carbon support (Vulcan XC-72). Therefore the peak at $2\theta \approx 40.04^\circ$ is reflection of the face centered cubic (f.c.c) crystal lattice of Pt {111}.

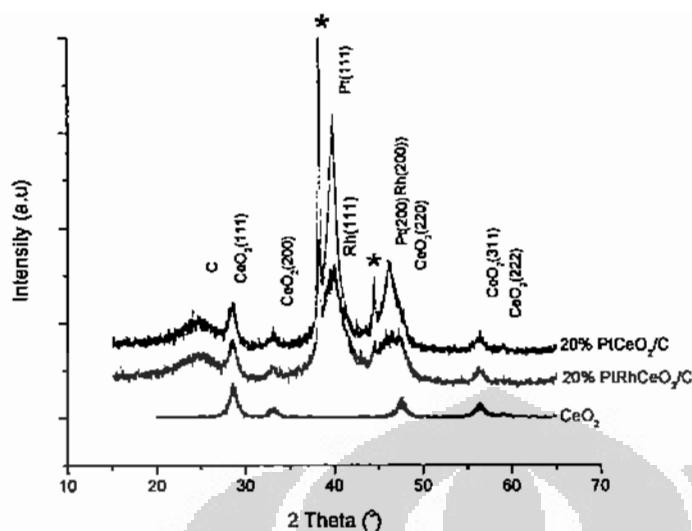


Figure 4.2 X-Ray diffraction pattern of PtCeO₂/C and PtRhCeO₂/C using in-house CeO₂, weight ratio Pt to CeO₂, 2:1

The peak patterns of Pt {111} and Pt {200} were at 40.04° and 46.5° respectively, whereas for Rh {111} and Rh {200} the peaks were at 40.7° and 47.4°. Since the peak pattern position is close among others, therefore the peak of Pt (200) probably merged with the peak of CeO₂(220) in the PtCeO₂/C catalyst, while the peak of Pt(200) merged with the peak of Rh (200) and CeO₂(220) in the PtRhCeO₂/C catalyst. Both of metals peak patterns (Pt and Rh) were detected in the PtRhCeO₂/C (A) catalyst. The peaks indicated with a star (*) in Fig.4.2 and Fig.4.3 was due to the sample holder.

Therefore, as a promoter in these catalysts, ceria peak pattern was visible in all of the synthesized catalysts (PtCeO₂/C and PtRhCeO₂/C).

The X-Ray diffraction patterns in Fig. 4.3 give evidence for the presence of Pt and Ceria in the PtCeO₂/C (B) catalyst. However, these patterns give no evidence for the presence of Pt or Rh in the PtRhCeO₂/C (B), it might be that the particles are too small or the amount is not enough to be detected [35-37].

Although the Pt and Rh in PtRhCeO₂/C (B) was not detected from XRD pattern, the presence of this Rh and Pt elements will be proved later on EDX characterization result and normal cyclic voltammogram for both metal catalysts.

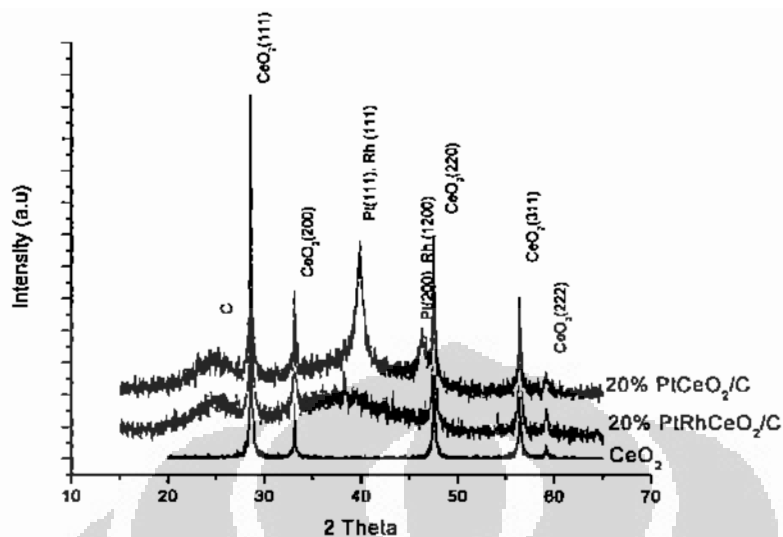


Figure 4.3 X-Ray Diffraction pattern of PtCeO₂/C and Pt₇-Rh₃-CeO₂/C with commercial CeO₂, weight ratio Pt to CeO₂, 2:1

The crystallite size (d_{XRD}) of the samples was estimated from XRD patterns by applying the full-width half-maximum (β) of the characteristic {1 1 1} peak to the Scherrer equation (4.1).

Scherrer equation:

$$d = \frac{K\lambda}{\beta \cos\theta} \quad (4-1)$$

where:

d is the mean crystallite size and β the width (in rad) of the peak at the half height (peak height is calculated from a baseline).

K = Constant

λ = wave length for X-Ray (0.154184 nm)

θ = the diffraction angle for the {111} plane

The estimation crystallite size by Scherrer formula (d_{XRD}) and average particle size from transmission electron microscopy (TEM) characterization result (d_{TEM}) was summarized in the Table.4.1. The values of the mean particle size obtained by TEM analysis are almost in good agreement with those calculated from the XRD results.

Table 4-1 mean crystallite size estimation (XRD) compared to TEM measurement result

Technique	CeO ₂	CeO ₂	20% PtCeO ₂ /C	20% PtCeO ₂ /C	20% PtRhCeO ₂ /C	20% PtRhCeO ₂ /C
	(A)	(B)	(A)	(B)	(A)	(B)
	d(nm)	d(nm)	d(nm)	d(nm)	d(nm)	d(nm)
XRD	9.1	19	3.1	3.4	2.7	-
TEM	8.5	20	2.9	3.2	2.6	2.0

4.1.2 Morphology of catalysts

Surface morphology of the catalyst was characterized by scanning electron microscopy (SEM) and Energy Dispersive of X-Ray (EDX). Fig.4.4 (a) shows the SEM picture and EDX spectra for PtCeO₂/C (A) catalyst, while Fig. 4.4 (b) shows the SEM picture and EDX spectra for PtCeO₂/C (B) catalyst. The white island in this picture shows the CeO₂ existence and distribution. The presence of ceria modifier on this surface was proved by the EDX spectra in Fig.4.4 (a). Distribution of the ceria commercial in the PtCeO₂/C(B) was similar to the PtCeO₂/C(A). However, the crystallite size for ceria commercial seems rather bigger than in-house ceria. From the SEM and EDX pictures in Fig 4.4 (a)& (b) can be seen that all of the component of PtCeO₂/C catalyst was exist.

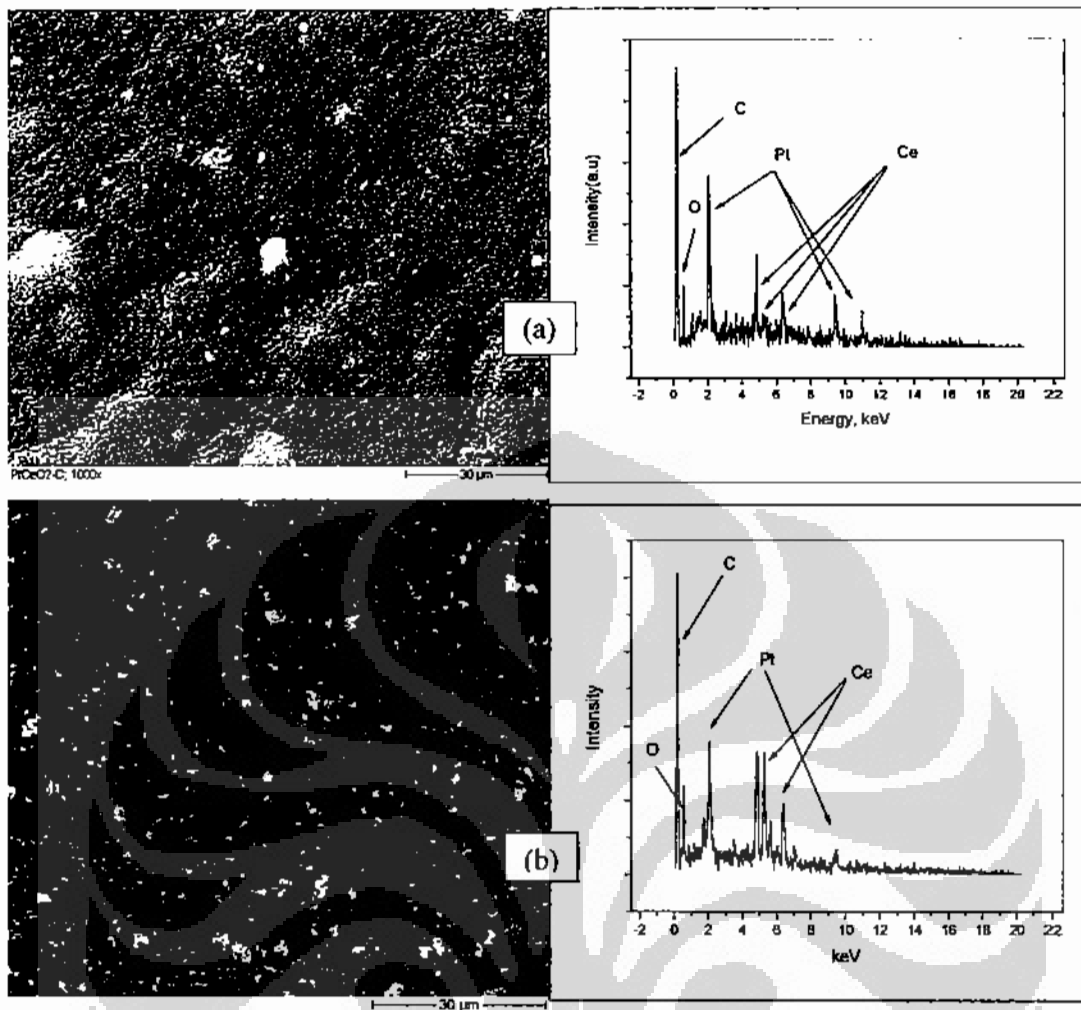


Figure 4.4 Pictures of (a) SEM & EDX of PtCeO₂/C (A) & (b) SEM & EDX of Pt-CeO₂/C (B) catalysts

SEM and EDX pictures of PtRhCeO₂/C (A) and PtRhCeO₂/C (B) catalysts was presented in Fig.4.5 (a) and (b). The white island in this picture indicated the ceria compound, while the metal catalyst of Pt and Rh were dispersed on catalyst. The presence of the Pt and Rh metal catalyst was proved by the EDX-spectra in Fig.4.5 (a) and (b). This EDX-spectra indicated that all of catalyst elements (Pt, Rh, Ce, O, C) was also detected by this technique for qualitative measurement. This SEM & EDX results can be used to verify the presence of Pt and Rh metal catalyst which was in the previous XRD results could not be detected.

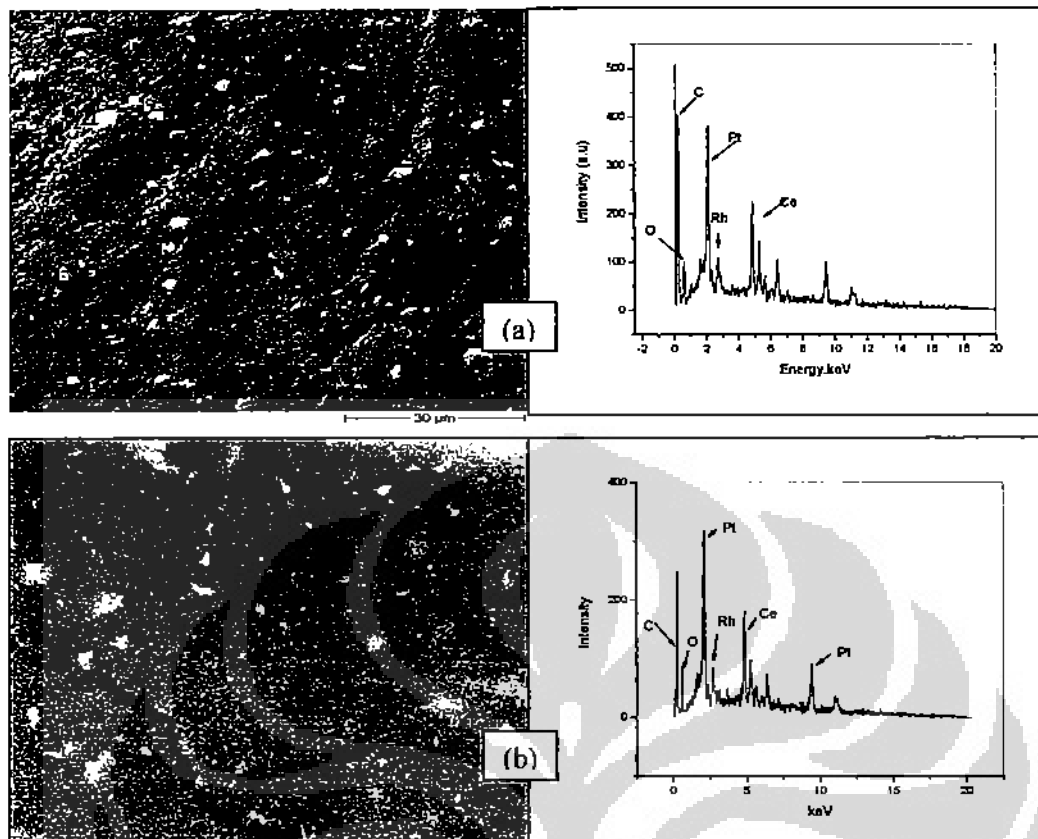


Figure 4.5 Pictures of (a) SEM & EDX of PtRhCeO₂/C (in-house CeO₂) & (b) SEM & EDX of Pt-RhCeO₂/C (Commercial CeO₂) catalysts

4.1.3 Particle Size of Catalysts

Fig.4.6 (a) shows the high resolution-transmission electron microscopy (HRTEM) image of in-house CeO₂ nano-particle. It shows that the d-spacing for lattice fringes in that image are 3.2 Å which correspond to the {111} facet of cubic CeO₂ crystal structure. The mean particle size of CeO₂ nano-particle was about 8-9 nm. The mean particle size was obtained by measuring the diameter of a sufficient number of particle to ensure a good statistical representation.

Fig. 4.6 (b) presents the particles distribution for nano-particles of 20% PtCeO₂/C (A).

In-set picture (Fig. 4.6 (b)) shows a histogram of particle size distribution of catalyst. The mean particle size of the PtCeO₂/C (A) catalyst was 2.9 ± 0.3 nm

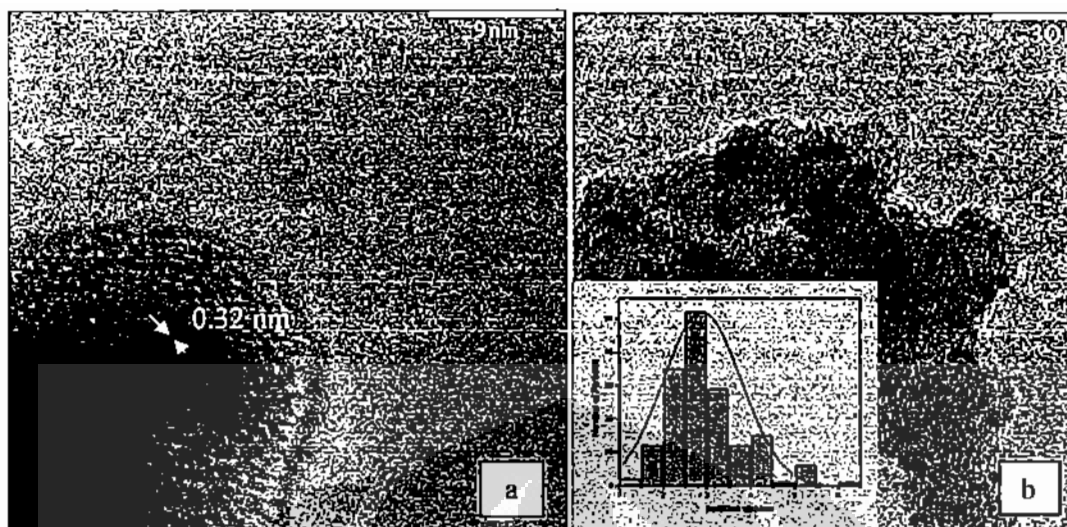


Figure 4.6 TEM image of (a) in-house-CeO₂ (HRTEM) (b) 20%Pt-CeO₂/C (A) catalyst

Estimated mean crystallite size by Scherer formula of XRD result measurements compared to the TEM measurement result for the catalysts was summarized in Table 4.1. TEM picture shows the particle of catalyst was well-dispersed with a weak agglomeration.

4.2 Electrochemical characterization of catalyst

Electrochemical characterization result in half cell setup will be presented in the following section. The electrochemical characterization comprise of the several technique, such as: normal Cyclic Voltammetry (CV), Chronoamperometry, CO stripping voltammetry and cyclic voltammetry in presence of ethanol. First, we characterized the catalyst of PtCeO₂/C (A) to look for the best composition of the Pt to CeO₂ by using normal CV and chronoamperometry technique. Similar characterization also performed to the PtRh/C catalyst. The best composition of Pt to CeO₂ and Pt to Rh was used in the catalyst synthesizing of PtRhCeO₂/C. Electrochemical characterization was performed in the acidic medium (H₂SO₄ solution) and alkaline medium (NaOH solution).

4.2.1 Electrochemical characterization in acid medium

Electrochemical characterization was carried out to all of catalysts in order to investigate its activity in ethanol oxidation in half cell setup.

4.2.1.1 Electrochemical measurement over 20% PtCeO₂/C catalyst

Fig. 4.7 shows the cyclic voltammogram of PtCeO₂/C catalysts with the targeted composition of Pt to CeO₂ was 1:1, 2:1 and 3:1 in weight ratio. This CV's obtained after cycled many times until the CV picture was reproducible. CV picture is recorded at the potential window of 0.0 V – 1.0 V vs. RHE. The graph in Fig.4.7 was a typical feature of the platinum in acid medium. CeO₂ it self hasn't any feature in CV, hence the CV for PtCeO₂/C catalyst was dominantly by platinum feature.

First region of potential window up to 0.25 V vs RHE is known as a hydrogen region, and between 0.25 – 0.5 V vs RHE is known as double layer region. The last region of this CV is known as oxygen region. If the CV continuing to the higher potential, the O₂ evolution will be taken place at potential of about 1.5 V vs. RHE..

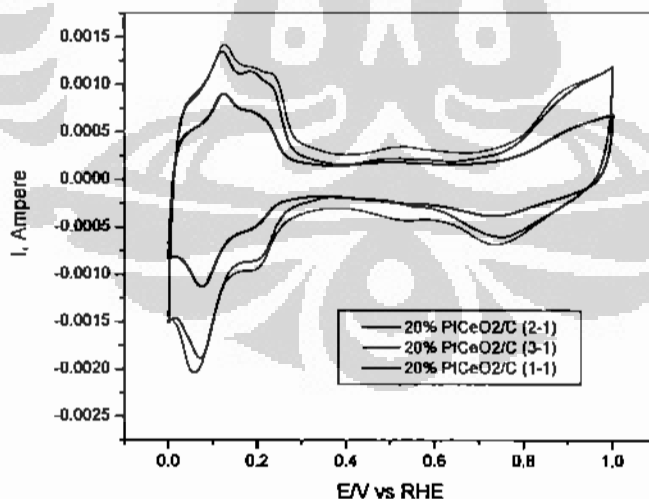


Figure 4.7 Cyclic Voltammogram of PtCeO₂/C varying with the composition Pt to CeO₂ at 30°C, scanrate 10 mV/s, 0.5 H₂SO₄

Altering of CeO_2 addition in the catalyst will affect the double layer splitting which is presented in Fig. 4.7 in normal CV. PtCeO_2/C catalyst with the composition 3:1 provided broader double layer splitting than with the composition of 1:1 and 2:1. This result in CV could be affected by property of ceria as an electronic insulator.

CeO_2 is a good supporting material for catalyst which is commonly used in the heterogeneous catalysis especially in three way catalyst [35-37]. However, direct utilization of ceria as support of an electrocatalyst will fail most likely [26], due to the limited electronic conductivity of the material. In order to determine of best catalyst composition with resulting of the best in catalyst activity, at the beginning of the research work we carried out variation of the Pt to CeO_2 composition. PtCeO_2/C with the composition of weight ratio Pt to CeO_2 : 1:1, 2:1, and 3:1 . All of those catalysts were synthesized by the same colloidal method (ethylene glycol reduction method).

After reproducible CV obtained, electrochemical characterization was continued by chronoamperometric measurements. The purpose of the measurement by using this technique was to investigate the current output at certain potential as function of time. Fig. 4.8 shows the current vs. time for PtCeO_2/c with the different in composition Pt to ceria.

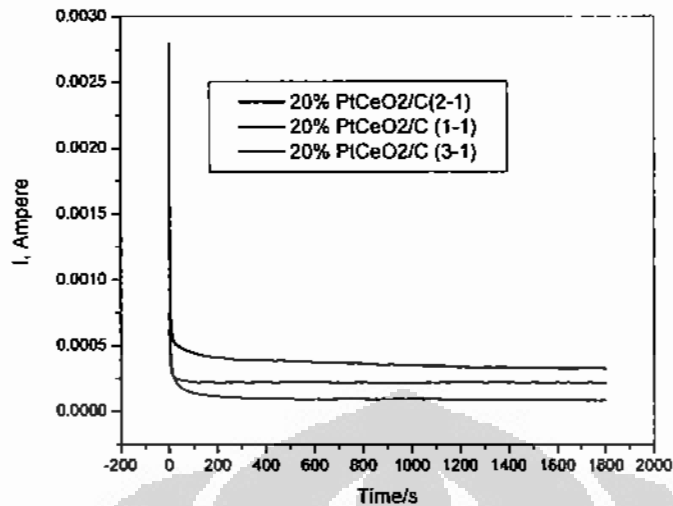


Figure 4.8 Chronoamperometry of PtCeO₂/C [A] varying with Pt to CeO₂ composition, at 0.6 V vs RHE, scanrate 10 mV/s at 30°C.

The potential was stepped from 0 V vs RHE to the 0.6 V vs RHE with scan rate 10 mV/s and at temperature 30 °C for 30 minutes. It was clearly seen that 20% PtCeO₂/C with the composition Pt to CeO₂ (2:1) provided higher current than the composition of 1:1 and 3:1. Increasing of the current of this catalyst composition associated to the presence and appropriate amount of CeO₂ modifier in the catalysts. Hence, modified ceria in the catalyst improved its activity without significant reduced an electrical conductivity of catalyst.

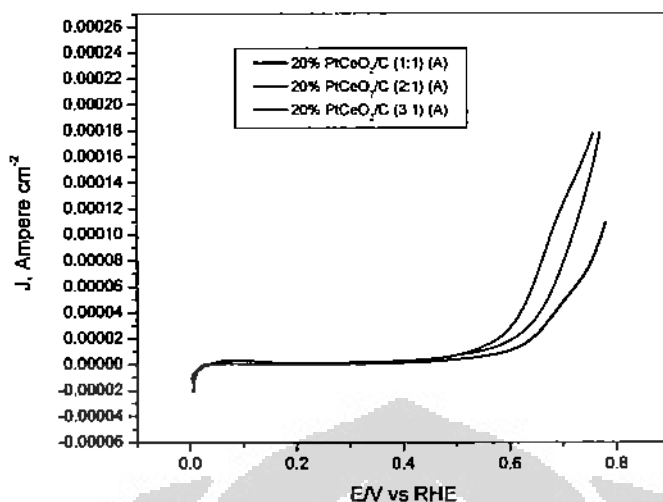


Figure 4.9 Ethanol electro-oxidation on PtCeO₂/C at 30°C, scanrate 10 mV/s, 0.5 H₂SO₄ and 1 M ethanol

Fig.4.9 shows the ethanol electro-oxidation reaction (EOR) over PtCeO₂/C catalysts with the composition Pt to CeO₂ was 1:1, 2:1, 3:1 (weight ratio). The results in Fig.4.9 was consistent to the previous result in chronoamperometry measurement that the catalyst with the composition Pt to CeO₂ (2:1) provided the best performance in EOR. The better performance in EOR is indicated by onset oxidation potential resulted by 20% PtCeO₂/C (2:1) (A) which is shifted to more negative potential then the other compositions. It means that PtCeO₂/C (2:1) (A) catalyst has a better activity in ethanol oxidation reaction compared to the other composition. Base on these results, we used this composition of Pt to CeO₂ (2:1) for further investigation.

4.2.1.2 Electrochemical measurement over 20% PtRh/C catalysts

In this experiment, we tried to optimize the composition of Pt to Rh in carbon supported binary PtRh catalyst. The aim of this experiment was to look for the best composition of Pt to Rh in binary/bimetal PtRh catalyst before we added ceria in the best composition catalyst. We varied Pt to Rh composition with the variation of Pt to Rh by 1:1, 4:1 and 7:3 atomic weight ratio.

All of these catalysts compositions performed in electrochemical cell by measured the normal CV, chronoamperometry and electro-oxidation reaction (EOR) or CV in presence of 1.0 M ethanol solution. Figure 4.10 shows the normal cyclic voltammogram of 20% PtRh/C in acid medium. It can be seen that feature of PtRh/C catalyst was bit different with the platinum feature in Fig.4.7, especially in the hydrogen region. In the CV feature of PtRh/C the two peak of hydrogen region was not clearly seen, and completely disappear on Pt₁Rh₁//C catalyst. It could be that in the composition of Pt₁Rh₁, platinum metal catalyst was not dominant anymore and the new dominant feature of CV was PtRh alloy or Rh metal catalyst.

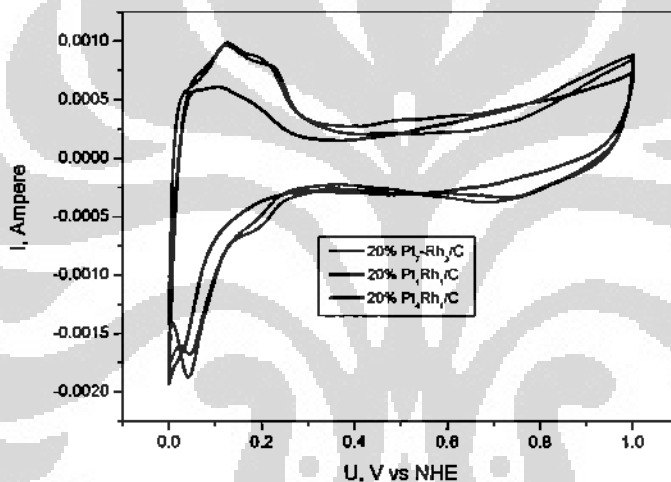


Figure 4.10 CV of PtRh/C catalyst in acid medium (0.5 M H₂SO₄) at 30°C , scanrate 50 mV/s

Fig.4.11 presents the chronoamperometric result of binary 20% PtRh/C at different atomic compositions of Pt to Rh. From the Fig.4.10 can be seen that the PtRh/c with the atomic composition ration 7:3 provided higher current compared to others. It was close in agreement with the result reported by J. P. I. de Souza et al [12], that they obtained optimum atomic ratio Pt to Rh at about 73:27.

Chronoamperometry result was match well with the result of ethanol oxidation reaction (EOR) as shown in Fig. 4.12. There were some improvements in EOR result which was indicated by onset potential shifting to more negative

over $\text{Pt}_7\text{Rh}_3/\text{C}$ than $\text{Pt}_4\text{Rh}_1/\text{C}$ and $\text{Pt}_1\text{Rh}_1/\text{C}$. The onset potential improvement was rather low between $\text{Pt}_7\text{Rh}_3/\text{C}$ than $\text{Pt}_4\text{Rh}_1/\text{C}$ catalyst.

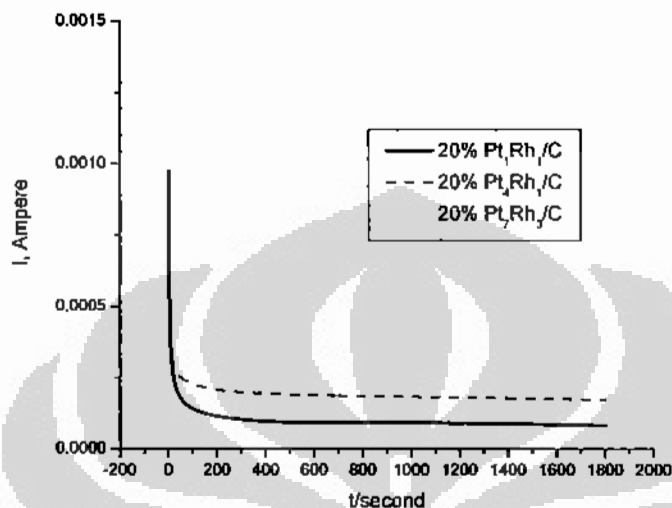


Figure 4.11 Chronoamperometry of PtRh/C catalysts varied with composition ratio Pt to Rh (1:1, 4:1, 7:3) in acid medium + 1 M ethanol at temperature 30°C , scanrate 10 mV/s.

However, Faradaic current both of catalyst was significantly different started from potential 0.6 V vs RHE, that $\text{Pt}_7\text{Rh}_3/\text{C}$ was yielded significant current improvement compared to $\text{Pt}_4\text{Rh}_1/\text{C}$ and $\text{Pt}_1\text{Rh}_1/\text{C}$ catalyst.

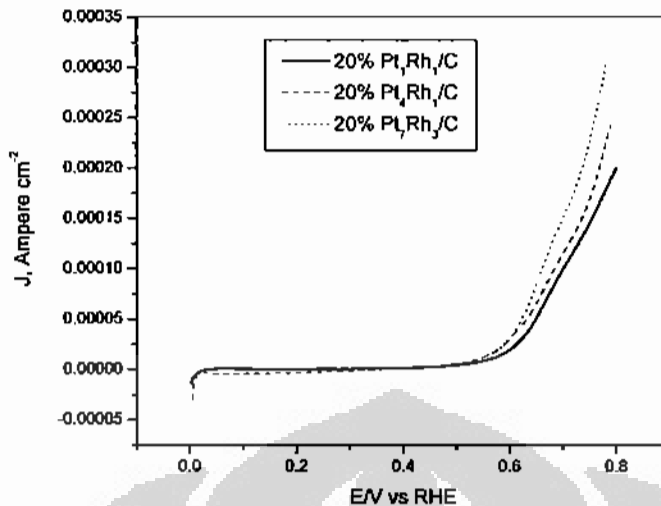


Figure 4.12 Ethanol electro-oxidation over PtRh/C catalysts varied with the composition Pt to Rh, 1:1, 4:1 and 7:3 atomic weight %, at temperature 30°C, scanrate 10 mV/s

After the best composition of Pt to CeO₂ and Pt to Rh were determined in this experiment, the following experiments is to carry out electrochemical characterization to the as-prepared catalysts by using in-house CeO₂ which denoted (A) and commercial CeO₂ which denoted (B).

4.2.1.3 Electrochemical measurement over PtRhCeO₂/C catalysts

Fig.4.13 shows the cyclic voltammogram (CV) of Pt/C (ref), PtCeO₂/C (A) & (B) and PtRhCeO₂/C (A) & (B) catalysts. From this CV we could interpret that addition double layer splitting both catalysts with and without ceria almost similar. This mean by addition of this amount of ceria modifier was not significantly reduced electrical conductivity of the catalyst.

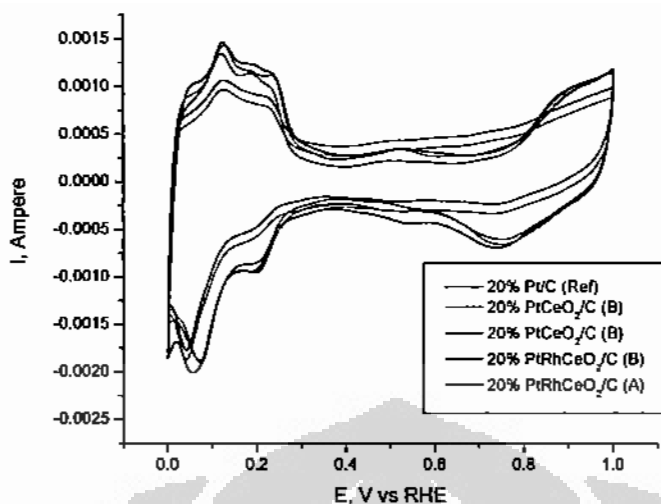


Figure 4.13 Cyclic Voltammogram of PtCeO₂/C (A&B) and PtRhCeO₂/C (A&B) at 30 °C scanrate 50 mV/s, 0.5 H₂SO₄

CO stripping voltammogram for of Pt/C (Ref), PtCeO₂/C (A) & (B) and PtRhCeO₂/C (A) & (B) catalysts were presented in Fig.4.14. The picture showed the CO adsorption peak which represented an electrochemical active surface area (EAS) for CO oxidations over those catalysts. The simplest approach for a base line subtraction was to consider double layer charging and oxide formation the same as in the absence of CO, *i.e.* to use the second cycle in the same experiment for base line subtraction and to contribute the difference between the first and the second cycle only to CO oxidation. Therefore the *EAS* in cm² was calculated with the formula as follows:

$$EAS = \frac{Q_{CO}}{0.420 \text{ mC.cm}^{-2}} \quad (4-2)$$

Where Q_{CO} is CO stripping charge (in mC) determined after 20 min of CO adsorption, and corresponds to a monolayer of adsorbed CO.

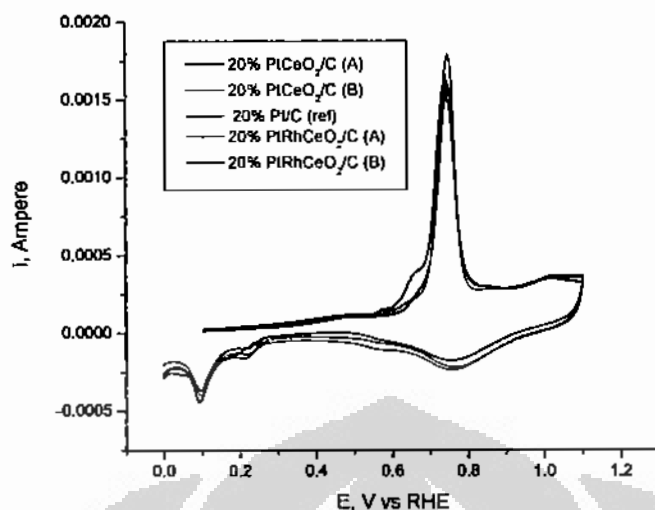


Figure 4.14 CO stripping Voltammetry of synthesized catalysts, at temperature 30 °C and scanrate 10 mV/s, in 0.5 M H₂SO₄

Table 4.2 summarized the electrochemical active surface area of synthesized catalysts that we used in this experiment. Most of the catalyst has similar (EAS), this mean by addition of ceria modifier on those catalysts were not reduced much of the EAS of the catalysts.

Table 4-2 Electrochemical Active Surface area (EAS) of synthesized catalysts

Catalyst	EAS (cm ²)
Pt/C (Ref)	23.8
PtCeO ₂ /C (A)	24.0
PtCeO ₂ /C (B)	24.2
PtRh/C	24.9
PtRhCeO ₂ /C (A)	25.1
PtRhCeO ₂ /C(B)	25.2

Apparent activation energy of ethanol electro-oxidation on 20% Pt/C and 20% Pt-CeO₂/C was calculated from Arrhenius Plot as shown in Fig. 4.15. Calculation of activation energy with this methods resulting value of about 30.5 kJ/mole over 20% Pt/C (ref) ,29 kJ/mole over Pt-CeO₂/C (A) and 26.6 kJ/mole over PtRhCeO₂/C (A)

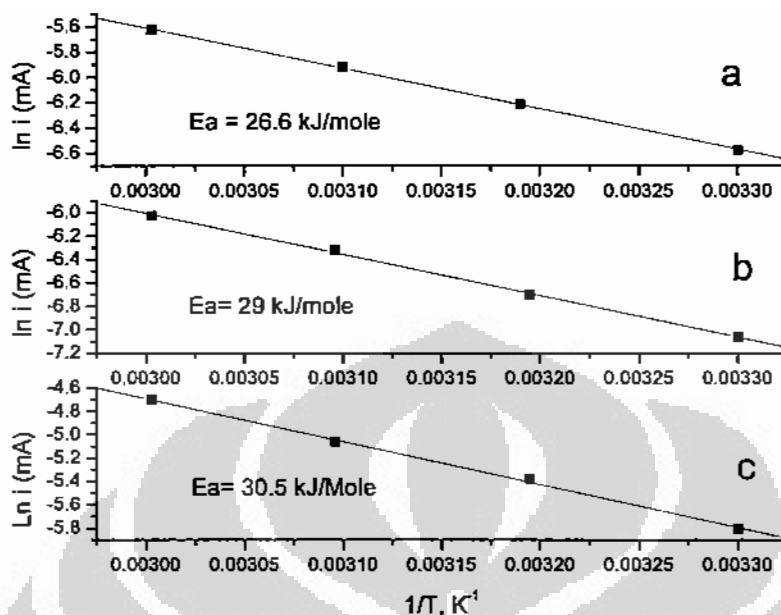


Figure 4.15 Arhenius plot over catalysts of (a) 20% PtRhCeO₂/C (A), (b) 20% PtCeO₂/C (A), (c) 20% Pt/C, at V= 0.6 V vs RHE, and at temperature range between 30°C-60°C.

These apparent activation energy value almost similar with the result from Jusys et.al., which obtained activation energy for ethanol electro-oxidation of about 32 kJ/mole over 40% Pt/C (ETEK) catalyst [18]. With these apparent activity value can be interpreted the trend of the catalyst activity in qualitatively was as follows; PtRhCeO₂/C > PtCeO₂/C > Pt/C.

Those activities of the catalyst also proved by the result of XRD and TEM related to the particle size of catalyst. The smaller particle size of PtRhCeO₂/C contributed to the activity of the catalysts. The smaller of energy activity of Arrhenius plot of PtRhCeO₂/C catalyst was also confirmed by EAS result for PtRhCeO₂/C in table 4.2, which has a higher value of EAS than PtCeO₂ and Pt/C.

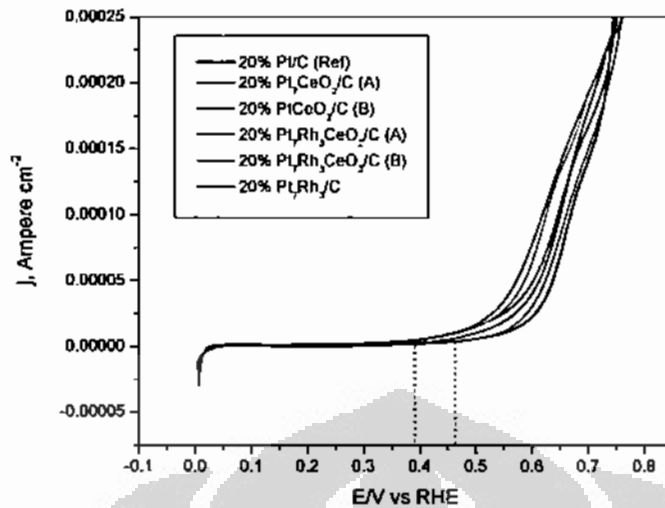


Figure 4.16 electro-oxidation of ethanol in acid medium (0.5 M H₂SO₄ + 1 M Ethanol), at 30°C , scanrate 10 mV/s

Ethanol electro-oxidation of many catalysts was summarized in Fig. 4.16. On-set potential of ethanol electro-oxidation over 20% Pt/C alfa aesar and 20% PtRh/C was at potential of 0.5 V and 0.48 V vs RHE respectively. The onset potential ethanol oxidation reaction was 0.4 V vs RHE and 0.38V vs RHE for PtCeO₂/C and PtRhCeO₂/C respectively. This onset potential was relative poor if for example we compared to electro-oxidation of methanol at 0.3 V vs RHE [6]. The higher (more positive) of the onset potential for ethanol oxidation than methanol was associated to the existing of C-C bond in ethanol.

4.2.2 Electrochemical characterization in alkaline Medium

In this work we also performed the catalysts (20% Pt/C , 20% PtCeO₂/C, 20% PtRhCeO₂/C (A) and 20% PtCeO₂/C, 20% PtRhCeO₂/C (B) in alkaline medium. Fig. 4.17 and 4.18 presented the CV in normal alkaline (NaOH 0.1 M) medium and in presence of ethanol (1 M).

Performance test of catalysts in alkaline medium shows the significant improvement of performance over CeO₂ modified catalysts. In alkaline medium, increasing Faradaic current over PtCeO₂/C catalyst in comparison to Pt/C (ref)

catalyst was by factor of 2, whilst the increasing Faradaic current over PtRhCeO₂/C was by factor of 2.5 at potential 0.6 V vs RHE. These result indicated that ethanol EOR more easily taken place at lower potential in alkaline medium than in acid medium. Those result agreed to the result reported by P.K.Shen [28] which performed PtCeO₂/C catalyst in alkaline medium (KOH)

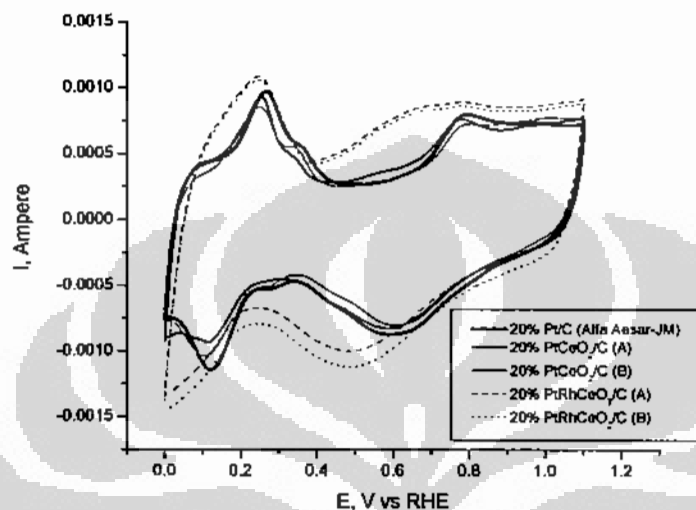


Figure 4.17 Cyclic Voltammety of different catalysts in alkaline medium (0.1 M NaOH), at 30 °C, with scanrate 50 mV/s.

The on-set potential of ethanol oxidation reaction (EOR) on 20% PtCeO₂/C was started at potential 0.32 V vs RHE and on 20% PtRhCeO₂/C was occurred at potential 0.27 V vs RHE at operating temperature 30°C. EOR on 20 Pt/C (Alfa Aesar-JM) was happened at more positive potential at 0.35 V vs RHE. These result indicated that activity of CeO₂ modified catalysts were better than activity of the Pt/C reference catalyst.

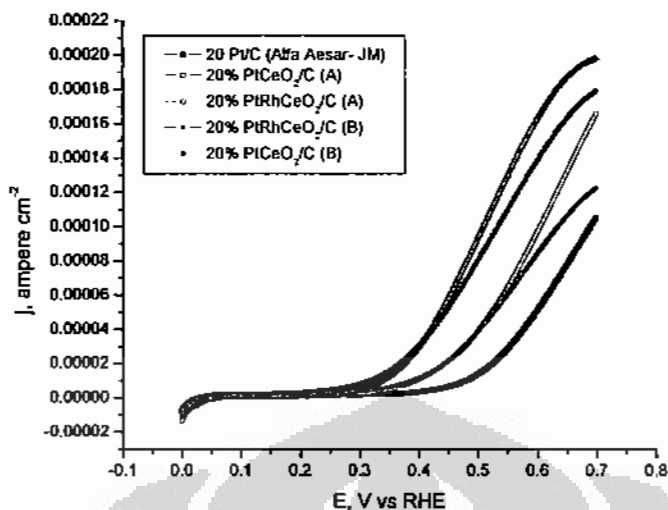


Figure 4.18 Electro-oxidation of ethanol in alkaline medium (0.1 N NaOH)+ 1 M ethanol , at 30°C scanrate 10 mV/s,

4.3 Electrochemical activity and selectivity of the catalyst in fuel cell setup: Potentiodynamics measurements

Steady state voltammogram for ethanol electrooxidation was taken place by dynamics scanning at potential window from 0-1.0 V , with scanrate 5 mV/S. The CV was recorded after several cycles

4.3.1 Potentiodynamics in-situ DEMS measurements of ethanol oxidation on Pt/C catalyst

Potentiodynamics of ethanol electro-oxidation on a 20% Pt/C, Pt-CeO₂/C , PtRh/C and Pt-Rh-CeO₂/C catalysts either with in-house CeO₂ or commercial CeO₂ at temperature 90°C and 0.1 M ethanol concentration are shown in figure 4.19 – 4.24

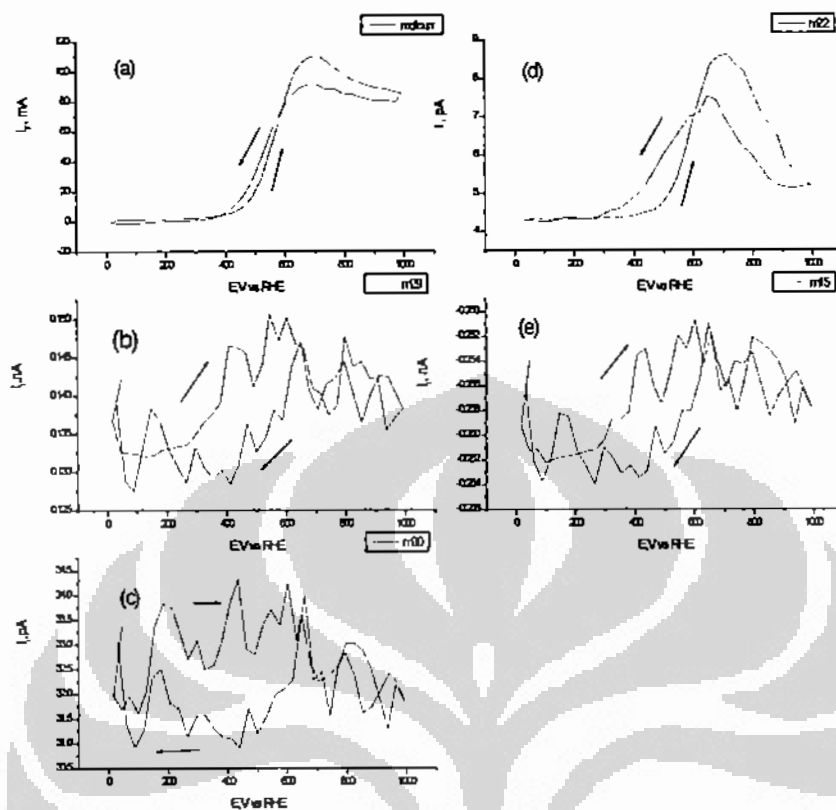


Figure 4.19. CV and MSCV of 20% Pt/C (Alfa Aesar-JM) catalyst at temperature 90°C, ethanol flowrate 5 ml/min, with scanrate 5 mV/s (a) CV (b) MSCV for $m/z = 29$ (c) MSCV for $m/z = 30$ (d) MSCV for $m/z = 22$ and (e) mSCV for $m/z = 15$

Those graphs in Fig.4.19 comprise of cyclic voltammogram (CV) /Faradaic current (a), and the mass spectrometric cyclic voltammogram (MSCV) for ion currents $m/z=29$ (b) $m/z=30$ (c), $m/z =22$ (d) and $m/z= 15$ (e),. Ion current $m/z=22$ was corresponding to mass spectrometric signal for CO_2 via the doubly ionized molecular ion signal. Ion current $m/z = 29$ was corresponding to mass spectrometric signal for acetaldehyde, $m/z= 30$ was corresponding to mass spectrometric signal for ethane, and $m/z =15$ was corresponding to methane.

Fig. 4.19 (d) shows the onset of CO_2 formation in the positive going scan of the steady state voltammogram occur at ca.0.5 V for 20% Pt/C catalyst . Electro-oxidation of ethanol at potential below ca.0.4V is largely blocked by adsorbed poisoning intermediates CO and hydrocarbon residues as shown in Fig.4.19 (a).

This result was in agreement with reported by Wang et al [18]. This result also shows that ion current $m/z = 22$ follow the Faradaic current. In Fig.4.19 (d) the MSCV of $m/z = 22$ has a peak at around 715 mV and after that it declines fast. It was because that at higher potentials, ethanol oxidation is hindered by PtO formation.

4.3.2 Potentiodynamics in-situ DEMS measurements of ethanol oxidation on PtRh/C catalyst

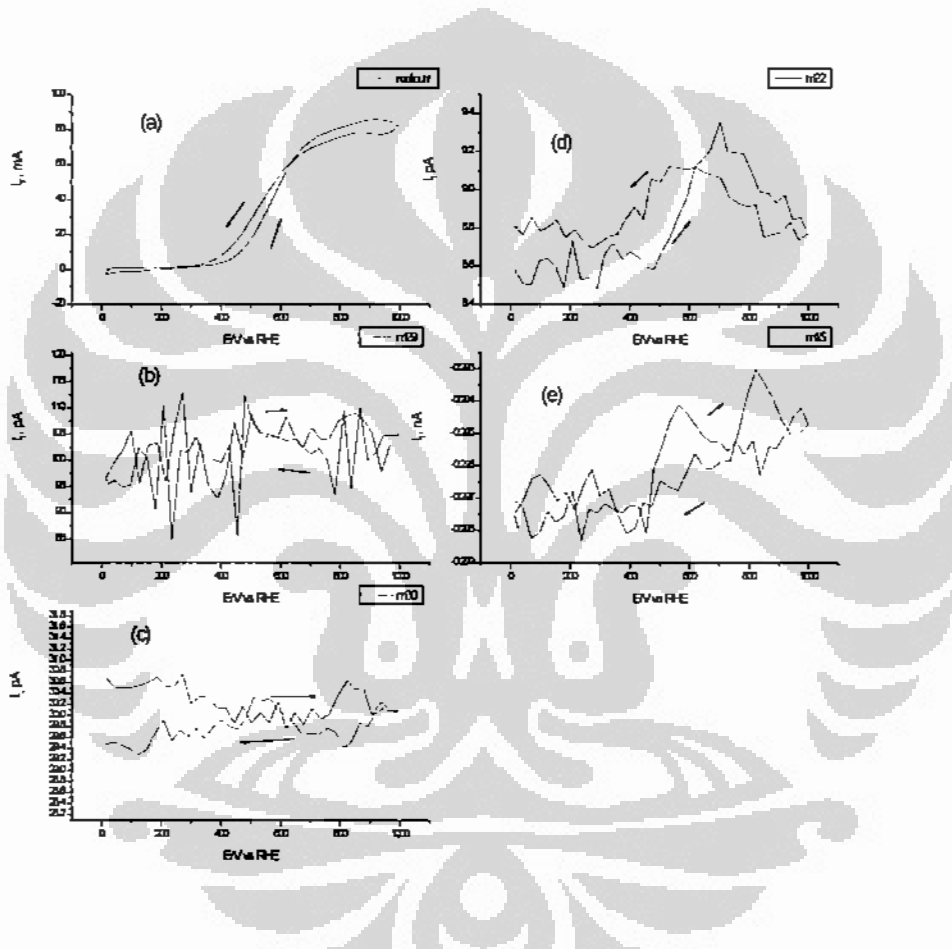


Figure 4.20 CV and MSCV of 20% Pt-Rh/C catalyst at temperature 90°C, ethanol flowrate 5 ml/min, with scanrate 5 mV/s(a) CV (b) MSCV for $m/z = 29$ (c) MSCV for $m/z = 30$ (d) MSCV for $m/z = 22$ and (e) mSCV for $m/z = 15$

Fig. 4.20 shows the cyclic voltammogram (CV) /faradaic current, and the mass spectrometric cyclic voltammogram (MSCV) for ion currents, $m/z=29$, $m/z=30$, $m/z =22$, and $m/z= 15$ over 20% PtRh/C catalyst. The trend of the ion current m/z

= 22 was similar to the ion current $m/z=22$ over 20% Pt/C catalyst (reference) in Fig.4.19 (d)

4.3.3 Potentiodynamics in-situ DEMS measurements of ethanol oxidation on PtCeO₂/C (A) and PtRhCeO₂/C (A) catalysts

Fig. 4.21 show the result of potentiodynamics DEMS measurements of PtCeO₂/C catalysts by using in-house CeO₂ as modifier.

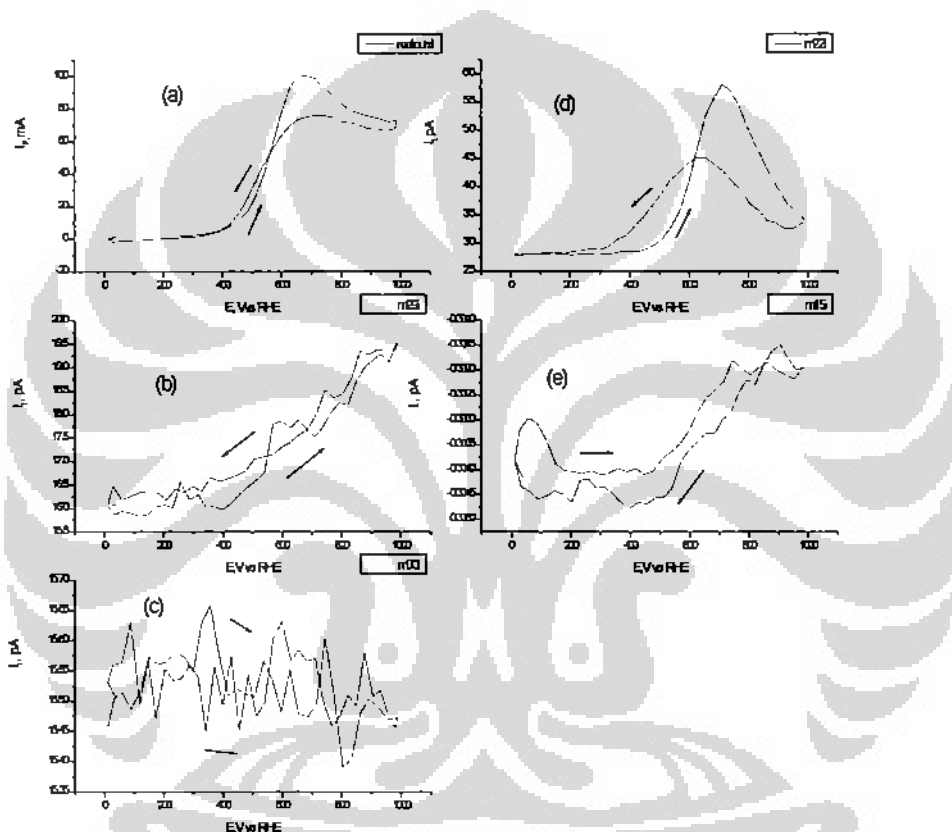


Figure 4.21. CV and MSCV of 20% Pt-CeO₂/C (A) catalyst at temperature 90°C, ethanol flowrate 5 ml/min, with scanrate 5 mV/s(a) CV (b) MSCV for $m/z = 29$ (c) MSCV for $m/z = 30$ (d) MSCV for $m/z = 22$ and (e) MSCV for $m/z = 15$

The trend of $m/z = 22$ and $m/z = 29$ which was corresponded to CO₂ and acetaldehyde formation was following the Faradaic current. However, for methane and ethane formation was not exactly following the Faradaic current. Methane was formed at initial of scanning potential then decreasing at potential of about

400 mV before increasing again to follow the Faradaic current trend. Meanwhile, the ethane formation trend completely different compared to Faradaic current trend. This ion current signal was detected at initial potential scanning and gradually decreasing along the positive going scan.

Fig. 4.22 show the result of potentiodynamics DEMS measurements of PtRhCeO₂/C catalysts by using in-house CeO₂ as modifier.

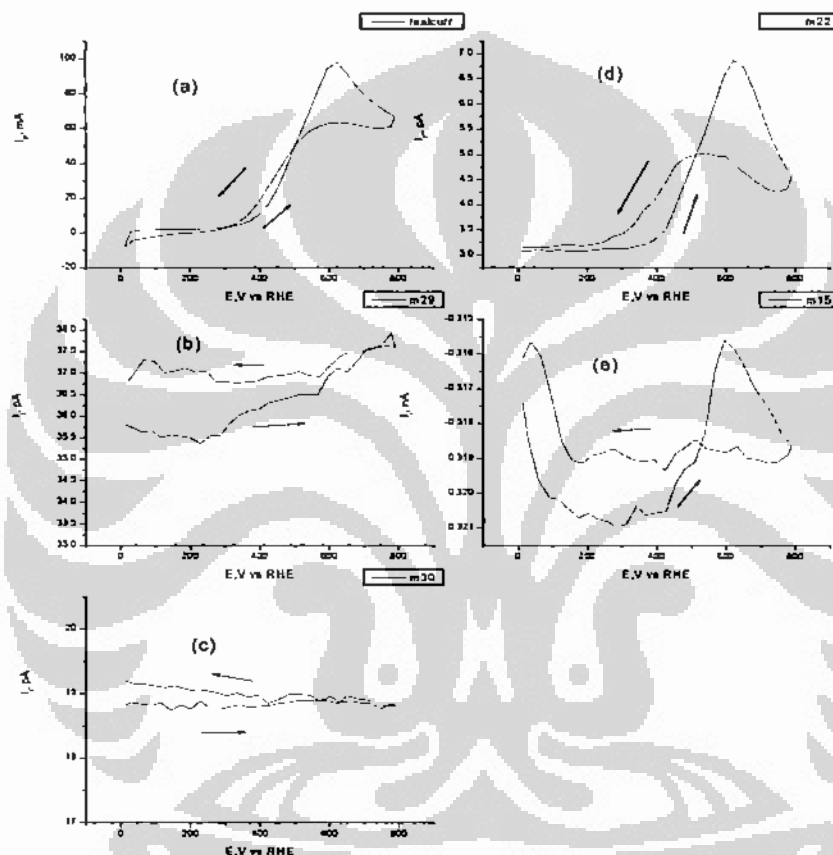


Figure 4.22. CV and MSCV of 20% Pt-Rh-CeO₂/C (A) at temperature 90°C, ethanol flowrate 5 ml/min, with scanrate 5 mV/s(a) CV (b) MSCV for m/z = 29 (c) MSCV for m/z = 30 (d) MSCV for m/z = 22 and (e) MSCV for m/z = 15

Detected ion current signal and the trend all of ion current signal almost similar to the result over PtCeO₂/C (A) in Fig.4.21, except for ion current signal m/z=29. Increasing ion current signal of acetaldehyde at positive going scan was not as much as trend over PtCeO₂/C (A) in Fig.4.21

4.3.4 Potentiodynamics in-situ DEMS measurements of ethanol oxidation on PtCeO₂/C (B) and PtRhCeO₂/C (B) catalysts

Fig. 4.23 show the result of potentiodynamics DEMS measurements of PtCeO₂/C catalysts by using commercial CeO₂ as modifier.

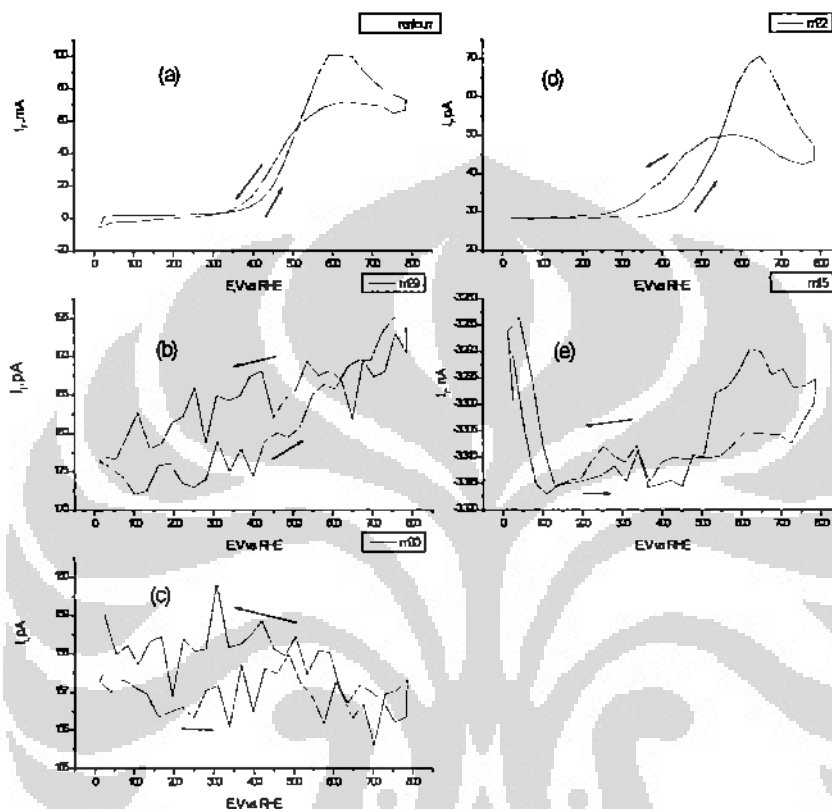


Figure 4.23. CV and MSCV of 20% PtCeO₂/C (B) at temperature 90°C, ethanol flowrate 5 ml/min, with scanrate 5 mV/s (a) CV (b) MSCV for m/z = 29 (c) MSCV for m/z = 30 (d) MSCV for m/z = 22 and (e) mSCV for m/z = 15

The trend of m/z=29 was again different between the result over catalyst of PtCeO₂/C (B) in Fig. 4.23 compared to result over PtRhCeO₂/C (B) catalyst as shown in Fig.4.24. The differences the trend of acetaldehyde ion current signal could be affected by presence of rhodium metal in the catalysts.

Fig. 4.24 show the result of potentiodynamics DEMS measurements of PtRhCeO₂/C catalysts by using commercial CeO₂ as modifier.

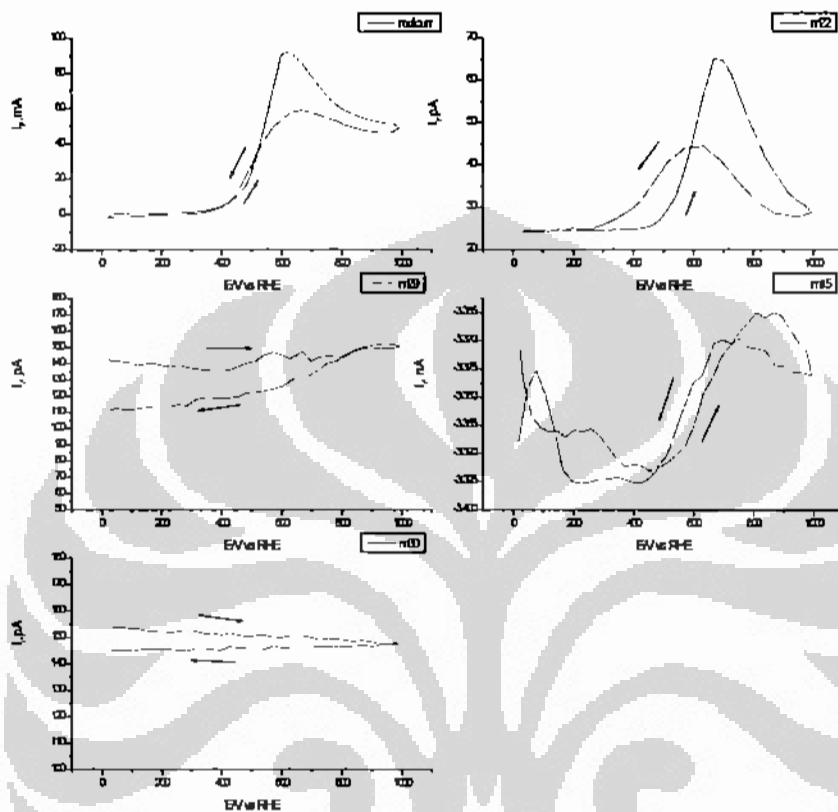


Figure 4.24. CV and MSCV of PtRhCeO₂/C (B), at temperature 90°C, ethanol flowrate 5 ml/min, with scanrate 5 mV/s(a) CV (b) MSCV for m/z = 29 (c) MSCV for m/z = 30 (d) MSCV for m/z = 22 and (e) mSCV for m/z = 15

Since Fig.4.21- 4.24 plotted for studied the tendency of each ion mass current, it was almost no significant differences between both kinds of ceria as modifier related to the ion mass current tendency. Simoultaneously potentiodynamics measurement of ethanol oxidation indicated that all of the CeO₂ modified catalysts which are employed in this experiment resulted product of CO₂, acetaldehyde, methane and ethane which is shown by ion currents m/z =22, m/z=29, m/z= 15, and m/z=30 as a function of the cell voltage. However,

acetic acid which was reported as one of the main product in ethanol electro-oxidation couldn't be seen in Fig. 4.21 – 4.24 due to its low volatility [6].

Figure 4.19-4.24 show the ion mass signal $m/z = 29$ as a function of electrode potential. $m/z=29$ (acetaldehyde) was attributed to major acetaldehyde fragment, CHO^+ . This signal tends to follow the faradaic current for catalyst 20 % Pt/C (Alfa Aesar-JM) (Fig.4.19). For ceria modified catalysts (Fig.4.21-4.24), tendency of increase of $m/z = 29$ follow faradaic current, however increasing ion current signal $m/z = 29$ over ceria modified PtRh catalyst was not as much as increasing over PtCeO₂/C catalyst. Therefore, ion current signal, $m/z = 29$ will not be decline at the same time with decreasing of Faradaic current for ceria added catalysts..

The results show that acetaldehyde formation was favor at high potential. The onset of acetaldehyde formation in the positive going scan occurs at potential ca. 0.35 V. It was simultaneously with the on set of ethanol oxidation. In correlation to CO₂ formation at low potential (<0.4V), it might be that at low potential incomplete oxidation is occurred. This result agreed with experiment result reported by Iwasita et al. [8] which investigated ethanol oxidation using infrared spectroscopy.

Ion mass signal $m/z = 15$ corresponds to CH_3^+ ion which was fragment from methane. Methane formation was reported by dehydrogenation of ethanol on the catalyst surfaces [1]. At positive going scan $m/z=15$ rises almost followed the $m/z=29$ (acetaldehyde).It was because of acetaldehyde also had ionic fragment CH_3^+ . At negative going scan, methane formation was occurs at potential <0.3 V. This result was agreed to result from Wang et al.[18] which used Pt porous electrode. We also monitored $m/z=30$ during ethanol oxidation for ethane formation. Similarly to methane that ethane formation occurs at negative going scan below potential 0.3 V. Ethane formation is reported by reduction of acetaldehyde at low potential (0.06 V) on Pt/C [18].

4.4 Electrochemical activity and selectivity of the catalyst in fuel cell setup: Potentiostatics measurements

Monitoring transient Faradaic current and ion mass current by stepping the potential from 0 V vs RHE to 0.5, 0.6, 0.7 ,and 0.8 V vs RHE (10 minutes for

each potential step), with scanrate 5 mV/s at temperature 90 °C for Cyclic Voltammogram and Mass Cyclic Voltammogram for ion currents $m/z = 22$, 29, 15 and 30

4.4.1 Potentiostatics in-situ DEMS measurements of ethanol oxidation on Pt/C, PtRh/C, PtCeO₂/C (A), PtRhCeO₂/C (A) and PtCeO₂/C (B) and PtRhCeO₂/C (B) catalysts

Fig. 4.25 shows the Faradaic current vs potential for different catalysts. Testing performance in DEMS was carried out at temperature 90 °C, 5 ml/minute ethanol flowrate, and with scanrate of 5 mV/s by potentiostatic DEMS measurements. This result indicated that Faradaic current of catalysts by using ceria modified catalyst resulted higher current at low potential (up to 0.6 V) in comparison to Pt/C catalyst reference. At high potential > 0.6 V, the Faradaic current resulted by Pt/C catalyst superior than ceria modified Pt based catalyst. The Faradaic current was representing the activity of the catalysts. This means that addition ceria on Pt-based catalyst could increase an activity of the catalysts at low potential. In application of fuel cell, increase of Faradaic current at low potential is more useful compared to increase of Faradaic current at high potential. Improvement of this activity was proved by the result of the apparent activation energy (E_{app}) in Fig.4.15. Both results indicated that PtRhCeO₂/C catalyst was more active than PtCeO₂/C. This improvement in activity of the PtRhCeO₂ if correlated to particle size of the catalyst was indicated that with smaller in particle size diameter would affect to the improvement in catalyst activity.

Faradaic currents improvement at potential 0.5-0.6V vs RHE is ranging from 5 - 15 %. Meanwhile at potential > 0.6 V, Faradaic current which is obtained over Pt/C catalyst was higher than the Faradaic current which is obtained over PtCeO₂/C. The difference was about 20-40%. Therefore we want to further investigate the increment of Faradaic current emphasizing at the lower potential to observe an ion mass number 22 as shown in Fig.4.26.

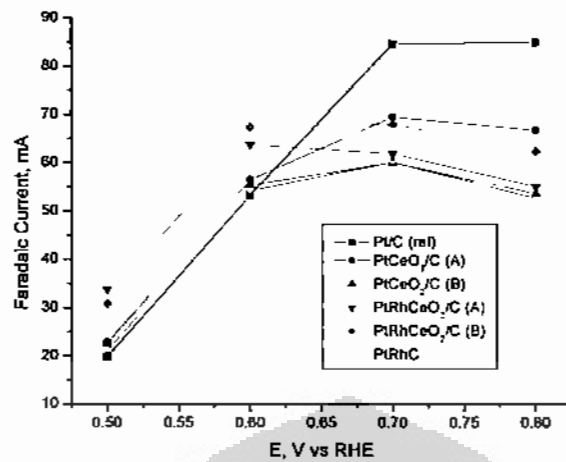


Figure 4.25. Faradaic current vs. potential for different catalysts at temperature 90°C, scanrate 5 mV/s, ethanol flowrate 5 ml/min.

Fig 4.26 shows relation between CO₂ current efficiency (CCE) versus potential. From this picture can be seen that an increase of Faradaic current which was taken place at low potential following with increase significantly of CCE. 20% Pt/C (ref) catalyst provide lower performance than ceria added catalysts, especially at low potential (< 0.6 V).

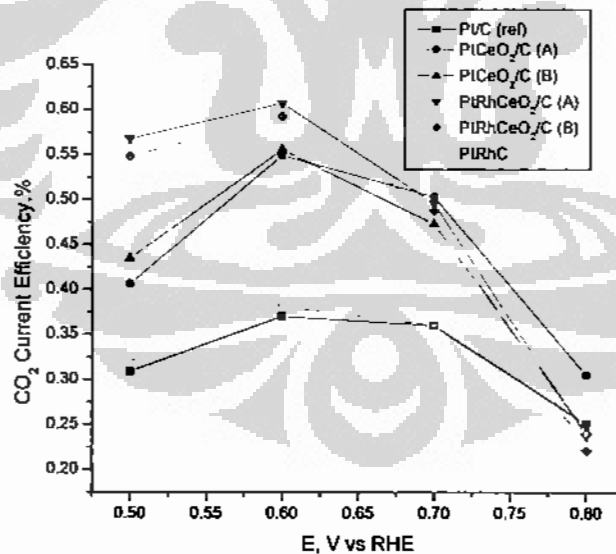


Figure 4.26. CO₂ current efficiency vs potential for different catalysts at temperature 90°C, scanrate 5 mV/s, ethanol flowrate 5 ml/min

Comparison of CCE for the CeO₂ modified catalysts to the reference catalyst at potential 0.6 V was summarized in Table 4.3.

Table 4-3. CCE for different catalysts at potential 0.6 V

Catalyst	Pt/C (ref)	PtCeO ₂ /C (A)	PtCeO ₂ /C (B)	PtRhCeO ₂ /C (A)	PtRhCeO ₂ /C (B)
CCE	0.37	0.55	0.56	0.61	0.59
Difference (abs)	-	18	19	24	22
Difference (%)	-	48.31	50.08	63.99	60.09

4.4.2 CO₂ Current Efficiency (CCE) base on platinum loading, on Pt/C, PtRh/C, PtCeO₂/C (A), PtRhCeO₂/C (A) and PtCeO₂/C (B) and PtRhCeO₂/C (B) catalysts

Figure 4.27 shows relation between CCE to the platinum loading of 20% Pt/C and 20% PtCeO₂/C(A&B) catalysts. The remark was with almost same in platinum loading provided equal value of CCE. This performance was also shown by 20% Pt-Rh-CeO₂/C (in-house and commercial) catalysts. With slight difference in Pt loading, we tried to compare these values to the reference catalyst (20% Pt/C (Ref)). The result shown that ceria modified catalysts provided a better performance than the reference catalyst.

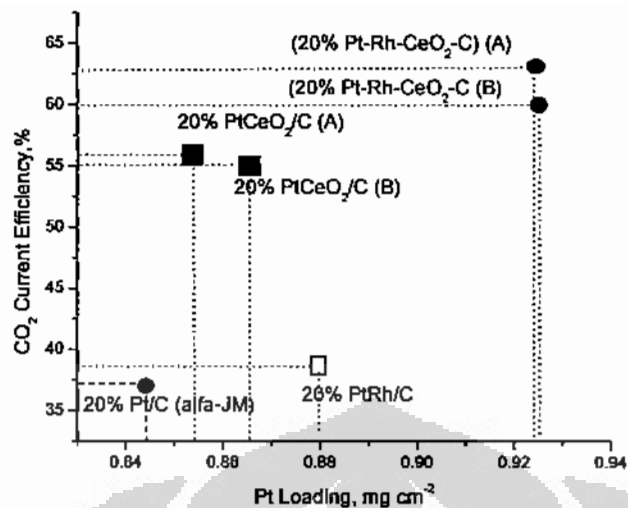


Figure 4.27. CO₂ current efficiency vs platinum loading for different catalysts at potential 0.6 V, temperature 90°C, scanrate 5 mV/s, ethanol flowrate 5 ml/min

4.4.3 Comparison of CO₂ Current Efficiency (CCE) base on CO stripping charge, on Pt/C, PtRh/C, PtCeO₂/C (A), PtRhCeO₂/C (A) and PtCeO₂/C (B) and PtRhCeO₂/C (B) catalysts

In Fig.4.28 shows relation between CO₂ current efficiency (CCE) and the CO stripping charge for different anode catalysts at potential 0.6 V vs. RHE and operating temperature at 90°C. CO stripping charge is linear correlated to Electrochemical Active Surface Area (EAS) by factor of about 420 μC/cm². Detail of the EAS calculation is reported elsewhere [20]. This graph clearly showed that base on the same of EAS between Pt/C and PtCeO₂/C (in-house and commercial), the catalysts provided different value of CCE.

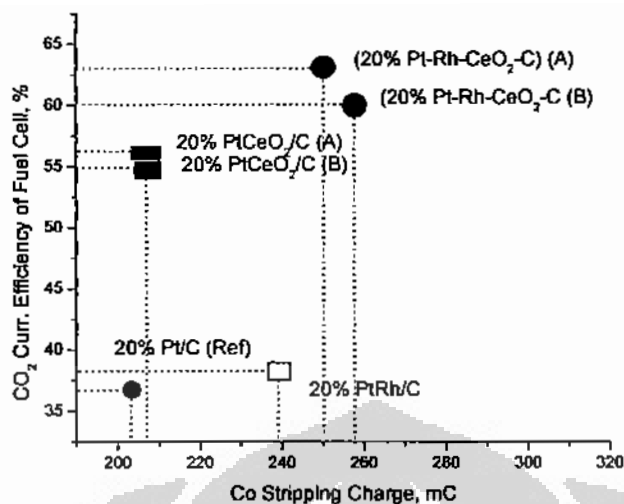


Figure 4.28. CO₂ current efficiency vs CO stripping charge for different catalysts at potential 0.6 V, temperature 90°C, scanrate 5 mV/s, ethanol flowrate 5 ml/min. denoted A means using in-house CeO₂, denoted B means using commercial CeO₂.

Table 4.4 present the CO stripping charge of synthesized and reference catalyst which prepared in membrane electrode assembly (MEA).

Table 4-4. CO Stripping charge of synthesized and reference catalysts in membrane electrode assembly (MEA)

No	Catalyst	CO stripping Charge
1	20% Pt/C (Alfa Aesar-JM)	204.8 mC
2	20% PtRh/C	240.3 mC
3	20% PtRhCeO ₂ /C (Commercial CeO ₂)	258.4 mC
4	20% PtRhCeO ₂ /C (In-house CeO ₂)	250.1 mC
5	20% PtCeO ₂ /C (Commercial CeO ₂)	206.1 mC
6	20% PtCeO ₂ /C (In-house CeO ₂)	208.2 mC

Result of the CO stripping charge indicated that the value which obtained over PtRh based catalyst were higher than the CO stripping charge of Pt-based catalysts. These result was in agreement with the result from T.H.M Housmans et al., [15], they reported that it was an enhancement of surface oxidation of the Pt-Rh in comparison to the Pt or Rh catalyst. From the CO stripping charge value

also indicated that PtRhCeO₂/C was more active than PtCeO₂/C and Pt/C catalyst reference.

4.5 Effect of Rh metal catalyst and CeO₂ modifier on Pt based catalyst

Rhodium is well known as a material in three way catalyst [39]. Rhodium also reported has a capability for breaking C-C bond in ethanol [12,15].

Remark of the results of DEMS measurements over PtRh/C indicated that it was slightly improvement of CO₂ formation which is shown in Fig. 4.25-4.27. However, increasing in activity for C-C bond dissociation is not followed by a higher overall reaction rate, as can be seen from the lower normalized current for the platinum- rhodium electrode compared to pure platinum. There are many possible reasons for the slower reaction rate of ethanol electrochemical oxidation on platinum-rhodium electrodes.

The possible reason of slow reaction over PtRh/C catalyst was related to the apparently strong Rh-CO_{ads} bonding. The bonding energy of adsorbed CO on surface Rh polycrystalline reported of about 134 kJ mol⁻¹, while the bonding energy of adsorbed CO on Pt polycrystalline was 25 kJ mol⁻¹. Its strongly CO-Rh bonding caused the difficulty of totally removing the CO_{ads} monolayer from the Rh surface.

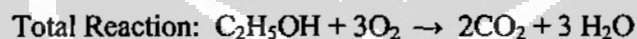
From the experiments results, we also found that it was very difficult to remove CO_{ads} in the CO stripping measurement after poisoning the surface of PtRh/C by CO saturated water. To remove CO_{ads}, its need more voltmetry cycle compared to Pt surface.

Fig.4.25 shows evidence that the activity of EOR over PtRh/C catalyst was slightly higher than activity over Pt/C reference catalyst which was shown by onset potential over PtRh/C catalyst. The onset potential of PtRh/C was shifted to more negative than over Pt/C catalyst. So, the impact of Rh addition in the combination of PtRh improved in C-C bond breaking, although not totally C-C bond breaking results was converted to CO₂ product.

Therefore, to further oxidize result of C-C bond over PtRh surface needed some promoter which helping to oxidize of CO_{ads} to CO_2 .

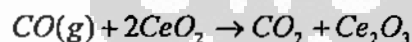
Addition of CeO_2 in the catalysts was aimed to enhance capability of the catalyst in converting CO_{ads} to CO_2 product and finally could drive the ethanol oxidation toward total oxidation reaction.

Effect of addition CeO_2 was shown in Fig.4.25 in PtCeO_2/C catalyst. By addition of CeO_2 improved the activity which is shown by increasing of Faradaic current at low potential less than 0.6 V vs RHE. In-situ DEMS measurements result indicated that the CO_2 current efficiency of EOR over PtCeO_2/C was increase compared to Pt/C catalyst. Increasing of CO_2 current efficiency as an indication that ethanol oxidation reaction was taken place through total oxidation reaction, obey the following reaction:



Improvement of the CO_2 current efficiency also as an indication that the C-C bonds breaking was occurred in the ethanol oxidation reaction. It was because mostly CO_2 product was resulted from oxidation of CO adsorption (CO_{ads}) species of ethanol as intermediate product of C-C bond breaking.

The role of CeO_2 in the oxidation of carbon monoxide was agreed to what reported by Thi at al. [14] :



The reaction mechanism could be explained that oxygen was extracted from an exposed surfaces of the CeO_2 , facilitated by reduction of Ce^{4+} to Ce^{3+} . This role of CeO_2 as oxygen storage container (OSC) was proved by the XRD result that CeO_2 in the of crystallite form. Therefore, in the case of CeO_2 application in electro-catalyst of direct ethanol fuel cells, the mechanism could be explained as follows:

According to the CeO_2 as an oxygen container, oxygen could be renewed from O of water molecule after water molecule activated on catalyst surface to form $\text{OH}^- + \text{H}^+$. The $\text{Pt-H}_{\text{ads}}^+$ reacted with $(\text{CH}_3)_{\text{ads}}$ to form CH_4 , meanwhile the OH^- further

5 CONCLUSIONS

New developed catalysts of PtCeO₂/C and PtRhCeO₂/C which was synthesized by colloidal method improved the activity and selectivity to CO₂ product in ethanol electro-oxidation toward total oxidation reaction in direct ethanol fuel cell. Whereas, effect addition of rhodium in the catalyst was to improve capability in C-C bond breaking, while effect addition of CeO₂ in the catalyst was to donor oxygen onto Pt surface to break C-C bond and to promote CO_{ads} intermediate to the CO₂ product on the surface of platinum.

Addition of rhodium to the carbon supported Pt catalyst improved in C-C bond breaking in ethanol electro-oxidation. However, the result of C-C bond breaking was not converted to CO₂ product totally, due to strongly adsorption of CO intermediate product on surface of PtRh. Therefore, it was only slightly increase of the activity and selectivity of ethanol electro-oxidation reaction (EOR) over PtRh/C compared to commercial Pt/C reference catalyst.

Addition of CeO₂ to the carbon supported catalyst improved the activity of catalysts in C-C bond breaking and improved the selectivity by promoted the oxidation of CO intermediate product to CO₂ on Pt surface. The ceria effect was associated to the capabilities of ceria to provide oxygen on Pt surface that finally could improve activity and selectivity of the catalyst in ethanol oxidation reaction.

Addition of Rh and CeO₂ to the carbon supported catalyst improved the activity of catalysts in C-C bond breaking and improved the selectivity for CO₂ formation. The improvements of activity and selectivity of the catalyst is due to a synergistic effect.

In the real fuel cell, improvement of an activity in electrochemical cell measurement was also obtained by in-situ differential electrochemical mass spectrometry. Increase in activity over ceria modified catalyst also led to increase in selectivity for CO₂ formation. Increasing in activity was indicated by increment of Faradaic current and the increasing selectivity of the catalysts to the CO₂

formation was indicated by increment of the CO₂ current efficiency. Both increasing of the activity and selectivity were occurred at low potential less than 0.6 V vs. RHE

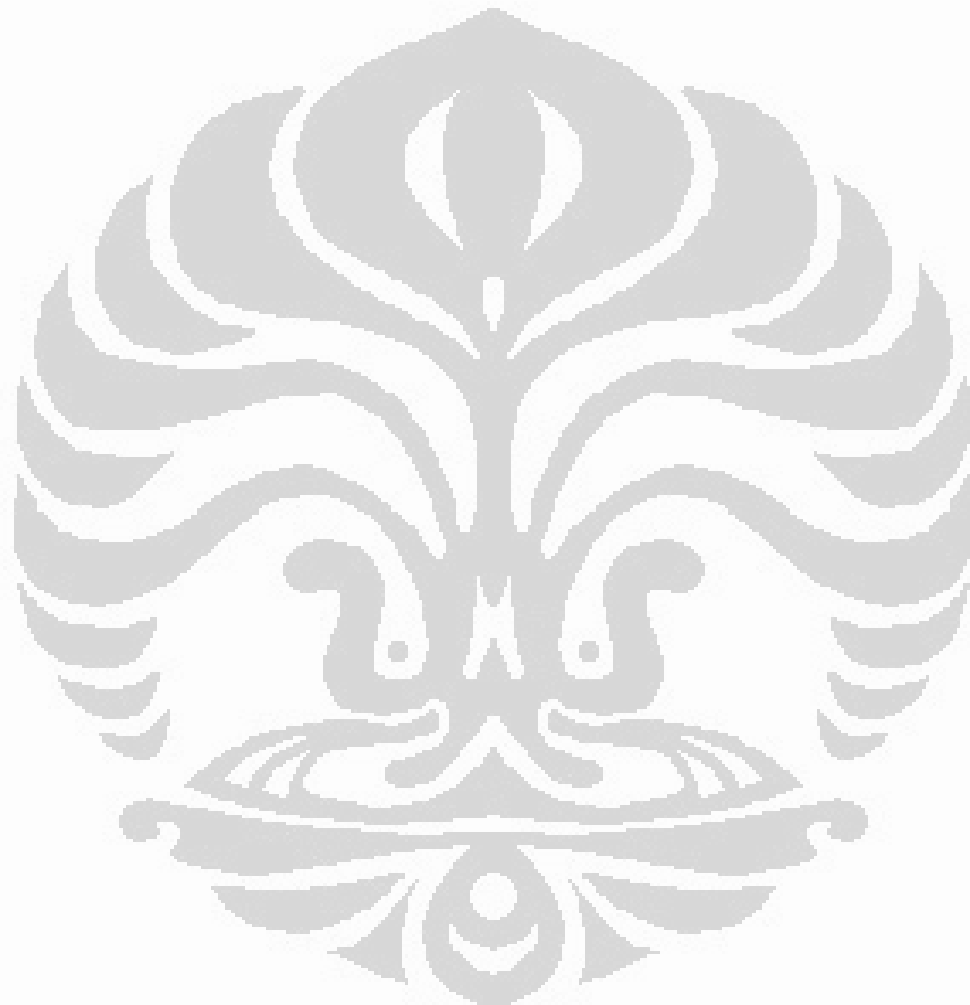
Increasing activity of ethanol oxidation over ceria modified Pt-based catalysts in comparison to reference catalyst (20% Pt/C) at potential 0.6 V are: 20% PtCeO₂/C (in-house CeO₂): 5.99%, 20% PtCeO₂/C (commercial CeO₂): 3.89%, 20% PtRhCeO₂/C (in-house CeO₂): 19.6%, 20% PtRhCeO₂/C (Commercial CeO₂): 26.3%.

The product of the ethanol oxidation reaction over Pt/C, PtCeO₂/C, PtRh/C and PtRhCeO₂/C which was investigated by in-situ DEMS were CO₂, acetaldehyde, methane, ethane. Meanwhile, acetic acid was not detected by DEMS due to low volatility. CO₂ current efficiency (CCE) was represented the selectivity to CO₂ formation of ethanol oxidation. Increasing CCE over ceria modified Pt-based catalysts in comparison to reference catalyst (20% Pt/C) at potential 0.6 V are: 20% PtCeO₂/C (in-house CeO₂): 20%, 20% PtCeO₂/C (commercial CeO₂): 19 %, 20% PtRhCeO₂/C (in-house CeO₂): 27%, 20% PtRhCeO₂/C (Commercial CeO₂): 24%.

SUGGESTIONS FOR FUTURE WORK

- Activity of ethanol electro-oxidation on PtCeO₂/C and PtRhCeO₂/C from electrochemical cell testing was indicated that the result of testing in alkaline medium was better than in acidic medium. This finding has a good challenge to be investigated further in real fuel cell setup by for example, in-situ differential electrochemical mass spectrometry.
- Although the synthesized catalysts modified by Ceria provided improvement in activity and selectivity of ethanol electro-oxidation, it is necessary to look for new ternary metal catalyst (Sn, Ru, etc.,) which capable to improve the performance of catalyst.

- It is necessary to investigate the intermediate product of ethanol electro-oxidation in order to explain more detail the mechanism of ethanol electro-oxidation over PtRhCeO₂ catalyst.



REFERENCES

- [1]. C. Lamy, S. Rousseau, E.M. Belgsir, C. Coutanceau, J.-M. Léger, *Recent progress in the direct ethanol fuel cell: development of new platinum–tin electrocatalysts*, *Electrochimica Acta* 49 (2004) 3901–3908
- [2]. A. S. Aricò P. Cretì, P. L. Antonucci and V. Antonucci, *Comparison of Ethanol and Methanol Oxidation in a Liquid-Feed Solid Polymer Electrolyte Fuel Cell at High Temperature*, *Electrochemical and Solid-State Letters*, 1 (2) 66-68 (1998)
- [3]. N. Fujiwara, K.A. Friedrich, U. Stimming, *Ethanol oxidation on PtRu electrodes studied by differential electrochemical mass spectrometry*, *Journal of Electroanalytical Chemistry* 472 (1999) 120–125
- [4]. T. Iwasita, E. Pastor, *Electrochim. Acta* 39 (1994) 531.
- [5]. C.Lamy, E.M. Belgirs, J.M. Leger, *Electrocatalyxs oxidation of aliphatic alcohols: applications to the direct alcohols fuel cell (DAFC)*, *Journal of appl. Electrochemistry* 31, 799-809, 2001
- [6]. X.H. Xia, H.-D. Liess, T. Iwasita, *Early stages in the oxidation of ethanol at low index single crystal platinum electrodes*, *Journal of Electroanalytical Chemistry* 437 (97) 233-241)
- [7]. J.-M. Leger, S. Rousseau, C. Coutanceau, F. Hahn, C. Lamy, *How bimetallic electrocatalysts does work for reactions involved in fuel cells? Example of ethanol oxidation and comparison to methanol*, *Electrochimica Acta* 50 (2005) 5118–5125
- [8]. G.A. Camara, R.B. de Lima, T. Iwasita, *The influence of PtRu atomic composition on the yields of ethanol oxidation: A study by in situ FTIR spectroscopy*, *Journal of Electroanalytical Chemistry* 585 (2005) 128–131
- [9]. Luhua Jiang, Gongquan Suna, Zhenhua Zhou, Weijiang Zhou, Qin Xin, *Preparation and characterization of PtSn/C anode electrocatalysts for direct ethanol fuel cell*, *Catalysis Today* 93–95 (2004) 665–670

- [10]. L. Colmenares , H. Wang, Z. Jusys , L. Jiang , S. Yan, G.Q. Sun, R.J. Behm, *Ethanol oxidation on novel, carbon supported Pt alloy catalysts— Model studies under defined diffusion conditions*, *Electrochimica Acta* xxx (2006) xxx–xxx
- [11]. www.princeton.edu
- [12]. J. P. I. de Souza, S. L. Queiroz, K. Bergamaski, E. R. Gonzalez, and F. C. Nart, *Electro-Oxidation of Ethanol on Pt, Rh, and PtRh Electrodes. A Study Using DEMS and in-Situ FTIR Techniques*, *J. Phys. Chem. B* (2002), 106, 9825-9830
- [13]. Linda Carrette, K. Andreas Friedrich, U. Stimming, *Fuel cells: principles, types, fuels, and applications*, *Chemphyschem* (2000), 1, 162-193
- [14]. Larminie J., Dicks A., *Fuel cell systems explained*, John Wiley and Sons Ltd, (2001)
- [15]. P.-Y. Sheng, A. Yee, G. A. Bowmaker, and H. Idriss, *H₂ Production from Ethanol over Rh–Pt/CeO₂ Catalysts: The Role of Rh for the Efficient Dissociation of the Carbon–Carbon Bond*, *Journal of Catalysis* 208 (2002), 393–403
- [16]. Thi X. T. Sayle, a Stephen C. Parker^b and Dean C. Sayle, *Phys. Chem. Chem. Phys.*, (2005), 7, 2936–2941
- [17]. Christina Bock, Chantal Paquet, Martin Couillard, Gianluigi A. Botton, and Barry R. MacDougall, *Size-Selected Synthesis of PtRu Nano-Catalysts: Reaction and Size Control Mechanism*, *J. Am. Chem. Soc.* (2004), 126, 8028-8037
- [18]. H. Wang, Z. Jusys, and R.J. Behm, *Ethanol electro-oxidation on Carbon Supported Pt catalyst*, *J Phys. Chem. B* (2004), 108, 19413–19424
- [19]. T. H. M. Housmans, J. M. Feliu, R. Gomez, and M. T. M. Koper, *ChemPhysChem* 2005, 6, 1522-1529
- [20]. Hariyanto, Widodo W. Purwanto, *Ethanol electro-oxidation on Pt based catalyst for direct ethanol fuel cell*, *Seminar Nasional Teknik Kimia UNSRI*, (2006), July 19-20
- [21]. Rao V., Hariyanto, Carsten Cremer, U. Stimming, *DEMS study on alkaline anion membrane fuel cell*, *Journal of Fuel Cells* (2007)

- [22]. Hariyanto, W.W. Purwanto, R.W. Soemantojo, *Ethanol electro-oxidation on Pt-Rh-CeO₂/C catalyst in direct oxidation fuel cell*, international symposium of solid state ionics,(2007), Serpong
- [23]. Hariyanto, W.W. Purwanto, R.W. Soemantojo, *Ethanol electro-oxidation on Pt-CeO₂/C catalyst*, 14th Regional Symposium of Chemical Engineering,(2007), Yogyakarta
- [24]. Hariyanto, W.W. Purwanto, R.W. Soemantojo, U.Stimming, *Ethanol electro-oxidation on PtCeO₂/C catalyst*, Journal of Chemical Engineering and Natural Resources Engineering, (Accepted)
- [25]. Hariyanto, W.W. Purwanto, R.W. Soemantojo, *CO₂ Current Efficiency in Direct Ethanol Fuel cell*, Journal Teknik Kimia Indonesia, (accepted)
- [26]. Carsten Cremers, Hariyanto, V. Rao, A. Racs, U. Stimming, *Direct Ethanol Fuel Cell*, Proceeding TFI,(2006), 28-29 March, Duisburg, Germany, p.327-332
- [27]. Hariyanto, Carsten Cremers, U. Stimming, *Ethanol electro-oxidation on PtRhCeO₂/C*, Fischer Symposium (2006), Benedict Bauern, Munich, Germany
- [28]. Chang Wei Xu, P.K.Shen, *Novel Pt/CeO₂/C catalysts for electro-oxidation of alcohols in alkaline media*, Chem.Comm.(2004),2238-2239
- [29]. H. Hitmi, E.M. Belgsir, J.-M. Leger, C. Lamy, R.O. Lezna, *Electrochim. Acta* 39 (1994) 407.
- [30]. EG& EG Services, *Fuel Cell Handbook*, Fifth Edition (2001), West Virginia
- [31]. Yuan Wang, Jiawen Ren, Kai Deng, Linlin Gui, and Youqi Tang, *Preparation of Tractable Platinum, Rhodium, and Ruthenium Nanoclusters with Small Particle Size in Organic Media*, Chem. Mater. 2000, 12, 1622-1627
- [32]. Boro Djuricic and Stephen Pickering, *Nanostructured Cerium Oxide: Preparation and Properties of Weakly-agglomerated Powder*, Journal of the European Ceramic Society 19 (1999) 1925±1934
- [33]. F. Zhang, Q. Jin, S.-W. Chan, J. Appl. Phys. 95 (2004) 4319–4326.

- [34]. Z. Yang, T.K. Woo, K. Hermansson, *Chem. Phys. Lett.* 396 (2004)384–392.
- [35]. www.herkules.oulu.fi
- [36]. T. Iwasita, B. Rasch, E. Cattaneo, W. Vielstich, *Electrochim. Acta* 34 (1989) 1073.
- [37]. H. Hitmi, E.M. Belgsir, J.-M. Leger, C. Lamy, R.O. Lezna, *Electrochim. Acta* 39 (1994) 407.
- [38]. J. Willsau, J. Heitbaum, *J. Electroanal. Chem.* 194 (1985) 27
- [39]. Carl H. Haman, Andrew Hamnett, W.Vielstich, *Electrochemistry*, 2nd (2007), Wiley WCH
- [40]. C. Suryanarayana, M. Grant Norton, *X-Ray Diffraction a Practical Approach*, (1998), 3-93
- [41]. James T. Richardson, *Principles of Catalyst Development*, (1989), New York
- [42]. Luo, H.Y. Zhang, W., Zhou, H. W., Huang, S. Y. Lin, P.Z. Ding, Y.J; *Appl. Catal., A* 214 (2001), 161
- [43]. Purnomo Yusgiantoro, *Indonesia's experience on biofuel development*, International biofuel conference, July 5th 2007, Brusell
- [44]. Larminie J., Andrew Dicks, *Fuel Cell Systems Explained*, John Wiley & Sons, LTD, West Sussex, England (2001)
- [45]. Satterfield C.N., *Heterogeneous Catalysis in Industrial Practice*, 2nd edition, McGraw-Hill, New York (1991)
- [46]. N. Toshima and T. Yonezawa, *New J. Chem.*, 1998, 22, 1179.
- [47]. H. Bonnemann and R. M. Richards. *Eur. J. Inorg. Chem.*, 2001,10, 2455.
- [48]. P. V. Kamat, *J. Phys. Chem. B*, 2002, 106, 7729.
- [49]. H. J. Freund, M. Baumer, J. Libuda, T. Risse, G. Rupprechter and S. Shaikhutdinov. *J. Catal.*, 2003. 216, 223.
- [50]. J. S. Bradley, in *Clusters and Colloids: from Theory to Applications*, ed. G. Schmid, VCH, Weinheim. 1994. pp. 459–536.
- [51]. X. M. Yan. J. Ni. M. Robbins. H. J. Park. W. Zhao and J. M. White, *J. Nanopart. Res.*, 2002. 4, 525.

- [52]. T. Sasaki, N. Koshizaki, S. Teuchi, H. Umehara, Y. Matsumoto and M. Koinuma. *Nanostruct. Mater.*, 1997, 8, 1077.
- [53]. A.D. Belapurkar, S. Kapoor, S.K. Kulshreshtha and J. P. Mittal, *Mater. Res. Bull.*, 2001, 36, 145.
- [54]. J. H. Hodak, A. Henglein and G. V. Hartland, *J. Phys. Chem. B*, 2000, 104, 9954.
- [55]. T. Fujimoto, S. Terauchi, H. Umehara, I. Kojima and W. Henderson, *Chem. Mater.*, 2001, 13, 1057.
- [56]. W. Chen, J. Zhang and W. Cai, *Scr. Mater.*, 2003, 48, 1061.
- [57]. P. Bindra and E. Yeager, *Electrochem. Soc. Proc.*, 1981, 233, PV 81-6.
- [58]. Lee, K. Y. Chan and D. L. Phillips, *Appl. Surf. Sci.*, 1998, 136,321.
- [59]. J. V. Zoval, J. Lee, S. Gorer and R. M. Penner, *J. Phys. Chem. B*, 1998, 102(7), 1166.
- [60]. M. T. Reetz and W. Helbig, *J. Am. Chem. Soc.*, 1994, 116, 7401.
- [61]. H. Bonnemann and R. M. Richards. *Eur. J. Inorg. Chem.*. 2001.10. 2455.
- [62]. P. V. Kamat, *J. Phys. Chem. B*. 2002, 106, 7729.
- [63]. Roucoux, J. Schulz and H. Patin. *Chem. Rev.*. 2002, 102,3757.
- [64]. Curtis, D. Duff, P. Edwards, D. Jefferso, B. Johnson, A. Kirkland and A. Wallace, *J. Phys. Chem.*, 1988, 92, 2270.
- [65]. G. Cardenas-Trivino, K. Klabunde and D. E. Brock, *Langmuir*, 1987, 3, 986.

CURRICULUM VITAE

Name : Hariyanto
Place & date of Birth : Wonogiri, March 01, 1970
Sex : Male
Marital status : Married
Kebangsaan : Indonesia



Formal Education

1. Sarjana Teknik, Jurusan Teknik Kimia, Fakultas Teknologi Industri, Institut Teknologi Sepuluh Nopember Surabaya (ITS), (1994)
2. Magister Teknik, Program studi Konversi Energi, Departemen Teknik Mesin, Fakultas Teknik, Universitas Indonesia, (2002)

Working Experiences

1994-2004 : Laboratorium Sumberdaya Energi, BPPT
2004- to date : Balai Besar Teknologi Energi (B2TE), BPPT

Publications

- [1]. Hariyanto, W.W. Purwanto, R.W. Soemantojo, U. Stimming, Ethanol electro-oxidation on PtCeO₂/C catalyst, *Journal of Chemical Engineering and Natural Resources Engineering*, (Accepted)
- [2]. V. Rao, Hariyanto, Carsten Cremer, U. Stimming, *DEMS study on alkaline anion membrane fuel cell*, *Journal of Fuel Cells* (2007)
- [3]. Hariyanto, Widodo W. Purwanto, *Ethanol electro-oxidation on Pt based catalyst for direct ethanol fuel cell*, Seminar Nasional Teknik Kimia UNSRI, (2006), July 19-20
- [4]. Hariyanto, W.W. Purwanto, R.W. Soemantojo, *Ethanol electro-oxidation on Pt-Rh-CeO₂/C catalyst in direct oxidation fuel cell*, international symposium of solid state ionics, (2007), Serpong
- [5]. Hariyanto, W.W. Purwanto, R.W. Soemantojo, U. Stimming, Ethanol electro-oxidation on Pt-CeO₂/C catalyst, 14th Regional Symposium of Chemical Engineering, (2007), Yogyakarta
- [6]. Hariyanto, W.W. Purwanto, R.W. Soemantojo, *CO₂ Current Efficiency in Direct Ethanol Fuel cell*, *Journal Teknik Kimia Indonesia*, (accepted)

- [7]. Carsten Cremmers, Hariyanto, V. Rao, A. Racs, U. Stimming, *Direct Ethanol Fuel Cell*, Proceeding TFI,(2006), 28-29 March, Duisburg, Germany, p.327-332
- [8]. Hariyanto, Carsten Cremers, U. Stimming, *Ethanol electro-oxidation on PtRhCeO₂/C* , Fischer Symposium (2006), Benedict Bauern, Munich, Germany
- [9]. Hariyanto, Bambang Sugiarto, *Pengaruh Humidifikasi gas reaktan terhadap efisiensi konversi energi pada fuel cell jenis polimer elektrolit membran*, Prosiding seminar Quality in Research"UI, Jakarta, 2001
- [10]. Hariyanto, *Hidrasi Elektrolit Membran Fuel Cell*, Prosiding Fundamental & Aplikasi Teknik Kimia 2001, ITS, Surabaya, 2001
- [11]. Hariyanto, *Sel bahan bakar dengan umpan langsung bahan bakar methanol*, Seminar Nasional Teknik Kimia 2003, SP01-SPO2
- [12]. Hariyanto, *Studi Eksesperimen Direct Methanol Fuel Cell Menggunakan Katalis platinum ruthenium berpenyangga karbon*, Prosiding Seminar Nasional Teknologi Proses Kimia 2003, UI, 2003



PAPER I

Ethanol Electro-oxidation on Pt-CeO₂/C catalyst in direct ethanol fuel cell

Ethanol Electro-oxidation on PtCeO₂/C Catalyst in Direct Ethanol Fuel Cell

Hariyanto^a, Widodo W. Purwanto^{a*}, Roekmijati.W-Soemantojo^a, U. Stimming^b

^a Department of Chemical Engineering, Faculty of Engineering, University of Indonesia, Depok 16424, Indonesia

^b Department of Physics, Technical University of Munich, D 85748 Munich-Germany

Abstract

Anode catalyst of 20% PtCeO₂/C was prepared by colloidal method using ethylene glycol as the reductant. The prepared catalyst was characterized by X-ray diffraction (XRD) and transmission electron microscopy (TEM) techniques. TEM images show uniform dispersion of spherical metal nano particles with average diameter of 2.9±0.3 nm and close agreement with those estimated by Scherer formula from XRD results. Activity of the catalyst for ethanol electro-oxidation reaction (EOR) was tested in an electrochemical cell by cyclic voltammetry technique and in real fuel cell by in-situ differential electrochemical mass spectrometry (DEMS). The DEMS of fuel cell was also used to investigate the selectivity toward CO₂ formation by measuring the CO₂ current efficiency. Pt loading of anode catalyst (20% PtCeO₂/C) was about 0.8 mg/cm² and 2.5 mg/cm² for cathode catalyst (commercial 40% Pt/C). The results show that 20% PtCeO₂/C catalyst provided better performance in comparison to 20% Pt/C commercial catalyst.

Keywords: ethanol electro-oxidation reaction (EOR), CeO₂, CO₂ current efficiency, activity, selectivity

1 Introduction

Fuel cell has received an increasing attention because of its advantage compared to conventional energy conversion devices [1]. Among of the fuel cells types, proton exchange membrane fuel cell (PEMFC) is a low temperature fuel cell which has been rapidly developing. However, there are some problems in application of PEMFC due to gaseous fuel utilization i.e. hydrogen or hydrogen rich gas [6]. Using gaseous hydrogen fuel is more complicated due to bulky hydrogen storage and required external fuel reformer. Compared to PEMFC, direct alcohol fuel cell (DAFC) are more compact

* Corresponding author: Widodo W. Purwanto, Telp: 062-21-7863516 Fax: 062-21-7863515
Email address: widodo@che.ui.edu

without the heavy and bulky external fuel reformer and can be applied especially to power electric vehicles. Liquid fuels, such as low-molecular weight alcohols (methanol and ethanol), have high energy densities and can be easily handled, stored and transported in comparison with gaseous fuels

Currently, direct methanol fuel cell (DMFC) is being widely investigated as a possible power source for electric vehicles and other portable applications in the future. However, it is well-known that methanol is volatile and relatively toxic; therefore it is not thought as a favorable and friendly fuel [1]. Other short chain organic chemicals, such as ethanol, ethylene glycol, and propanol were also tested as fuels for direct liquid electro-oxidation [1-5]. Among alternative fuels, ethanol is safer and has higher energy density compared to methanol (8.01 kWh kg^{-1} versus 6.09 kWh kg^{-1}). Moreover, ethanol can be easily produced by fermentation of sugar-containing raw materials. Therefore, ethanol is more attractive than methanol for direct alcohol oxidation fuel cells operating at lower temperature. The adsorption and oxidation of ethanol for fuel cells at lower temperature values have already been investigated, but most of the prior studies were restricted to the analysis of ethanol anodic oxidation mechanism and the identification of the reaction intermediates and products [7]. The complete ethanol electro-oxidation to CO_2 involves releasing of 12 electrons per molecule and many adsorbed intermediates. Besides, ethanol is electrochemically oxidized through different pathways on different catalytic surfaces or in different media. Thus, it is more difficult to elucidate exactly the mechanism of ethanol electro-oxidation [2,5].

High activity and stability of Pt, especially under acidic environment, makes it a suitable electrocatalyst for electro-oxidation of many small chemical molecules.

However, at room or moderate temperature values pure platinum is not a very good anode catalyst for ethanol or methanol electro-oxidation, because it is readily poisoned by the strongly adsorbed intermediates, including CO adsorption (CO_{ads}) which is always considered as one of the main poisoning species at low operating temperature.

CeO_2 is well known as catalyst modifier in heterogeneous catalyst [13]. It was due to property of CeO_2 as a good oxygen donor and oxygen container. The oxygen storage capacity associated with the ability to undergo a facile conversion between Ce(IV) and Ce(III) is one of its most interesting properties for electro-catalyst application to enhance in C-C bond breaking and convert intermediate product of CO to CO_2 .

Preliminary study of PtCeO_2/C catalyst for ethanol oxidation in alkaline medium was conducted by Shen et al. [12]. By testing in electrochemical cell, they found that PtCeO_2/C gave better performance than Pt/C catalyst.

In this work, PtCeO_2/C electro-catalyst with Pt: CeO_2 weight ratio of 2:1, was prepared by alcohol reduction process [6]. Systematic study was carried out by testing the catalyst for ethanol oxidation using cyclic voltammetry in electrochemical cell and using in-situ differential electrochemical mass spectrometry (DEMS) of fuel cell. The aim of this research work is to investigate of PtCeO_2/C for ethanol electro-oxidation in direct ethanol fuel cell (DEFC) to improve capability for C-C bond breaking toward total oxidation reaction of ethanol.

2 Materials and Methods

2.1 Material and Chemicals

The starting materials which was used in this experiment were: cerium nitrate hexahydrate ($\text{Ce}(\text{NO}_3)_3 \cdot 6\text{H}_2\text{O}$, anal., Alfa-Johnson Matthew), hydrogen peroxide (30%

H₂O₂, p.a., Merck) and ammonium hydroxide (NH₄OH, 25 vol% p.a., Merck). H₂PtCl₆·6H₂O (Johnson Matthew) was used as precursors of PtCeO₂/C catalysts. Material of carbon support was Vulcan-XC-72 from Cabot Co.

In all experiments, 0.5 M sulfuric acid prepared from concentrated sulfuric acid (Merck suprapur), 0.1 sodium hydroxide (Merck suprapur) and water from a Milli-Q system (18 MΩ cm) was used as electrolyte. One molar ethanol in 0.5M sulfuric acid solution was prepared, using ethanol (LiChrosolv, 99,99 %) from Merck. High purity Ar (Linde Gas, 4.8) and CO (Linde Gas, N 4.7) were employed for electrolyte purging and CO saturation.

2.2 Preparation of CeO₂ and carbon supported PtCeO₂ catalyst.

Synthesis of ceria was carried out by a two step precipitation method. The procedure is briefly described as follows; separate solutions of 0.1 mol Ce (III) nitrate in water and of 30 vol.% hydrogen peroxide were cooled to 5°C and then mixed together under constant stirring. After 8-10 min, the solution turned to first yellow then orange-yellow, but remained transparent. Ammonium hydroxide solution was then added to increase the pH value to 10. The solution was then refluxed at 90°C in oil bath for 2 hours. Precipitation therefore occurred in two stages. The solution was decanted and the precipitate was washed and dried at 80-85°C, then calcined at 500 °C in air for 3 h.

The needed amount of H₂PtCl₆·6H₂O was added into ethylene glycol solution and stirred for 30 min. Prior to the synthesis of colloidal solution, ethylene glycol was dried using molecular sieve. Then the pH value of the solution was adjusted to 12 with sodium hydroxide (0.5 M) and the solution was heated under reflux to 160 °C in an oil bath, and

kept at this temperature for 2 h to obtain brown–black sol. The solution then cooled to room temperature and the calculated amount of as prepared CeO₂ and carbon Vulcan XC-72 was added to the sol and stirred for another 12 h. The obtained black product was then filtered and extensively washed with distilled water, and dried at 80°C for overnight.

2.3 Physical characterization

X-Ray diffraction was performed using instrumentation of Bruker D8 Advanced diffractometer equipped with a Cu anticathode, adjustable divergence slit, graphite monochromator on the diffracted beam and proportional detector. Data acquired at 2 θ range from 20 to 65°, scan step of 0.02° and fixed counting time of 6 s for each step.

Transmission electron microscopy (TEM) investigations were carried out using the JEOL JEM 2000 EX microscope operating at 120 kV. High Resolution Transmission Electron Microscopy (HRTEM) images were taken on JEOL JEM 2010 F operating at 200 kV.

2.4 Electrochemical characterization in half cell setup

10 mg catalyst sample was suspended in 0.3 mL distilled water and 0.5 mL of 10.0 wt.% Nafion in alcohol was added as binder and proton conductor. The mixture was ultrasonically processed for 10 min to form homogeneous ink. Then 13.5 micro liter of ink were pipetted on a vitreous electrode with 6 mm diameter to act as the working electrode.

An electrolyte solution was prepared by adding ethanol to a sulfuric acid solution to obtain concentration of 1 mol dm⁻³ ethanol + 0.5 mol dm⁻³ H₂SO₄. After deaerating the solution with Argon gas, electrochemical measurements were conducted on this solution

using potential control methods (Potentiostat, Autolab PGstat 20) which involve the electrode of the comparative samples as a working electrode and a platinum wire as a counter electrode, while Hg/Hg₂SO₄ (0.5 M) was used as a reference electrode.

2.5 Preparation of membrane electrode assembly (MEA)

In-house PtCeO₂/C catalyst was used for preparation of anode. 40% Pt/C commercial catalyst (E TEK) was used as cathode catalyst. In order to make MEA, a suspension of catalyst powder, Nafion® solution (from Du Pont) and isopropanol were treated in an ultrasonicator. The ink was sprayed onto porous carbon backing layer (Toray paper from ETEK, TGPH 060, no wet proofing) held at 110°C. The 1.2 cm² patches of the Toray paper comprising sprayed catalyst layers were then cut and hot pressed with the Nafion® 117 membrane in between at 140°C for 5 min at a pressure of 1 kN.cm². In order to keep the thickness of the anode electrocatalyst layer constant, we kept the amount of catalyst powder (Pt loading) around 0.8 mg cm⁻² for anode catalyst and of around 2.5 mg cm⁻² for cathode catalyst.

2.6 In-situ differential electrochemical mass spectrometry (DEMS) of fuel cell

The DEMS setup that consisted of two differentially pumped chambers, a Balzers QMS 200 mass spectrometer, AGEF potentiostat and computerized data acquisition system. The DEMS sensor was located at the outlet channel of anode compartment, it consist of a cylindrical detection volume with a diameter of 7 mm and a height of 2 mm through which anode outlet flow passes. This volume was separated from the vacuum system of the mass spectrometer by a Microporous Teflon membrane (Schleicher &

Schuell, TE30) with a pore size of 0.02 micrometer and a thickness of 110 micrometer.

The membrane is supported by a Teflon disc of 2 mm in diameter, with holes.

The fuel cell consist of two stainless steel plates with integrated serpentine medium distribution channels. This DEMS measurement was carried out in the fuel cell setup with cell dimension 1.2 cm².

Cathode with Pt loading (2.5mg/cm²) and continuous hydrogen flow works as counter and reference both. Potential of the cathode is assumed to be same as of the reversible hydrogen electrode (RHE). All potential are reported in reference to this.

The anode flow system comprised of a tank filled with ethanol solution and a tank filled with water. These tanks were connected via heated tubes with the three-way valve at the fuel cell inlet. The ethanol solution and the Millipore water were deaerated with argon gas for 40 min. A dosing pump between the cell outlet and exit tank controls the flow of ethanol solution and water through the cell. To avoid the gas bubble formation due to the large gas production and low solubility of CO₂ at elevated temperature, the anode flow system was pressurized at 3 bars overpressure. The cathode overpressure was kept at 1 bar to limit the crossover of H₂ to anode side. Schematic diagram of DEMS setup is shown in Fig.1

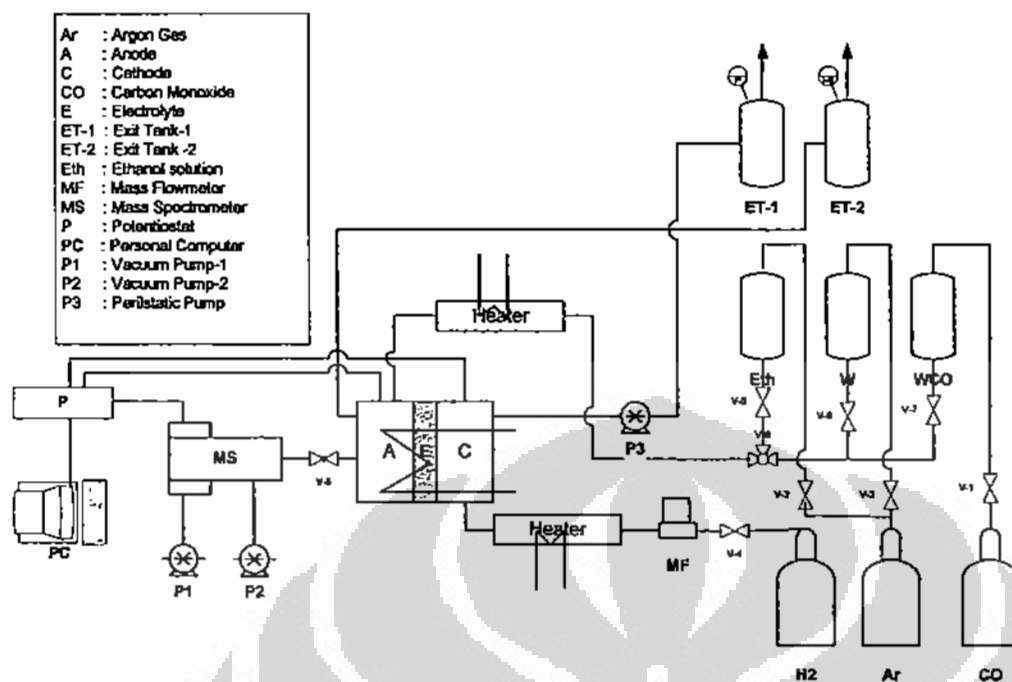


Figure 1. Schematic diagram of DEMS setup

3 Results and Discussion

The XRD patterns of Pt/C and Pt-CeO₂/C are shown in Fig. 2. From the Fig. 2 (a), the characteristic peaks located at 2θ : 28.5°, 33.1°, 47.5°, 56.3° and 59.01° are corresponding to {111}, {200}, {220}, {311} and {222} planes, respectively. These match well with the peaks of cubic fluorite CeO₂ crystal structure in XRD-pattern database.

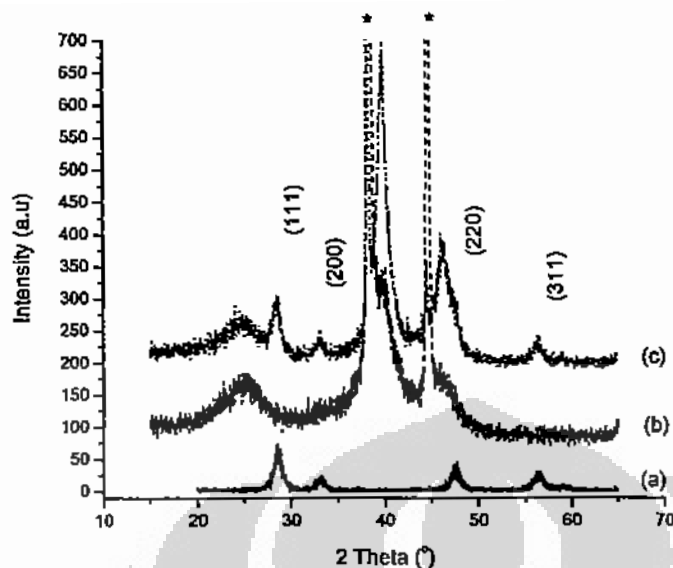


Figure 2 XRD pattern of (a) CeO_2 (solid line) (b) Pt/C (JM) (dashed line) and (c) Pt- CeO_2/C (dot line)

Fig 2 (b), represent the XRD pattern of commercial catalyst Pt/C (JM). The first peak at $2\theta \approx 23^\circ$ originates from the Vulcan XC-72 carbon support. The peaks at $2\theta \approx 40.04^\circ$ are reflections of the face centered cubic (f.c.c.) crystal lattice of Pt {111}. The peaks indicated with a star (*) was due to the sample holder. Fig.2 (c) presents the XRD pattern of Pt CeO_2/C catalyst. All of the peak which is corresponding to CeO_2 , platinum and carbon was exist in the XRD pattern result. This clearly indicates that the Pt CeO_2/C catalyst was successfully prepared by ethylene glycol reduction method.

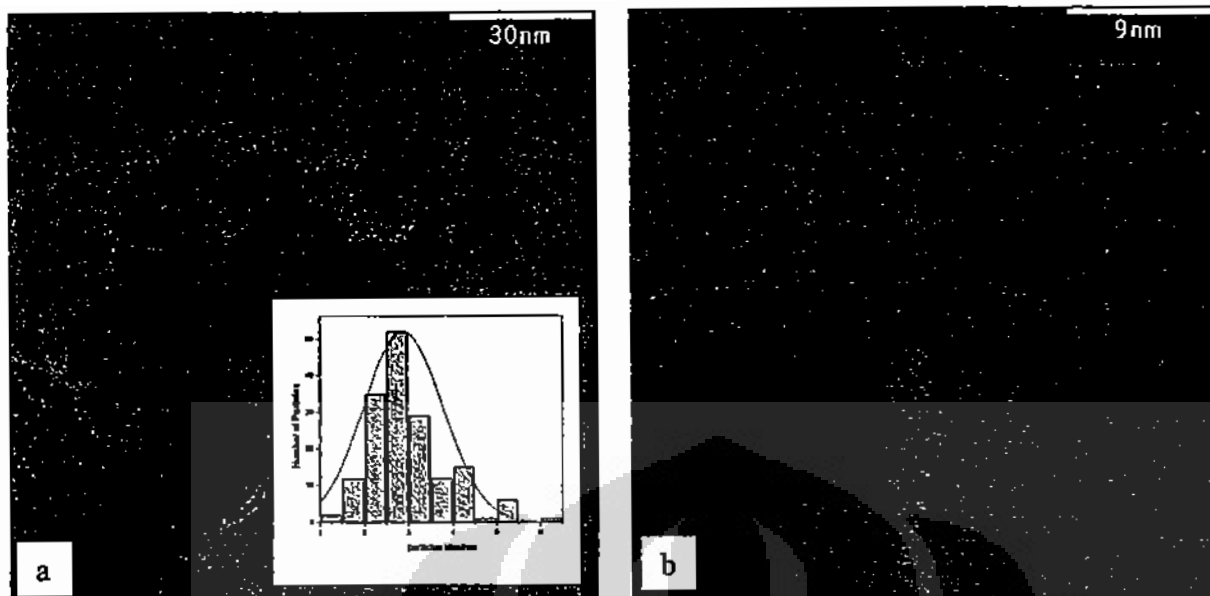


Figure 3 TEM and High Resolution of TEM (HRTEM) of (a) PtCeO₂/C catalyst and (b) CeO₂

Both XRD and TEM results indicate that all catalysts investigated in present work have similar nano particle sizes and the method is suitable to prepare nanometer catalysts with higher metal loading. From the TEM micrographs, it was found that metal particles of PtCeO₂/C catalyst are uniform. The mean particles size obtained by TEM analysis is 2.9 ± 0.3 nm. The mean particles size value is in good agreement with those calculated from the XRD results using Scherer formula of about 3.1 nm.

3.1 Activity test in electrochemical cell

Fig 4 shows the results of CV test of commercial carbon supported platinum and the carbon supported Pt-CeO₂ catalyst prepared in this study. From the Fig.4 (a) can be seen that there is no differences between CV of Pt/C and PtCeO₂/C, because of CeO₂ itself hasn't any feature of CV. However, in presence of ethanol Fig. 4 (b), it is clear that addition of the CeO₂ to Pt results in the negative shift of the on set potential oxidation of

ethanol. The on set potential oxidation of ethanol on PtCeO₂/C catalyst at about 0.40 V (vs. reference hydrogen electrode (RHE)) and on Pt/C at about 0.5 V (vs. RHE). It means that PtCeO₂/C catalyst was more active for ethanol oxidation than Pt/C catalyst. This result agreed to the results from Shen et al. which studied in the alkaline medium [12]. However, it is important to gain more understanding of the ethanol electro-oxidation reaction (EOR) especially to study the selectivity to CO₂ product. EOR mechanism in alkaline medium is difficult to investigate because the main product CO₂ is highly soluble in aqueous alkaline electrolytes, due to the formation of carbonates and bicarbonates which renders it difficult to observe with technique such as differential electrochemical mass spectrometry (DEMS).

The current density in Fig.4 (b) is the current which is obtained and normalized by electrochemical active surface area (EAS). This EAS was determined from CO stripping voltammetry [9]. EAS value which is obtained in these experiments for Pt/C and PtCeO₂/C catalysts are 23.6 and 23.8 cm² respectively.

At almost the same of EAS for CO adsorption, PtCeO₂/C catalyst was more active than Pt/C catalyst for electro-oxidation of ethanol.

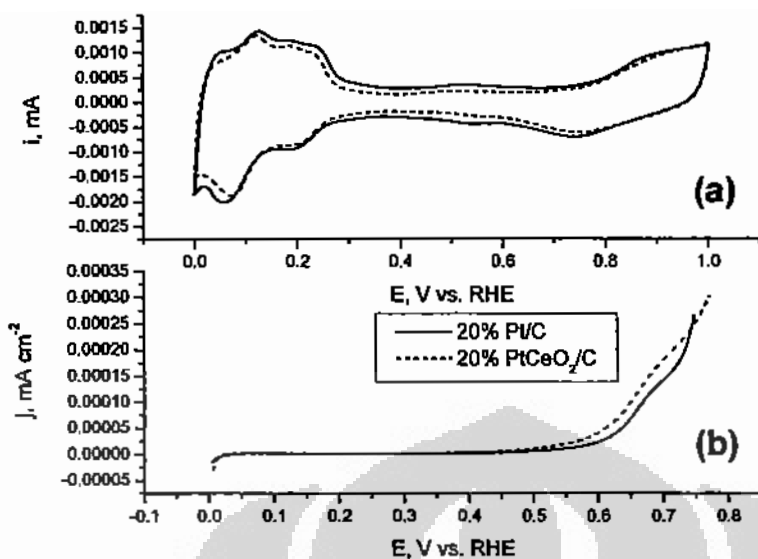


Figure 4 Cyclic voltammogram of 20% Pt/C (solid line) and 20% PtCeO₂/C (dashed line) at 30°C, scan-rate 10 mVs⁻¹, in 0.5M H₂SO₄ solution (a) in 0.5M H₂SO₄ solution + 1.0M ethanol.

From the linear slopes of the integrated charges in the Arrhenius plots in Fig.5 we determined the averaged apparent activation energies (E_{app}) for the overall ethanol electro-oxidation reaction. From the Faradaic current plot in Fig.5, we determined E_{app} was about 29 kJ/mol for ethanol oxidation over a PtCeO₂/C catalyst and of about 30.5 kJ/mol over Pt/C catalyst at temperature range of 30-60 °C. This means that electro-oxidation of ethanol over PtCeO₂/C catalyst is slightly active than over Pt/C reference catalyst. However, these values were higher when compared to the E_{app} of methanol which was reported as 21 kJ/mol [10]. The rather high value of E_{app} over PtCeO₂/C and Pt/C catalyst for ethanol electro-oxidation, is because the (complete) oxidation of ethanol to CO₂ includes a C-C bond cleavage, which is mostly requires higher activation energies.

From the values of E_{app} for ethanol electro-oxidation over PtCeO₂/C and Pt/C indicated that the ethanol oxidation favor occurred on PtCeO₂/C than Pt/C catalyst.

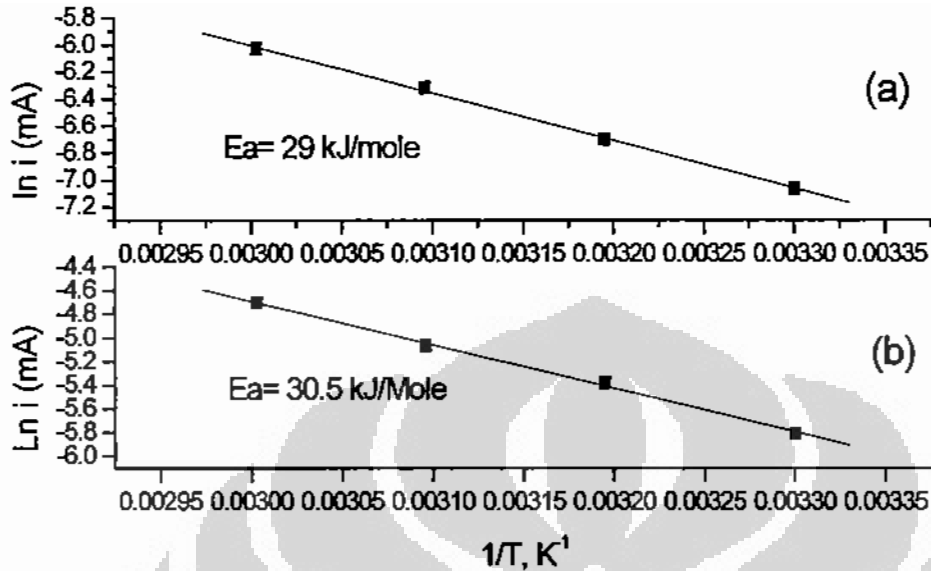


Figure 5 Arrhenius plot (a) for 20% PtCeO₂/C and (b) 20% Pt/C

3.2 Activity and selectivity test by in-situ differential electrochemical mass spectrometry of fuel cell

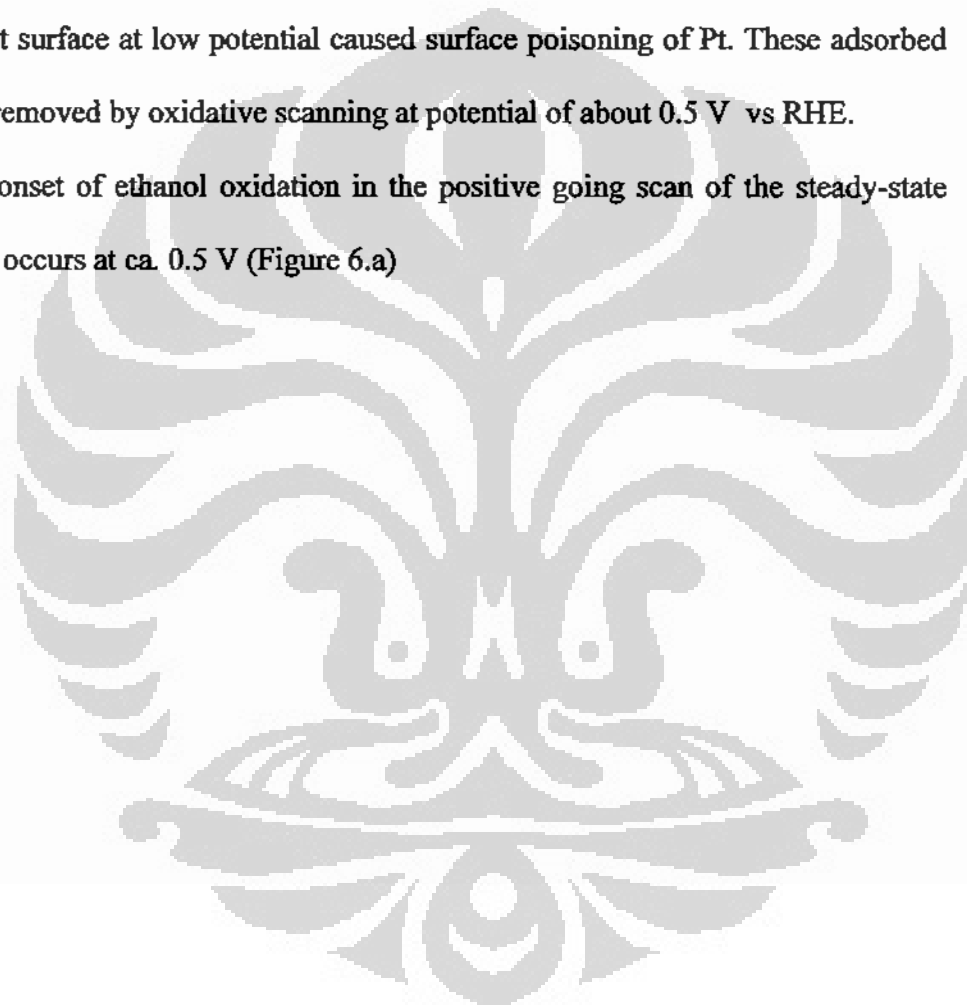
The product distribution of the ethanol oxidation over 20 % Pt/C reference catalyst and as prepared 20 % Pt CeO₂/C catalyst was performed. It is known that the different oxidation products of ethanol are carbon dioxide, acetaldehyde and acetic acid [4]. However, only the first two products were detected by using DEMS technique, due to low volatility of acetic acid.

Ethanol electro-oxidation products on Pt/C catalyst at temperature 90 °C in 0.1 M ethanol and 0.5 M H₂SO₄ was shown in Fig.6. This includes the Faradaic current cyclic voltammogram (CV) (a) and the corresponding mass spectrometric cyclic voltammogram (MSCV) for the ion currents $m/z = 29$ (b), $m/z = 30$ (c), $m/z = 22$ (d), and $m/z = 15$ (e).

The steady-state cyclic voltammogram for ethanol electro-oxidation on the Pt/C (Vulcan-XC72) catalyst was recorded after several cycles as shown in Fig. 6.

The electro-oxidation of ethanol on Pt/C at potential below 0.4 vs RHE could be largely blocked by intermediate product like CO and hydrocarbon residue. Xia et al. found the CO is one of an intermediate product in ethanol electro-oxidation over Pt/C catalyst by fourier transform infrared spectroscopy (FTIR) technique [5]. The CO was adsorbed strongly onto Pt surface at low potential caused surface poisoning of Pt. These adsorbed species can be removed by oxidative scanning at potential of about 0.5 V vs RHE.

Therefore, the onset of ethanol oxidation in the positive going scan of the steady-state voltammogram occurs at ca. 0.5 V (Figure 6.a)



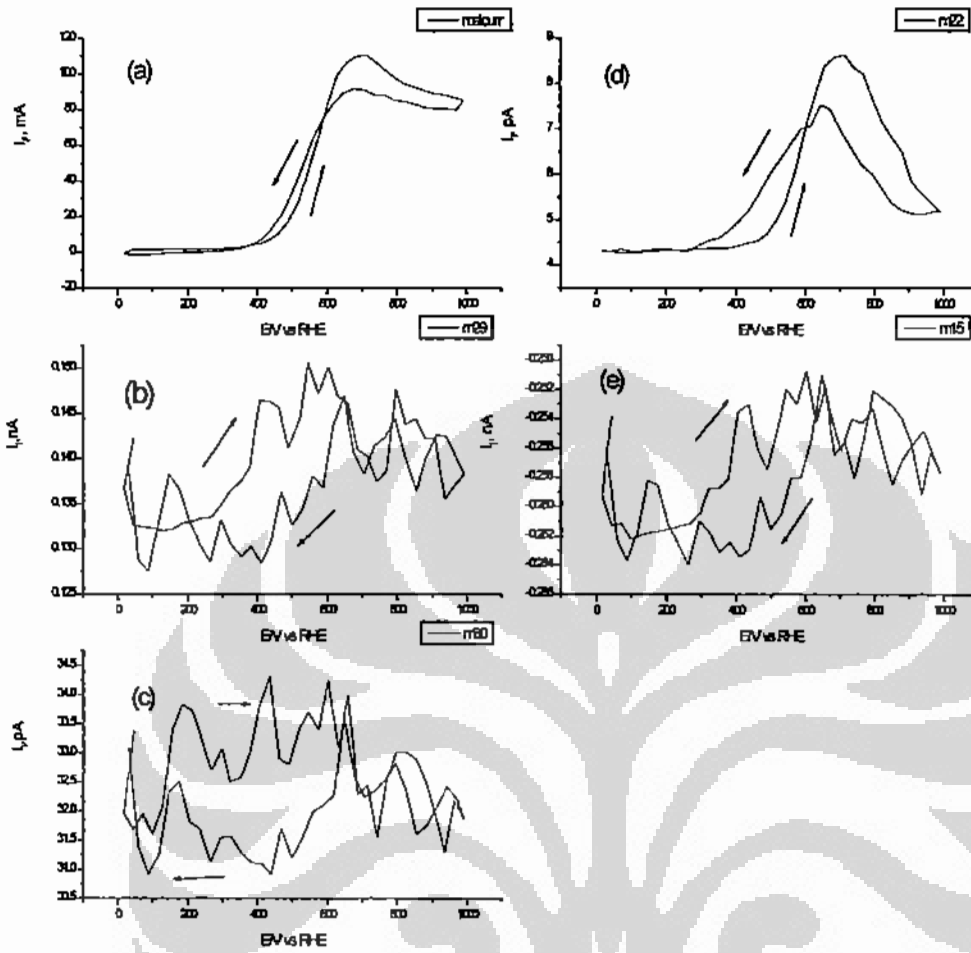


Figure 6. cyclic voltammogram (CV) and mass spectrometric cyclic voltammogram (MSCV) of 20% Pt/C catalyst at temperature 90°C, ethanol flowrate 5 ml/min, scanrate 5 mV/s (a) CV (b) MSCV for $m/z = 29$ (c) MSCV for $m/z = 30$ (d) MSCV for $m/z = 22$ and (e) MSCV for $m/z = 15$

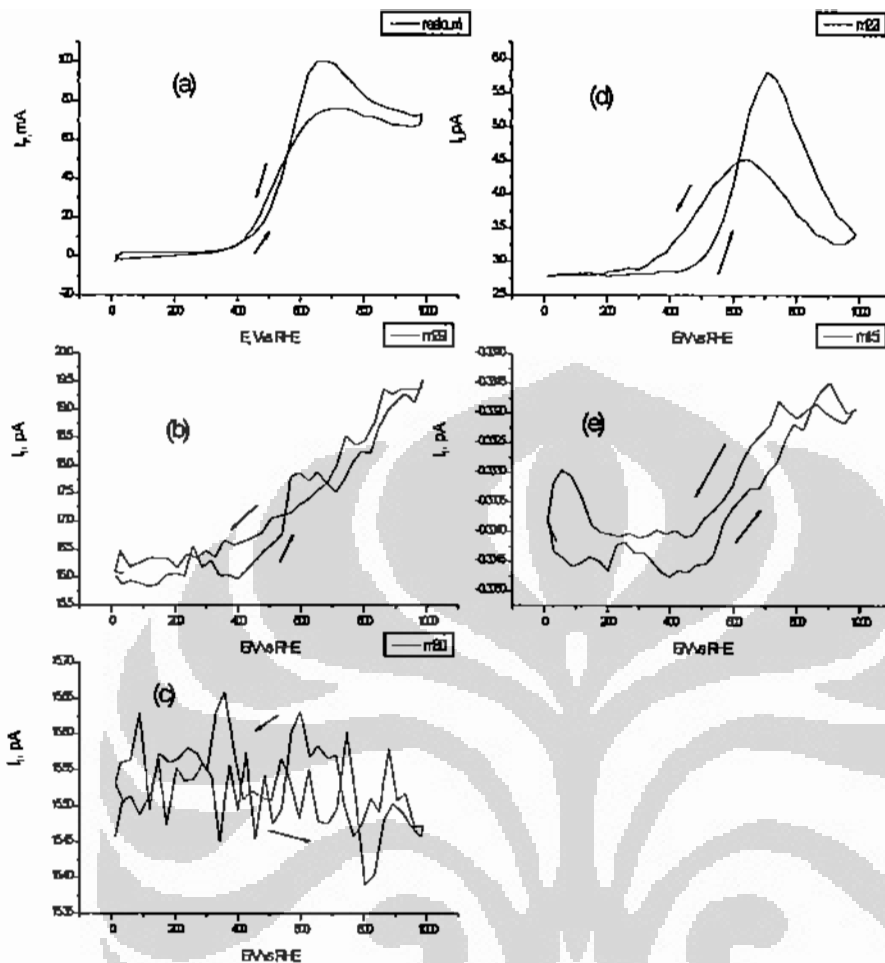


Figure 7. CV and MSCV of 20% Pt-CeO₂/C catalyst at temperature 90°C, ethanol flowrate 5 ml/min, with scanrate 5 mV/s (a) CV (b) MSCV for m/z = 29 (c) MSCV for m/z = 30 (d) MSCV for m/z = 22 and (e) MSCV for m/z = 15

Electro-oxidation of ethanol on PtCeO₂/C catalyst under the same conditions to the Pt/C reference catalyst was presented in Fig.7. CV of Faradaic current in Fig. 7(a) indicated that the on-set of ethanol oxidation reaction on PtCeO₂/C was shifted to the negative potential in comparison to the Pt/C catalyst (Fig.6(a)). The on-set potential of ethanol over PtCeO₂/C occurred at potential of about 0.4 V vs. RHE.

Mass spectrometric cyclic voltammogram (MSCV) for the ion currents $m/z = 29$ (b), $m/z = 30$ (c), $m/z = 22$ (d), and $m/z = 15$ (e) show the results which was similar trend for both of catalysts.

The PtCeO₂/C catalyst was more active for ethanol electro-oxidation reaction in fuel cell setup than commercial Pt/C catalyst. These results agreed with the previous results in electrochemical half cell test. This reaction resulted products like: CO₂, acetaldehyde, methane and ethane which was can be detected by in-situ DEMS technique. While, acetic acid which was reported could be detected by FTIR [4], cannot be detected by this DEMS measurement.

3.3 CO₂ current efficiency

Fig. 8 shows the Faradaic current vs potential for different catalysts. Testing performance in DEMS is conducted at temperature 90 °C , 5 ml/min ethanol flowrate, and with scanrate of 5 mV/s by potentiostatic measurements. This result indicates that Faradaic current of catalysts with added ceria provides higher current at low potential (up to 0.6 V) in comparison to commercial Pt/C catalyst reference. At potential > 0.6 V, the Faradaic current resulted from Pt/C catalyst is higher than the PtCeO₂/C catalyst. This means that by adding ceria on Pt-based catalyst, activity could be increased of the catalysts at low potential, although this elevation in Faradaic current was not so high. Increase of Faradaic current over PtCeO₂/C catalyst compared to Pt/C catalyst at potential up to 0.6V vs RHE was 5 - 15 %. Meanwhile, at potential > 0.6 V vs RHE, increase of Faradaic current over Pt/C catalyst compared to PtCeO₂/C was 20-40%. This increase of the Faradaic current at low potential was more useful in fuel cell application, because

magnitude of the overall cell potential is still significant. Therefore we want to further investigate increase of Faradaic current at the low potential by analyzing ion mass current at $m/z = 22$ as shown in Fig.9.

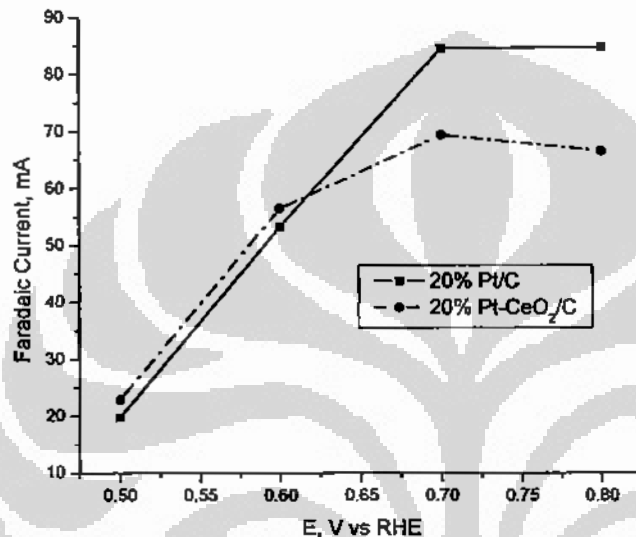


Figure 8. Faradaic current vs. potential of fuel cell setup at temperature 90°C, scanrate 5 mV/s, anode catalyst loading 0.8 mg/cm² for 20% PtCeO₂/C (dashed line) and 20% Pt/C (solid line), cathode catalyst loading 2.5 mg/cm² (40% Pt/C)

Fig 9. shows relation between CO₂ current efficiency (CCE) versus potential. It is shown that the CO₂ current efficiency is a strongly dependent on the potential. Furthermore an increase in Faradaic current which is observed at low potential (Fig.8) was followed by significantly increasing of CO₂ current efficiency. Hence, commercial Pt/C reference catalyst provided lower performance for ethanol oxidation reaction than PtCeO₂ catalyst, especially at low potential (≤ 0.6 V).

The CO₂ current efficiency maximum was obtained at potential 0.6 V vs RHE. At this potential, increasing CCE over PtCeO₂/C was about 18 % in comparison to reference catalyst. This trend can be explained by the fact that electro-oxidation of ethanol at potential below ca. 0.4 V is largely blocked by adsorbed poisoning intermediates (CO and hydrocarbon residues). The decrease in CO₂ current efficiency after 0.6 V is a bit surprising result, since the peaks of Faradaic current and ion current $m/z=22$ were occurred at potential of about 0.7 V vs RHE (Fig.7). Although we can expect that at potentials > 0.8 V the Pt surface is mostly covered by PtO, which may hinder the complete oxidation of ethanol, but will support formation of oxidation by-product like acetaldehyde or acetic acid which was detected using FTIR technique by Xia et al.[5].

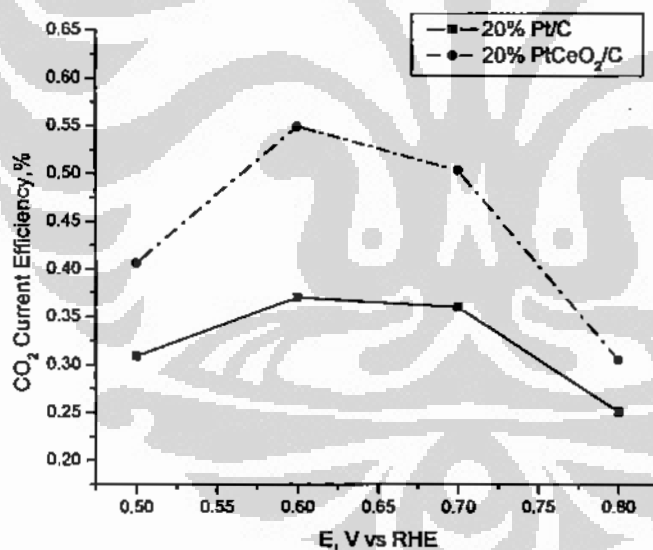


Figure 9. CO₂ current efficiency vs. potential, at temperature 90°C, scanrate 5 mV/s, anode catalyst loading 0.8 mg/cm² for 20% PtCeO₂/C (dashed line) and 20% Pt/C (solid line), cathode catalyst loading 2.5 mg/cm² (40% Pt/C).

It is clearly that modified Pt catalyst by CeO₂ increasing performance of catalyst for ethanol electro-oxidation reaction. Increasing of CO₂ current efficiency as an indication that ethanol oxidation reaction was taken place through total oxidation reaction.

Improvement of the CO₂ current efficiency also as an indication that the C-C bonds breaking was occurred in the ethanol oxidation reaction. It was because mostly CO₂ product was resulted from oxidation of CO_{ads} species of ethanol as an intermediate product of C-C bond breaking. The role of CeO₂ in the oxidation of carbon monoxide was agreed to what reported by Thi et al. [14] :



The mechanism could be explained that oxygen was extracted from an exposed surfaces of the CeO₂ that promote oxidation of CO_{ads} on Pt surface to CO₂ product , facilitated by reduction of Ce⁴⁺ to Ce³⁺ at low potential ≤ 0.6 V vs RHE.

4 Conclusion

20% PtCeO₂/C catalyst which is prepared by colloidal methods was an active catalyst for ethanol electro-oxidation reaction compared to the commercial Pt/C catalyst. Increasing performance in activity for EOR was indicated by increment of Faradaic current either in half cell electrochemical test or in DEMS of fuel cell test. Moreover, the increasing in selectivity to the CO₂ formation was indicated by increment of the CO₂ current efficiency in DEMS of fuel cell test. Both increasing of the activity and selectivity were occurred at low potential less than 0.6 V vs. RHE.

Increase of Faradaic current over PtCeO₂/C catalyst compared to Pt/C catalyst at potential 0.6V vs RHE was about 6 %. Increasing of selectivity toward CO₂ formation on PtCeO₂/C catalyst was about 18% at potential 0.6 V vs RHE in comparison to Pt/C catalyst.

5 Acknowledgments

We thank to Dr. Cristina Tealdi (Univ. Pavia Italy) for X-ray Diffraction measurement and Petra Belle (TU-Munich) for TEM measurement and discussion. Financial support by DAAD under contract A/03/41170 was also acknowledged.

6 References

- [1] Parson, Inc. *Fuel cell handbook*. 2000. West Virginia: U.S Department of Energy
- [2] Lamy C., E.M. Belgsir, J.-M. Léger. 2001. Electrocatalytic oxidation of aliphatic alcohols: application to the direct alcohols fuel cells, *J. Appl. Electrochem.* 31: 799.
- [3] Zhou W.J., S.Q. Song, W.Z. Li, G.Q. Sun, Q. Xin, S. Kontou, K. Poulianitis, P. Tsiakaras. 2004. Pt-based anode catalysts for direct ethanol fuel cells, *Solid State Ionics*. 175: 797–803
- [4] Camara G.A., R.B. de Lima, T. Iwasita. 2004. Catalysis of ethanol electro-oxidation by PtRu: the influence of catalyst composition, *Electrochemistry Communications*. 6 :812–815.
- [5] Xia X.H., H.-D. Liess, T. Iwasita. 1997. Early stages in the oxidation of ethanol at low index single crystal platinum electrodes, *Journal of Electroanalytical Chemistry* .437 : 233-241
- [6] Baldauf, W. Preidel. 2001. Experimental results on the direct oxidation of methanol in PEM fuel cell, *Journal of applied electrochemistry* .31:781-786

- [7] Vigier F., Contanceau F., Hahn F, Belgsir E.M., Lamy C. 2004. On the mechanism of ethanol electro-oxidation on Pt and PtSn catalyst, *journal of electroanalytical chemistry* .563 :81-89
- [8] Lamy C., S. Rousseau, E.M. Belgsir, C. Coutanceau, J.-M. Léger.2004. Recent progress in the direct ethanol fuel cell: development of new platinum–tin electrocatalysts, *Electrochimica Acta* .49:3901–3908
- [9] Hariyanto, W.W. Purwanto.2006. Ethanol electro-oxidation on Pt-Sn catalyst, *Proceeding Seminar Nasional Teknik Kimia UNSRI, Palembang*. 471-476
- [10] Cremers C., Hariyanto, V. Rao, A. Racs.2006. Direct ethanol fuel cells, *proceeding workshop of TFI, IASI, Duisburg-Germany* :327-331
- [11] Schmidt T.J., H. A. Gasteiger, R.J. Behm.1999. Methanol electrooxidation on a colloidal PtRu-alloy fuel cell catalyst, *Electrochemistry Communication I* :1-4
- [12] Shen P.K., Xu C.2005, Electrochemical oxidation of ethanol on Pt-CeO₂/C Catalyst, *Journal of Power Sources* .142:27-29.
- [13] Trovarelli.1996. *A. Catal. Rev. Sci. Eng.* 38: 439
- [14] Thi X. T. , Stephen C. Parkerb and Dean C. Sayle.2005. *Phys . Chem. Chem. Phys .* 7 :2936 – 2941



PAPER II

CO₂ current efficiency in direct ethanol fuel cell

CO₂ CURRENT EFFICIENCY IN DIRECT ETHANOL FUEL CELL

Hariyanto^{a,b}

^a Department of Chemical Engineering, Faculty of Engineering, University of Indonesia
Kampus Depok 16424, Indonesia

^b Energy Technology Center, B2TE, Puspiptek Serpong 15314 Tangerang-Indonesia

Widodo W. Purwanto and Roekmijati W. Soemantojo

Department of Chemical Engineering, Faculty of Engineering, University of Indonesia
Kampus Depok 16424, Indonesia

E-mail: hariyt@yahoo.com

Abstract

In this present work, a systematically study on 20% PtCeO₂/C catalyst for ethanol electro-oxidation in direct ethanol fuel cell were carried out. For cathode catalyst, a commercial catalyst of 40% Pt/C from ETEK was applied. Catalysts were printed on to carbon paper of TGPH 060 and sandwiched into membrane electrode assembly (MEA) and then arranged in fuel cell with the geometric area 1.2 cm². As an electrolyte, we used Nafion 117 from Du Pont. On-line Differential Electrochemical Mass Spectrometry (DEMS) measurement in fuel cell setup was carried out in order to determine the activity and selectivity which was indicated by result of Faradaic current and CO₂ current efficiency of ethanol electro-oxidation respectively. PtCeO₂/C was significantly improving the selectivity to form of CO₂ in comparison to the commercial catalyst of 20% Pt/C from Alfa Aesar- Johnson Mattews. Increasing of selectivity was shown by the increase of CO₂ current efficiency of ethanol oxidation of about 20 percent in comparison to references catalyst of 20% Pt/C (Alfa Aesar-JM)

Keywords : Ceria, Membrane Electrode Assembly (MEA), DEMS, Ethanol Electro-Oxidation

Abstrak

Pada penelitian ini dilakukan kajian sistematis terhadap katalis 20% PtCeO₂/C yang di akan digunakan pada elektro-oksidasi etanol pada fuel cell etanol langsung. Untuk katalis katoda, digunakan katalis komersial 40% Pt/C dari ETEK. Katalis tersebut diterapkan pada kertas karbon TGPH 060 dan diselipkan pada rangkaian membran elektroda (MEA) dan kemudian disusun pada fuel cell yang memiliki luas geometris 1.2 cm². Sebagai elektrolit, digunakan Nafion 117 produksi Du Pont. Pengukuran On-line Spektometri Massa Elektrokimia Diferensial atau Differential Electrochemical Mass Spectrometry (DEMS) pada pemasangan fuel cell telah dilakukan untuk menentukan aktivitas dan selektivitasnya yang dapat ditunjukkan masing-masing oleh hasil arus Faradaic dan efisiensi arus CO₂ dari elektro-oksidasi etanol. Dari hasil percobaan diperoleh bahwa PtCeO₂/C dapat secara signifikan meningkatkan selektivitas untuk membentuk CO₂ dibandingkan terhadap katalis komersial 20% Pt/C dari Alfa Aesar- Johnson Mattews. Kenaikan selektivitas ditunjukkan oleh kenaikan efisiensi arus CO₂ pada oksidasi etanol sebesar 20 persen dibandingkan terhadap katalis rujukan 20% Pt/C (Alfa Aesar-JM).

Kata Kunci : Ceria, Membrane Electrode Assembly (MEA), DEMS, Elektro-Oksidasi Etanol

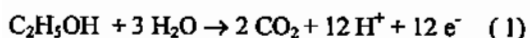
1. Introduction

Direct oxidation fuel cell (DOFC) is one of candidates for application in vehicle and portable power. The advantage of DOFC is that additional equipment like fuel reformer is not necessary. Alcohol and mainly methanol are widely proposed as possible fuel for direct methanol fuel cell (DMFC). One of the main advantages of methanol is its availability, its low price and the easiness of its storage as a liquid. However, there is a problem that methanol is toxic for human. Based on these aspects of DMFC, there are several kinds of fuel which are investigated as a fuel of direct type fuel cell. Ethanol is one of them. It is well known that ethanol is not toxic for human and is easily produced from biomass. This means that carbon dioxide (CO₂) emitted from direct type fuel cell using ethanol as a fuel can be recycled by planting. Ethanol as alternative fuel for direct ethanol fuel cell (DEFC) also has a relative high energy density (8 kWh/kg) and for comparison methanol energy density was 6 kWh/kg.

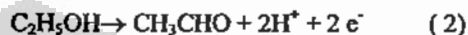
The case of oxidation of ethanol is more complicated than methanol which is necessary to break C-C bond to obtain the total oxidation reaction. To obtain this, it is necessary to modify the structure or composition of anode catalyst. Electrocatalytic oxidation of ethanol using platinum or platinum alloy catalyst has been investigated [1-3], and the products formed by the electrocatalytic oxidation of ethanol and the oxidation reactivity of ethanol were discussed from many aspects. Iwasita and Pastor studied the adsorb behavior of ethanol on a polycrystalline platinum using a differential electrochemical mass spectroscopy (DEMS) and FTIR [1]. They reported many adsorbed species formed by the oxidation of ethanol and observed the evolution of CO₂. The aim of the present paper is to investigate the activity and selectivity of the PtCeO₂/C catalyst for electro-oxidation of ethanol. The result was compared to the commercial Pt/C catalyst from Alfa Aesar-Johnson Matthews.

2. Fundamental

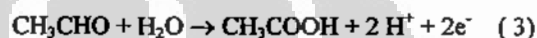
The energy of a chemical reaction depends on difference in energy of the reacting species before and after the complete reaction. In the case of the ethanol the chemical reaction with oxygen can be used in propulsion motors for automobiles. For the electrochemical route, the complete oxidation at the anode to CO₂ is:



using platinum as a basic catalyst for ethanol oxidation, the observed open circuit potential at room temperature is > 0,4 V, i.e., the overvoltage is similar to that of methanol [7]. The main problem in electrocatalysis of ethanol oxidation is the scission of the C-C bond; therefore low yields of CO₂ are observed, in particular at smooth Pt electrodes. The partial oxidation to acetaldehyde and acetic acid release 2 and 4 e⁻ respectively:



and



According to the reaction (1-3) several pathways for the ethanol reaction are possible.

In order to investigate the CO₂ product of ethanol electro-oxidation, in this research work, we conducted the performance test of newly prepared catalyst PtCeO₂/C to CO₂ formation by on-line differential electrochemical mass spectrometry (DEMS). The CO₂ product of ethanol electro-oxidation investigated by calculating the CO₂ current efficiency in real direct ethanol fuel cell setup in this research work.

3. Methodology

In this experiment we used 20% PtCeO₂/C catalyst (prepared at Technical University of Munich) as anode catalyst and 20% Pt/C (Alfa Aesar- Johnson Matthew) as reference catalyst. As cathode catalyst is used 40% Pt/C (from ETEK). Catalyst ink was prepared by mixing the required amount of catalyst powder with 20 % Nafion® solution (Du Pont) to give 30% wt. of Nafion, and then diluted with a mixture of millipore™ water and 2-propanol. The resulting ink then placed in an ultrasonic bath for 10 minutes or until the catalyst powder had fully dispersed. This ink then sprayed onto a piece of carbon Toray paper TGPH 060 which was kept at 110°C throughout the process, in order to assist the binding of the catalyst to the backing layer. The spraying machine consisted of motorised X-Y table controlled by a CNC automation controller. The catalyst layer on carbon paper then sandwiched into carbon paper to make the membrane electrode assembly (MEA)

The DEMS setup which consisted of two differentially pumped chambers, a Balzers QMS 200 mass spectrometer, AGEF potentiostat and computerized data acquisition system. The DEMS

sensor was located at the outlet channel of anode compartment, it consist of a cylindrical detection volume with a diameter of 7 mm and a height of 2 mm through which anode outlet flow passes. This volume is separated from the vacuum system of the mass spectrometer by a Micro porous Teflon membrane (Schleicher & Schuell, TE-30) with a pore size of 0.02 micrometer and a thickness of 110 micrometer. The membrane is supported by a Teflon disc of 2 mm in diameter, with holes.

The fuel cell consisted of two stainless steel plates with integrated serpentine medium distribution channels. Six threaded studs and nuts held the two plates together. The fuel cell can be operated in both modes half-cell and full cell. Generally during the investigation of anode it is used as a half-cell. Cathode with Pt loading ($2.5\text{mg}/\text{cm}^2$) and continuous hydrogen flow works as counter and reference both. Potential of the cathode is assumed to be same as of the reversible -

-hydrogen electrode (RHE). All potential are reported in reference to this. Schematic diagram of DEMS setup is shown in Fig. 1.

The main products of ethanol electro-oxidation are carbon dioxide, acetaldehyde and acetic acid [8]. From those three products, they were only carbon dioxide and acetaldehyde that can be monitored by DEMS measurement because its high volatility. The main problem in DEMS measurement is because the mass number of both CO_2 and CH_3CHO is the same at 44. to monitor both together is not possible at $m/z = 44$. To solve this problem, Fujiwara et al.[4],used deuterated ethanol ($\text{CD}_3\text{CH}_2\text{OH}$) for determining reaction products that had same mass number. Due to the high cost of this material, extensive utilization is limited. To avoid interference between CO_2^+ and CH_3CHO^+ ion current (both at $m/z = 44$), which are the major ethanol electrooxidation products, carbon dioxide and acetaldehyde was monitored at m/z

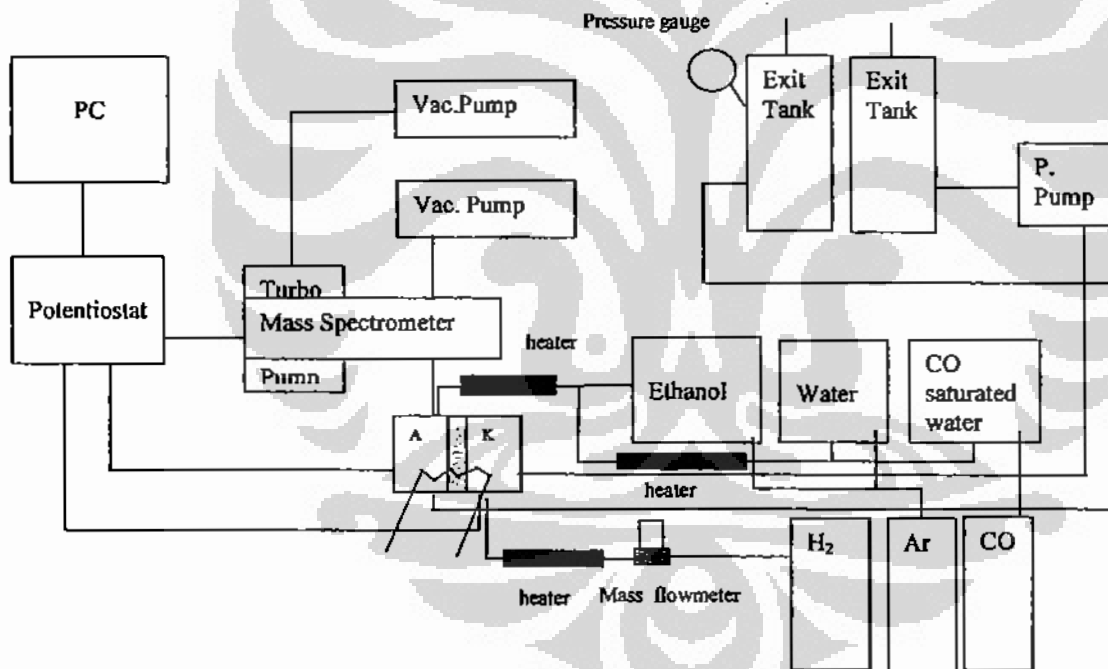


Figure 1. Differential electrochemical mass spectrometry (DEMS) of fuel cell setup

$m/z = 22$ and $m/z = 29$ respectively. The calibration of DEMS for CO_2 is performed with H_2 oxidation current interference and potentiostatic bulk CO oxidation.

Potentiodynamic measurements: Cyclic Voltammogram and Mass Cyclic Voltammogram for ion currents $m/z = 22, 29, 15$ and 30 from $0 - 1.0$ V vs RHE with scanrate 5 mV/s at temperature 90°C . Steady state voltammogram for

ethanol electrooxidation was recorded after several cycles.

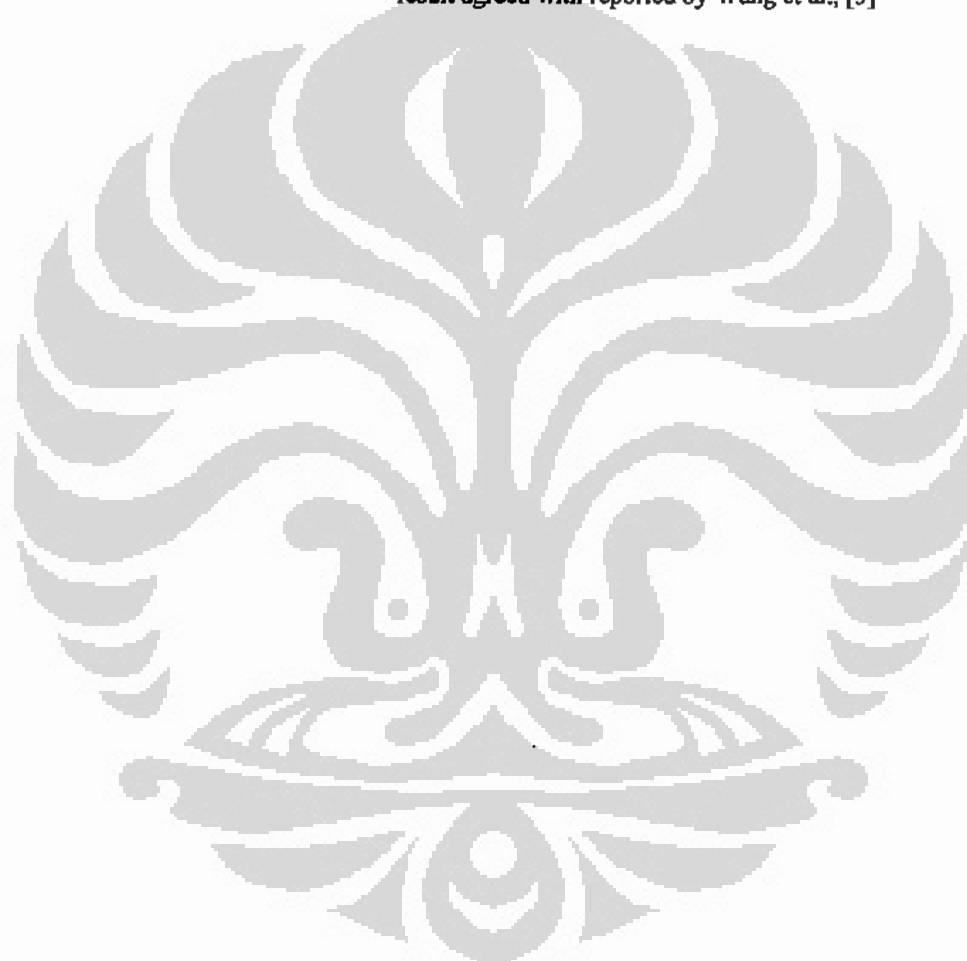
Potentiostatic DEMS measurements: monitoring transient faradaic current and ion mass current by stepping the potential from 0 V vs RHE to $0.5, 0.6, 0.7,$ and 0.8 V vs RHE (10 minutes for each potential step), with scanrate 5 mV/s at temperature 90°C for Cyclic Voltammogram and Mass Cyclic

Voltammogram for ion currents $m/z = 22, 29, 15$ and 30

4. Result and Discussion

Fig. 2 and Fig. 3 show the CV and MSCV for PtCeO₂/C and Pt/C catalyst respectively as function of cell potential by potentiodynamics measurement technique. These figures comprise of cyclic voltammogram (CV) /Faradaic current, and the mass spectrometric cyclic voltammogram (MSCV) for ion currents $m/z = 22, m/z=29, m/z=15,$ and $m/z=30$.

Ion current $m/z=22$ was corresponding to mass spectrometric signal for CO₂ via the doubly ionized molecular ion signal. The onset of CO₂ formation in the positive going scan of the steady state voltammogram took place at ca. 0.47 V vs. RHE for 20% Pt/C catalyst, while for catalyst 20% PtCeO₂/C the onset of CO₂ formation occurred at ca. 0.4 V vs. RHE. The CO₂ formation at rather high potential can be explained because of electro-oxidation of ethanol at potential below ca. 0.4V is largely blocked by adsorbed poisoning intermediates CO and hydrocarbon residues. This result agreed with reported by Wang et al., [5]



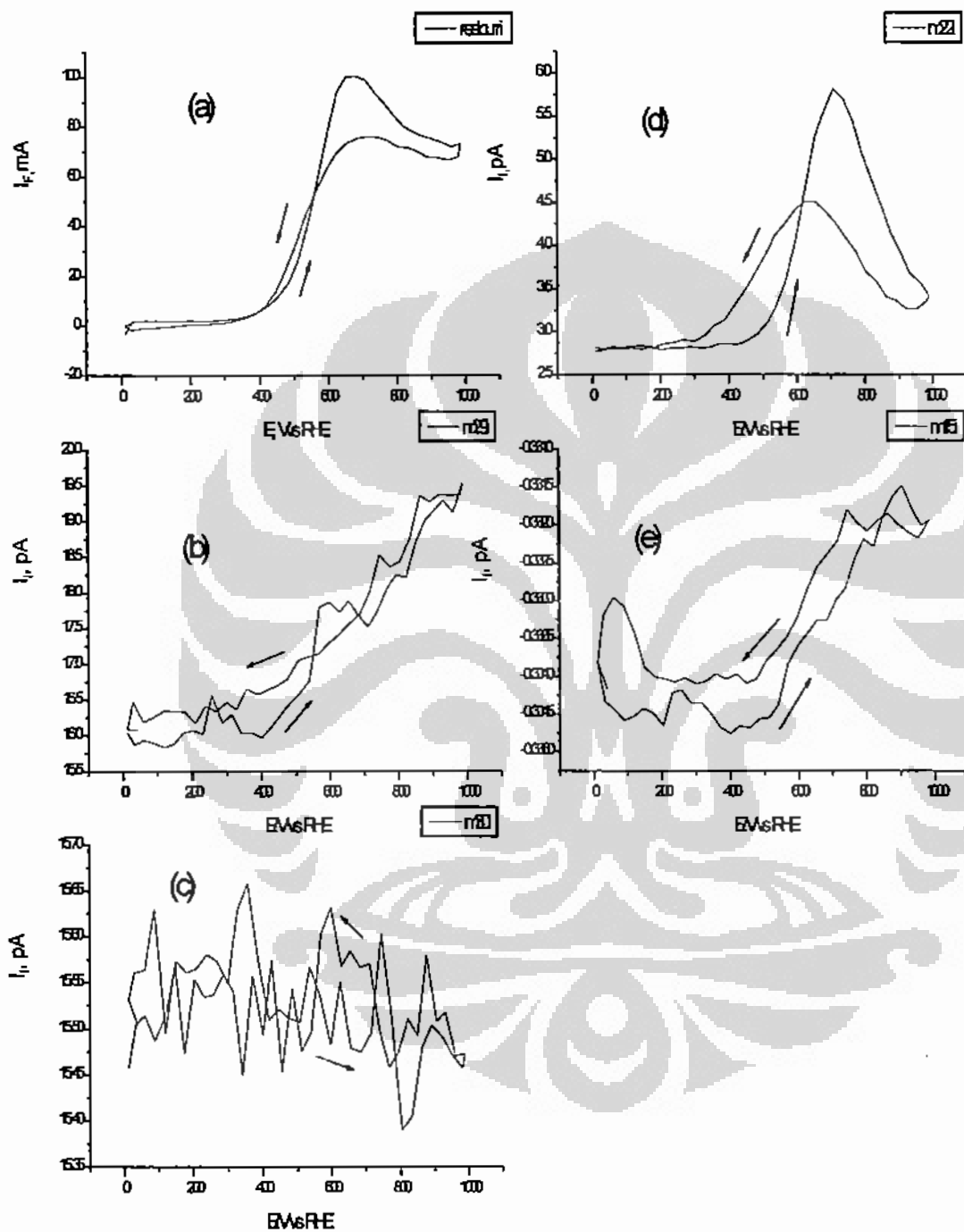


Figure 2. Typical CV and MSCV of 20% Pt-CeO₂/C catalyst at temperature 90°C, ethanol flowrate 5 ml/min, with scanrate 5 mV/s(a) CV (b) MSCV for $m/z = 29$ (c) MSCV for $m/z = 30$ (d) MSCV for $m/z = 22$ and (e) mSCV for $m/z = 15$

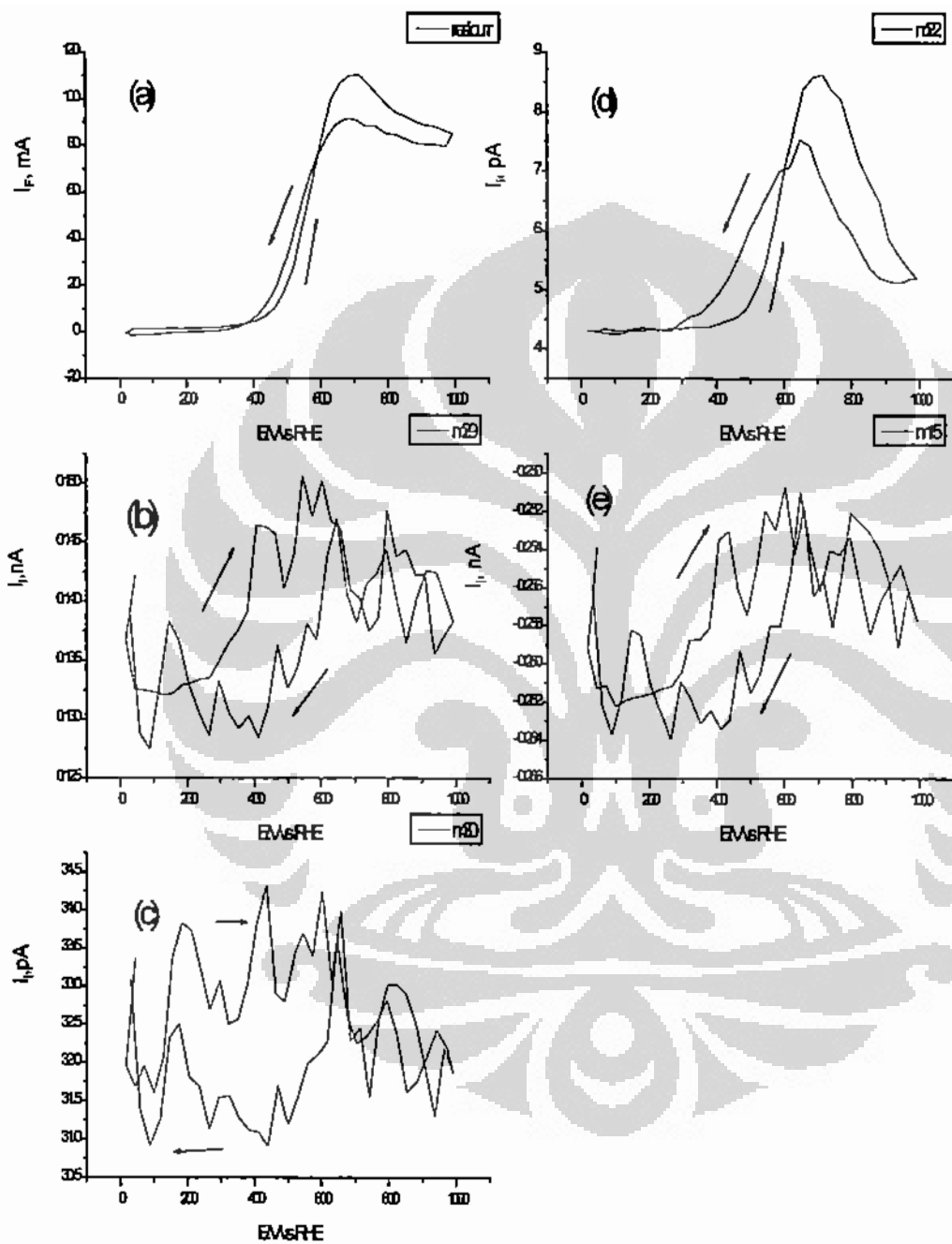


Figure 3. CV and MSCV of 20% Pt/C catalyst at temperature 90°C, ethanol flowrate 5 ml/min, with scanrate 5 mV/s (a) CV (b) MSCV for $m/z = 29$ (c) MSCV for $m/z = 30$ (d) MSCV for $m/z = 22$ and (e) MSCV for $m/z = 15$

Fig. 4 shows the Faradaic current vs potential for different catalysts. Testing performance in DEMS is conducted at temperature 90°C, 5 ml/minute ethanol flowrate, and with scanrate of 5 mV/s by potentiostatic measurements. This result indicated the Faradaic current of modified ceria catalyst (PtCeO₂/C) provided higher current at low potential (up to 0.6 V) in comparison to Pt/C (Alfa Aesar-JM) catalyst reference. This result was reproducible for two different PtCeO₂/C catalysts (denoted 1 and 2). Its mean, addition of ceria on Pt-based catalyst could increase an activity of the catalysts at low potential, although this enhancement in Faradaic current was not so high. In fuel cell applications, improvement of Faradaic current at low potential is more useful compared to the improvement of Faradaic current at high potential. The usual improvement of Faradaic current is until 0.5 V vs RHE. Therefore we want to further investigate increment of Faradaic current at the lower potential by analyzing of ion mass number m/z= 22 as shown in Fig. 5.

Fig. 5 shows relation between CO₂ current efficiency (CCE) versus potential. From this

picture can be seen that increase of Faradaic current which is took place at low potential is followed by significantly improvement of CCE. 20% Pt/C (Alfa Aesar-JM) as our reference catalyst provide lower performance than ceria modified catalysts, especially at low potential (< 0.6 V). Increase of the CO₂ current efficiency, indicated that oxidation reaction was occurred at a total oxidation reaction or mostly happen the C-C bond breaking of ethanol. It was because mostly CO₂ product was result from oxidation of CO_{ad} species of ethanol. These increases in CO₂ current efficiency (CCE) may effect of addition of ceria in the catalyst. The role of ceria in the oxidation of carbon monoxide agreed to what reported by Thi sayle at al. [6] which was followed the reaction:



Where, oxygen was extracted from exposed surfaces of the CeO₂, facilitated by reduction of Ce⁴⁺ to Ce³⁺.

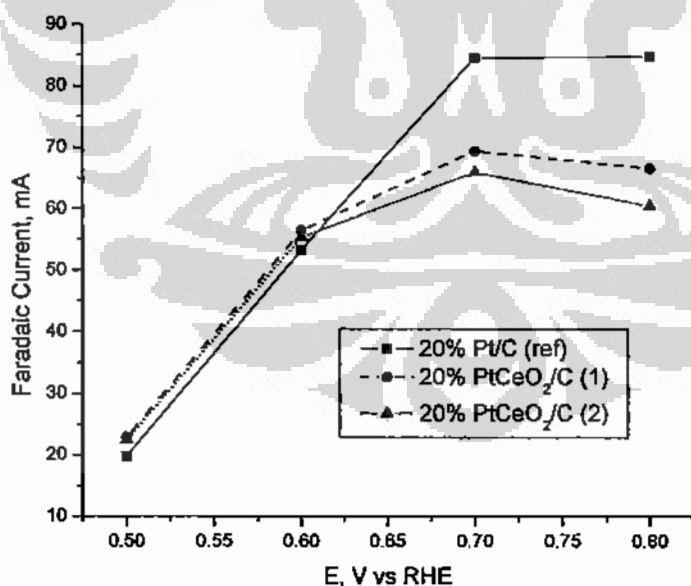


Figure 4. Faradaic current vs. potential, at temperature 90°C, scanrate 5 mV/s, anode catalyst loading 0.8 mg/cm² for 20% PtCeO₂/C (dashed line) and 20% Pt/C Alfa Aesar-JM (solid line), cathode catalyst loading 2.5 mg/cm² (20% Pt/C ETEK).

Fig.6 shows the correlation between CCE to the platinum loading of catalysts. Comparison of 20% PtCeO₂/C catalyst to the 20% Pt/C commercial catalyst which is almost equal in platinum loading (PtCeO₂/C = 0.855 and 0.85 mg/cm² and Pt/C = 0.845 mg/cm²), known that

PtCeO₂/C catalyst provided higher value of CCE. For fuel cell application, by improvement of CCE on PtCeO₂ catalyst in the same catalyst loading will reduce cost of catalyst in comparison to the Pt/C reference catalyst.

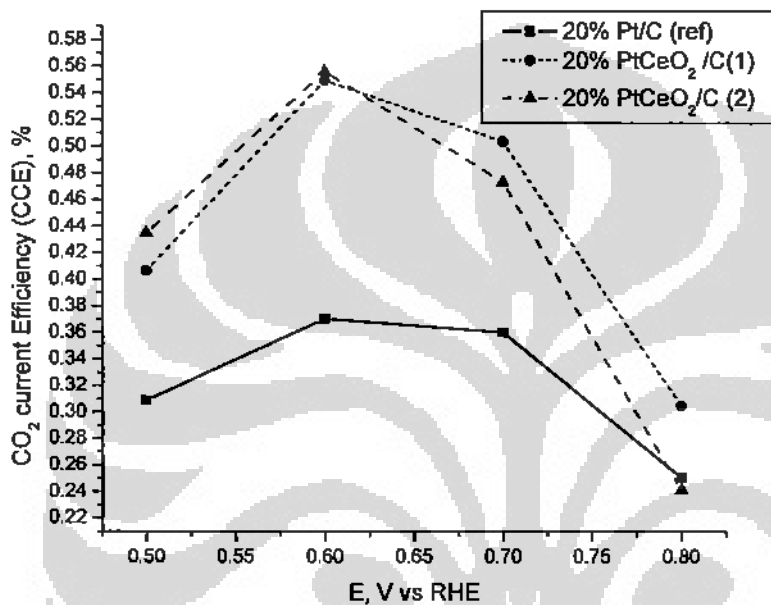


Figure 5. CO₂ current efficiency vs. potential, at temperature 90°C, scanrate 5 mV/s, anode catalyst loading ± 0.8 mg/cm² (20% PtCeO₂/C (1) & (2) (dashed and dot line) and 20% Pt/C Alfa Aesar-JM (solid line)), cathode catalyst loading 2.5 mg/cm² (20% Pt/C ETEK).

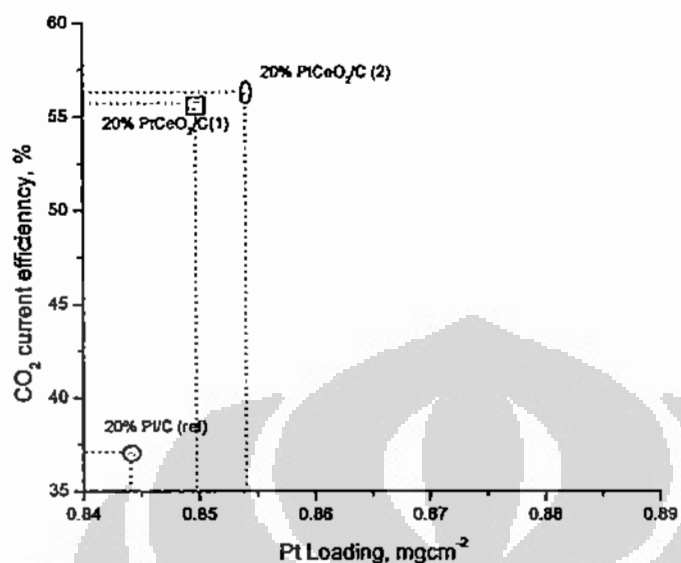


Figure 6. CO₂ current efficiency vs Pt loading catalyst for different catalysts at potential 0.6 V , temperature 90°C, scanrate 5 mV/s, ethanol flowrate 5 ml/min

5. Conclusion

The product of ethanol oxidation reaction (EOR) over Pt/C and PtCeO₂/C catalysts which investigated by in-situ DEMS were CO₂, acetaldehyde, methane, ethane. While acetic acid couldn't detect by DEMS due to its low volatility. Performance comparison from DEMS measurement result between 20% PtCeO₂/C and 20% Pt/C reference catalyst indicated that over PtCeO₂/C catalysts provided higher activity than Pt/C (ref) which is indicated by increase of Faradaic current and provided higher selectivity of the catalysts which is indicated by increasing of CO₂ current efficiency. Both increase of activity and selectivity were occurred at low potential (<= 0.6 V). Improvement of CO₂ current efficiency of ethanol oxidation was about 20 % in comparison to references catalyst of 20% Pt/C (ref).

Acknowledgement

Gratefully acknowledge to Prof. U. Stimming for guidance during this research work at TU-Munich Germany and the Deutscher Akademischer Austausch Dienst (DAAD) for financial support under contract A/03/41170 was also acknowledged.

Notation

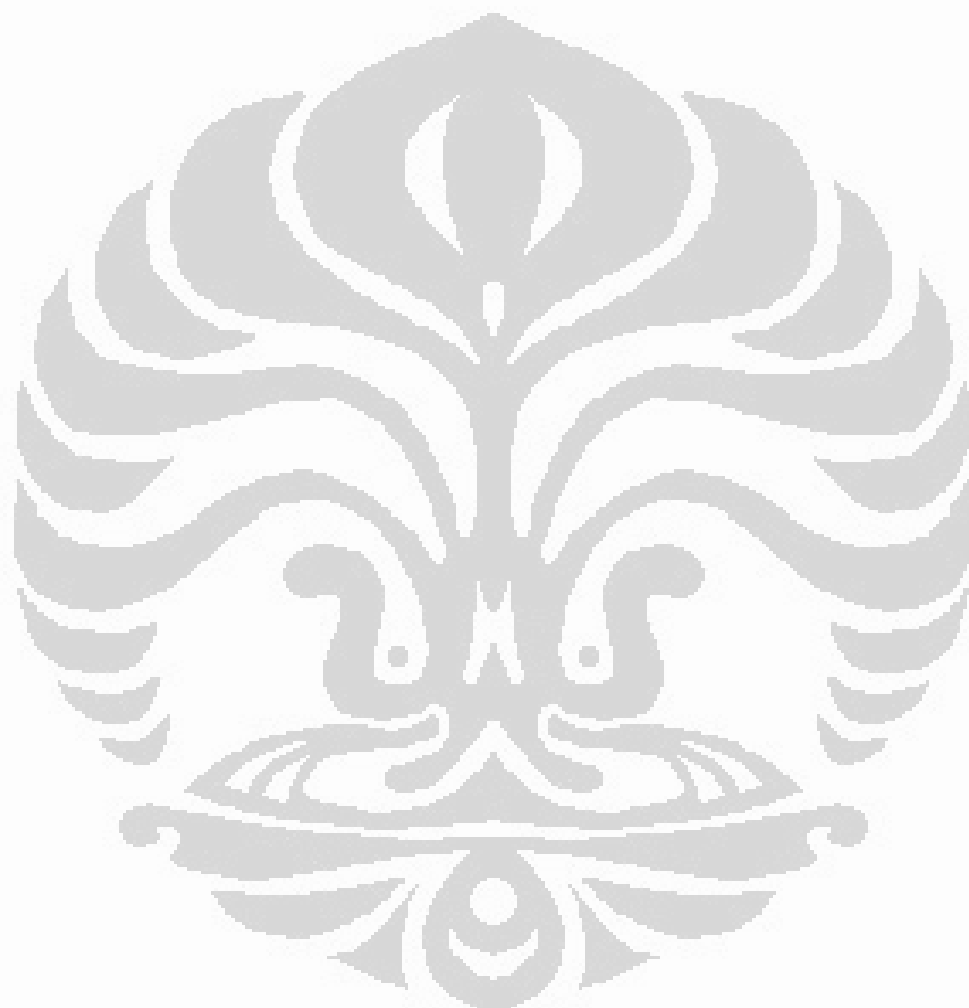
A = Anode

K = Cathode
H₂ = Gas Hydrogen
Ar = Gas Argon
CO = Gas of Carbon Monoxide
PC = Personal Computer
DEMS = Differential Electrochemical Mass Spectrometry
CV = Cyclic Voltammogram
MSCV = Mass spectrometric cyclic voltammogram

References

- [1] Iwasita T., E. Pastor, Parallel pathways of ethanol oxidation: The effect of ethanol concentration, *Electrochim. Acta* 39 (1994) 531.
- [2] Camara G.A., R.B. de Lima, T. Iwasita, Catalysis of ethanol electrooxidation by PtRu: the influence of catalyst composition, *Electrochem. Commun.* 6 (2004) 812.
- [3] Fujiwara N., K.A. Friedrich, U. Stimming, Ethanol oxidation on PtRu electrodes studied by differential electrochemical mass spectrometry, *J. Electroanal. Chem.* 472 (1999) 120.
- [4] Carsten Cremers, Hariyanto, V. Rao, A. Racs, Direct ethanol fuel cells, proceeding workshop of TFI, Duisburg Germany, (2006),76

- [5] Wang H, Z. Jusys, and R. J. Behm, Ethanol Electrooxidation on a Carbon-Supported Pt Catalyst: Reaction Kinetics and Product Yields, *J. Phys. Chem. B* 108, (2004) 19413-19424
- [6] Thi X. T. Sayle, Stephen C. Parker and Dean C. Sayle, *Phys. Chem. Chem. Phys.*, (2005), 7, 2936 – 2941
- [7] Carl H. Hamann, Andrew Hammnet, Wolf Vielstich, *Electrochemistry*, 2nd edition, Wiley-VCH (2007)
- [8] Xia X.H, H.-D. Liess, T. Iwasita, *Early stages in the oxidation of ethanol at low index single crystal platinum electrodes*, *Journal of Electroanalytical Chemistry* 437 (1997) 233-241





PAPER III

**Ethanol electro-oxidation on carbon supported
PtCeO₂ catalyst for direct ethanol fuel cell**



ETHANOL ELECTRO-OXIDATION ON Pt-CeO₂/C CATALYST

Hariyanto^{a,b}, W.W Purwanto^a, Roekmijati.W-Soemantojo^a, U. Stimming^c

^a Department of Chemical Engineering, Faculty of Engineering, University of Indonesia, Depok 16424, Indonesia

^b Energy Technology Center, B2TE-BPPT, Kawasan Puspiptek Serpong 15314, Indonesia

^c Department of Physics, Technical University of Munich, D 85748 Munich-Germany
hariyt@yahoo.com

Abstract

Ethanol appears to be an interesting alternative fuel for direct oxidation fuel cell (DOFC). Electro-oxidation of ethanol was studied on 20% PtCeO₂/C catalyst in this research work. The aim of this present paper is to investigate an effect of addition CeO₂ to the carbon supported Pt catalyst for ethanol electro-oxidation reaction (EOR). Synthesis of PtCeO₂/C is carried out by colloidal methods using ethylene glycol to obtain nanosize particle catalyst. Physical characterization was carried out by X-Ray diffraction and Transmission Electron Microscopy (TEM). Electrochemical characterization of the prepared catalyst was carried out by deposited the catalyst onto gold polycrystalline working electrode with the geometric surface area of about 0.28 cm² and comprised of technique: cyclic voltammetry, CO stripping voltammetry and ethanol electrooxidation. Therefore, EOR was performed in acidic solution (0.5M H₂SO₄) and alkaline solution (0.1M NaOH). As reference electrode was used Hg/Hg₂SO₄ (0.5 M) for acid medium and Hg/HgO (0.1 NaOH) for alkaline medium. X-ray diffraction pattern was indicated that peak of Pt and CeO₂ in the PtCeO₂/C catalyst was existed. Meanwhile, TEM image show the uniform particle dispersion with the mean particle size of catalyst was about 3.2 ± 0.3 nm. Electrochemical characterization results indicated that addition of CeO₂ on carbon supported Pt catalyst could improve its activity for ethanol electro-oxidation in comparison to the reference catalyst 20% Pt/C.

Keywords: ethanol, electro-oxidation, direct oxidation fuel cell, PtCeO₂/C

I. Introduction

In recent years, the development of fuel cell as alternative power sources has become in interest topic of research. Low temperature fuel cell base on proton exchange membrane fuel cell (PEMFC) or hydrogen-oxygen fuel cell is one of type of fuel cell which is rapidly developed by researchers worldwide. It was due to the widely potential application of PEMFC such as for power supply vehicle, portable power or stationary application.

However, hydrogen as fuel in fuel cell is still problematic due to its storage and transportation. The use alternative fuel like alcohols in direct alcohol fuel cells (DAFCs) appears then advantageous for two main reasons: they are liquids (which simplifies the problem of storage) and their theoretical mass energy density is rather high (6.1 and 8.0 kWh/kg for methanol and ethanol, respectively). Direct methanol fuel cell (DMFC) is the most intensively investigated one as the direct type fuel cell. However, there is a problem that methanol is toxic for human. It is well known that ethanol is not toxic for human and is easily produced from biomass. This means that carbon dioxide (CO₂) emitted from direct type fuel cell using ethanol as a fuel can be recycled by planting. This CO₂ recycling leads to balance of amount CO₂ at the atmosphere.

In the case of ethanol as the fuel in a direct ethanol fuel cell (DEFC), the problem is again more complicated than methanol because ethanol contains two atoms of carbon, and a good electro-catalyst towards the complete oxidation of ethanol to CO₂ must activate the C-C bond breaking. Electro-catalytic oxidation of ethanol using platinum or platinum alloy catalyst has been investigated [1-4], and the products formed by the electro-catalytic oxidation of ethanol and the oxidation reactivity of ethanol were discussed from many aspects. Iwasita and Pastor studied the adsorb behavior of ethanol on a polycrystalline platinum using a differential electrochemical mass spectroscopy (DEMS) and FTIR [1].



To increase the electro-reactivity of ethanol is crucial together to obtain its complete oxidation into carbon dioxide which is still a hard challenge [6–9]. Ceria was reported as a good catalyst material in heterogeneous catalysis. The aim of the present paper is to investigate the influence of the modification of Pt by addition of ceria for the electro-oxidation of ethanol. 20% PtCeO₂ catalyst was synthesized by colloidal methods. After carefully physical characterization, activity of the catalyst for ethanol oxidation is tested in half cell electrochemical measurement. As reference catalyst, we used commercial 20% Pt/C catalyst purchased from Alfa Aesar-Johnson Matthews.

II. Experiment

Preparation of PtCeO₂/C catalyst

The research work was initiated by preparation of CeO₂ nano particles by two step precipitation methods [10]. As synthesized CeO₂ and H₂PtCl₆·6H₂O were used as precursors of PtCeO₂/C catalysts. Carbon Vulcan XC-72R from Cabot and ethylene glycol (EG) was used as a support and reducing agent, respectively. Detailed of ethylene glycol method is presented in elsewhere [11,12]. Following is a brief description of the preparation method: the required amounts of H₂PtCl₆·6H₂O was added to the mixture of EG and deionized water with stirring to form homogeneous slurry. The slurry was heated to 160°C and kept at this temperature in an oil bath for 3 h. The slurry was then cooling down to the room temperature while continue stirring. Carbon-XC-72 then added to the slurry and stirring for overnight. Then the black solid sample was filtered, washed and dried at 80°C for 10 h in a vacuum oven. The nominal loading of Pt in the catalysts was 20 wt.%.

Characterization of catalysts

X-Ray Diffraction measurement of the catalyst is carried out by using instrumentation of Bruker D8 Advance diffractometer equipped with a Cu anticathode, adjustable divergence slit, graphite monochromator on the diffracted beam and proportional detector. Data acquired at 2θ range from 20 to 65°, scan step of 0.02° and fixed counting time of 6 s for each step.

TEM measurement was carried out by using instrumentation of JEOL JEM 2000 EX. Sample preparation on holey carbon Cu-grids TEM 120 keV bright field dry preparation on grid data storage 1024x1024, 150 kX magnification.

Electrochemical characterization

The cyclic voltammetry spectra were recorded using a potentiostat/galvanostat (autolab model PG30). Ten milligram of Pt-based catalyst was suspended in 300 μl of distilled water and 500 μl of 0.1 % Nafion® solution to prepare catalyst ink. Then 13 μl of ink was transferred with an injector to clean gold disk electrode (with area of 0.2826 cm²). After the ethanol volatilization, the electrode was heated at 60°C for 5 min.

For surface area determination, CO stripping voltammetry by CO adsorption method was used. The electrochemical active surface area (S_{co}) was determined as follows:

$$S_{co} = \frac{Q_{co}}{0.420 \text{ mC cm}^{-2}} \quad (1)$$

Where Q_{co} was CO stripping charge (in mC) determined after CO adsorption, and 0.420 mC cm⁻² correspond to a monolayer of adsorbed CO.

For acid medium, a mixture solution containing 0.5M H₂SO₄ and 1.0 M ethanol was used as electrolyte, which was saturated by pure argon in order to expel oxygen in the solution. The scan rate was 10 mV/s, and a Hg/Hg₂SO₄ (0.5 M) was used as reference electrode, and a platinum wire was used as counter electrode.

For alkaline medium, a mixture solution containing 0.1M NaOH and 1.0 M ethanol was used as electrolyte, which was saturated by pure argon in order to expel oxygen in the solution. The scan rate was 10 mV/s, and a Hg/HgO (0.1 M NaOH) was used as reference electrode, and a platinum wire was used as counter electrode.

III. Result and Discussion

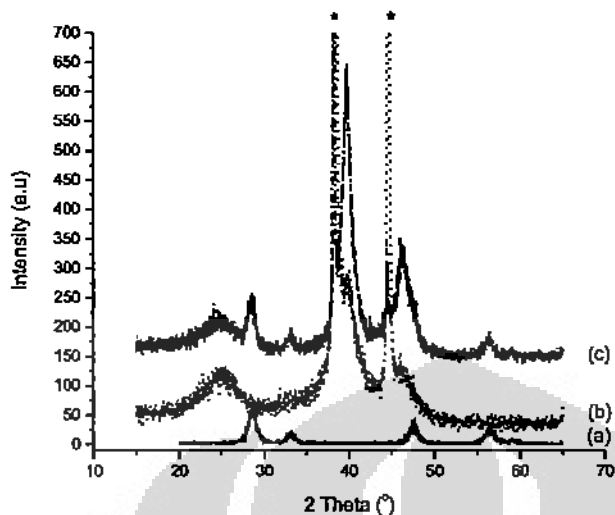


Figure 1 XRD pattern of (a) CeO₂ (b) Pt/C (JM) and (c) Pt-CeO₂/C

The XRD patterns of Pt/C and Pt-CeO₂/C were shown in Fig. 1. From the Fig. 1 (a), the characteristic peaks located at 2θ : 28.5°, 33.1°, 47.5°, 56.3° and 59.01° are corresponding to (1 1 1), (2 0 0), (2 2 0), (3 1 1) and (2 2 2) planes, respectively. These match well with the peaks of cubic fluorite CeO₂ crystal structure in XRD-pattern database. Fig 1 (b), represent the XRD pattern of commercial catalyst Pt/C (JM). The first peak at $2\theta \approx 23^\circ$ originates from the Vulcan XC-72 carbon support. The peaks at $2\theta \approx 40.04^\circ$ are reflections of the face centered cubic (f.c.c) crystal lattice of Pt (111). The peaks indicated with a star (*) was due to the sample holder. Fig.1 (c) presented the XRD pattern of PtCeO₂/C catalyst. All of the peak which is corresponding to CeO₂, platinum and carbon was exist in the XRD pattern result.

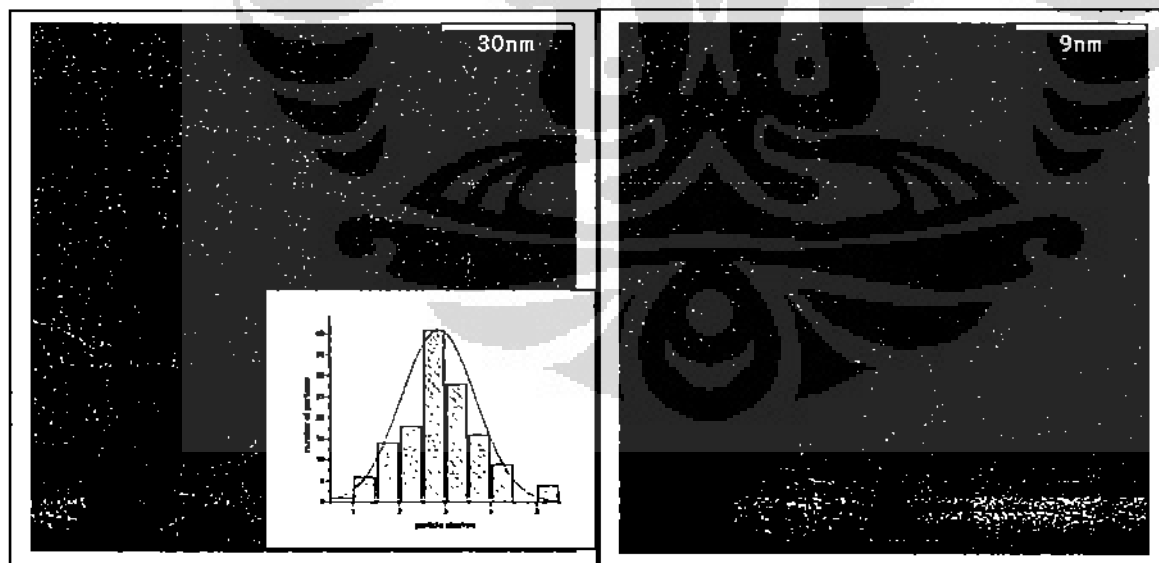


Figure 2 TEM and High Resolution of TEM (HRTEM) of PtCeO₂/C catalyst and as prepared CeO₂

High resolution transmission electron microscopy (HR-TEM) with 500 kX magnification picture for CeO_2 was shown in Fig.2. The particle size of the CeO_2 crystal is about 8-9 nm. As prepared nanoparticle CeO_2 then used as modifier in PtCeO_2/C catalyst.

The particle size (d_{XRD}) of the samples can be estimated from XRD patterns by applying the full-width half-maximum (s) of the characteristic (1 1 1) peak to the Scherrer equation. By this method, the estimated particle size of PtCeO_2/C was about 3.1 nm. The values of the mean particle size obtained by TEM analysis was about 2.9 ± 0.3 nm and was almost in good agreement with those calculated from the XRD results. The TEM results show that the present method is suitable to prepare nanometer-sized PtCeO_2/C catalysts.

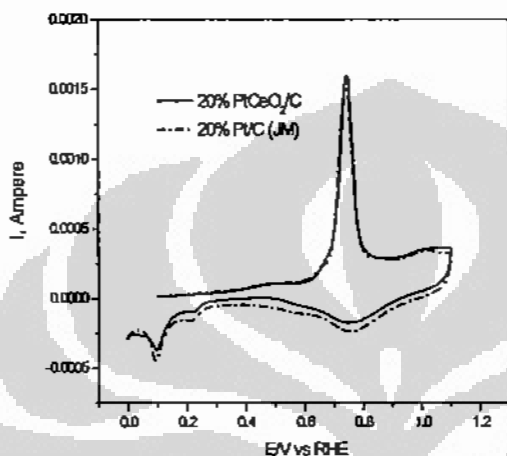


Figure 3 CO stripping voltammetry for Pt/C and PtCeO_2/C catalysts

Fig. 3 shows the CO stripping voltammetry for Pt/C and PtCeO_2/C catalysts. CO stripping charge was determined by integrate a peak from first CV scan. Therefore, the electrochemical active surface area (EAS) of both catalysts can be calculated by using equation (1). The EAS of Pt/C and PtCeO_2/C was about 23.8 cm^2 and 23.9 cm^2 respectively. It means that by adding ceria on Pt/C catalyst would not reduce the EAS of the catalyst and we could easily compare the performance of PtCeO_2/C with our reference catalyst.

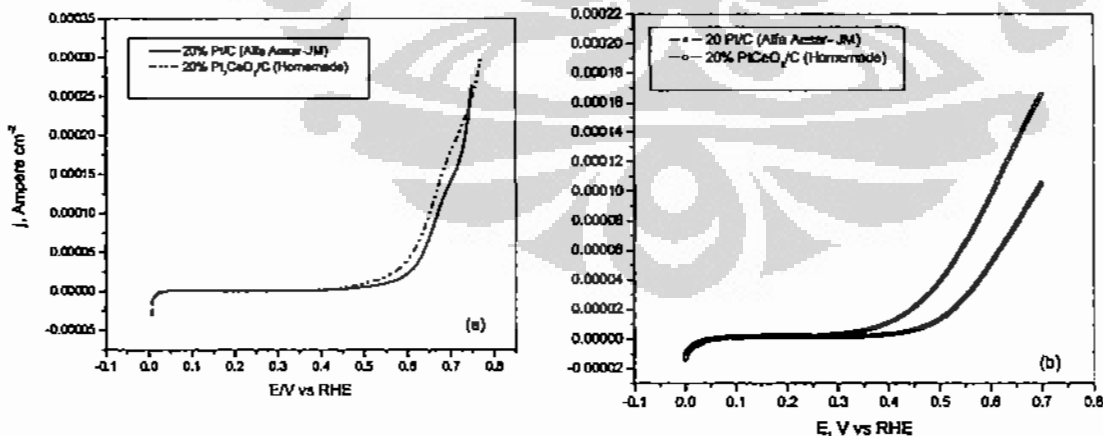


Figure 4 (a) EOR on PtCeO_2/C in acidic medium (b) EOR on PtCeO_2/C in alkaline medium



Activities of the catalysts were electrochemically tested in half cell arrangement. The electrochemical testing was carried out either in acid or alkaline medium. It is well known that in alkaline medium ethanol electrooxidation reaction (EOR) over Pt catalyst was more active than in acid medium. However, increasing of performance of PtCeO₂/C catalyst in alkaline medium was higher than in acid medium. It was shown by the onset oxidation potential which shifted to more negative potential in alkaline medium. Over PtCeO₂/C catalyst, the onset oxidation potential was about 0.3 V vs. RHE, while over Pt/C catalyst was about 0.44 V vs RHE. Increasing Faradaic current over PtCeO₂/C at potential 0.6 V vs. RHE was about factor of 2 compared to the reference catalyst. The higher activity in alkaline medium probably due to the C-C bond breaking could easily happen in this medium. In order to further study of the reaction product of EOR, in the next will be carried out experiment by in-situ differential electrochemical mass spectrometry in fuel cell setup.

IV. Conclusion

Electro-oxidation of ethanol is a very complex reaction because several reaction products and intermediates may be formed. Electro-oxidation of ethanol on PtCeO₂/C either in acid medium or in alkaline medium could increase the activity of the catalyst in comparison to the Pt/C reference catalyst. The increase performance at potential 0.6 V vs RHE over PtCeO₂/C catalyst was about factor of 1.5 in acid medium and factor 2 in alkaline medium compared to the reference Pt/C commercial catalyst.

Acknowledgment

We thank to Dr. Cristina Tealdi (Univ. Pavia Italy) for X-ray Diffraction measurement and Petra Belle for TEM measurement and discussion. Financial support by DAAD under contract A/03/41170 was also acknowledged.

References

- [1.] T. Iwasita, E. Pastor, *Electrochim. Acta* 39 (1994) 531.
- [2.] J.P.I. Souza, J.B. Rabelo, I.R. de Moraes, F.C. Nart, *J. Electroanal. Chem.* 420 (1997) 17.
- [3.] N. Fujiwara, K.A. Friedrich, U. Stimming, *J. Electroanal. Chem.* 472 (1999) 120.
- [4.] G.A. Camara, R.B. de Lima, T. Iwasita, *Electrochem. Commun.* 6 (2004) 812.
- [5.] E.V. Spinace, A.O. Neto, M. Linardi, *J. Power Sources* 129 (2004) 121.
- [6.] H. Hitmi, E.M. Belgsir, J.-M. Léger, C. Lamy, R.O. Lezna, *Electrochim. Acta* 39 (1994) 407.
- [7.] T. Iwasita, E. Pastor, *Electrochim. Acta* 39 (1994) 531.
- [8.] X.H. Xia, H.D. Liess, T. Iwasita, *J. Electroanal. Chem.* 437 (1997) 233.
- [9.] S.C. Chang, L.W. Leung, M.J. Weaver, *J. Phys. Chem.* 94 (1990) 6013.
- [10.] Boro Djuricic and Stephen Pickering, *Journal of the European Ceramic Society* 19 (1999) 1925-1934
- [11.] Hariyanto, W. Purwanto, ethanol electrooxidation on Pt-based catalyst, Seminar Nasional Teknik Kimia, UNSRI, Palembang, 2006
- [12.] Christina Bock, Chantal Paquet, Martin Couillard, Gianluigi A. Botton, and Barry R. MacDougall, *J. AM. CHEM. SOC.* 2004, 126, 8028-8037



PAPER IV

Direct alcohol fuel cell

Direct Alcohol Fuel Cells

Carsten Cremers, Hariyanto, Vineet Rao, Alexander Racz, Werner Seliger, Franz Schweiger, Ulrich Stimming

Abstract—Alcohols can be derived from biomass and offer energy densities similar to liquid hydrocarbons. They are therefore attractive fuels for direct converting fuel cells, even in the low temperature regime. Nevertheless, some improvements are still needed to achieve acceptable power densities in low temperature fuel cells, in particular if alcohols with C-C bonds like ethanol are used as fuels. To achieve this goal, improved catalysts with better reaction kinetics are required, as well as improved electrode structures. It would be also an advantage, if the operating temperature of the cells could be increased around 200 °C. In this paper we present some results of ongoing work in the areas of fuel cell catalysts development, fuel cell electrode structures and high temperature proton conducting membranes.

Index Terms—Direct Alcohol Fuel Cells, Methanol, Ethanol, Anode Catalyst, Cathode Catalyst, High Temperature PEMFC

INTRODUCTION

Fuel cells employing alcohols directly as fuel – direct alcohol fuel cells (DAFC) – are attractive power sources for mobile, stationary and portable applications. In such fuel cells the alcohol is directly fed to the anode, where it is oxidised, while oxygen taken from air is reduced at the cathode. Using alcohols directly as fuels, any problem related to the production, purification, distribution or storage of hydrogen can be avoided. In addition alcohols provide energy densities of e.g. methanol 6 kWh/kg, ethanol 8 kWh/kg or ethylene glycol 5.29 kWh/kg, which are comparable to those of hydrocarbon fuels like petrol. Also no additional weight and volume for a fuel processor is necessary.

In order to achieve competitive power densities still some improvements, for the electrode processes on the anodic and cathodic side in particular, are necessary. Using catalysts presently available, the anodic oxidation of alcohols is quite slow, therefore high amounts of catalysts are required increasing the costs of the fuel cells. The problem becomes even more prominent when alcohols with C-C bonds like ethanol are used as fuel instead of methanol. At the same time the oxygen reduction has likewise slow kinetics which is further hindered by

alcohols crossing the membrane. So, the primary development targets are to find anode catalysts having a higher activity for the alcohol oxidation and to find cathode catalyst having a higher selectivity towards the oxygen reduction reaction. In addition, a further enhancement of the catalyst utilisation in the electrode layer of the membrane electrode assembly (MEA) is required. This can be achieved by improving the simultaneous connection of the catalyst particles to the ion and the electron conducting phases, as well as by improving the transport of the reactants to the catalysts by facilitating mass transport in the catalyst layer, e.g. through a more open porous structure.

To further improve the oxidation kinetics for the alcohols, additionally an increase of the operating temperature of the cells would be highly beneficial. Using standard polymer electrolyte membranes this option is limited by the temperature stability of the membrane and the loss of humidification, needed to maintain a high conductivity. New membrane materials allowing for a higher operating temperature about 200 °C would therefore be a plus.

In this paper we will present results on the some ongoing work covering the different topics introduced above. Based on these results we further show that joining our

forces will help to develop direct alcohol fuel cells for the Indonesian market.

Catalyst Developments

Alcohol tolerant cathode catalyst

The formation of a mixed potential at the cathode of direct methanol fuel cells (DMFC) by methanol crossing the membrane is one of the important problems of DMFC. Therefore, numerous efforts have been made to find methanol tolerant cathode catalysts. One of the most promising approaches is the use of ruthenium modified with selenium. Such catalysts were first proposed by Alonso-Vante and co-workers [1,2] and are currently investigated by a number of groups [3,4,5]. One of the main drawbacks of these materials is their still low activity for the oxygen reduction reaction (ORR) compared to platinum. In this work the possibility to increase the activity by applying the catalyst onto an appropriate supporting material, e.g. Cabot Vulcan XC-72R carbon black, was investigated. To prepare the supported catalyst the synthesis used by Alonso-Vante and co-workers [1,2] was modified. Selenium was dissolved in refluxing *o*-xylene under vigorous stirring. At the same time the support material was dispersed in *o*-xylene at room temperature. Then the desired amount of $\text{Ru}_3(\text{CO})_{12}$ was added to this dispersion and dissolved and the prepared mixture was slowly added to the refluxing selenium solution using a dropping funnel. The reaction mixture was subsequently kept refluxing for 20 hours. After letting cool down the mixture, the solid product was filtered off and thoroughly rinsed with diethyl ether on the funnel and dried in air at ambient conditions. In this way catalysts with a varying ratio of ruthenium to selenium were prepared. The catalysts were characterised structurally by XRD, and TEM-EDX measurements. Electrochemically, the activity for the oxygen reduction reaction (ORR) was determined by rotating disk electrode (RDE) measurements on a gold disk. Furthermore, the electrochemically active surface area was determined by Cu under potential deposition.

Finally MEA were prepared and tested in full cell tests.

The results showed that the highest activity is obtained for a 3:1 weighted-in ratio of Ru:Se. Analysis of some nanoparticles from this sample revealed that the Se concentration in the nanoparticles themselves is even lower at about Ru:Se = 9:1. However, the activity for the ORR is still lower than for state-of-the-art Pt catalysts, resulting in an overpotential which is about 100 mV higher than for a commercial 40% Pt/C reference catalyst by E-TEK. However, the electrochemically active surface area of the catalyst was likewise small, in the range of a few square meters per gram of metal, so that the activity per active surface area compares to that of the Pt-based catalyst in absence of methanol. Due to the methanol tolerance of the RuSe_x/C catalysts it can be expected, the activity per active surface area in presence of methanol will be higher than that of the Pt/C reference.

Fuel cell tests showed a lower performance for MEA with RuSe_x/C cathode compared to MEA with a Pt/C cathode. In contrast to MEA with Pt/C cathode however, the MEA using RuSe_x/C at the cathode proved to be tolerant for very high methanol concentration at the anode side (up to 10 mol/l) which lead to a severe performance breakdown with Pt-based cathode electrodes.

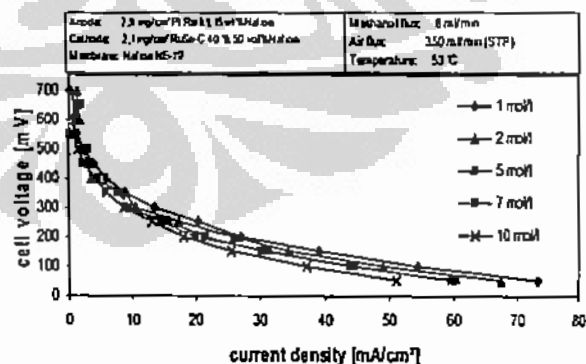


Fig. 1: U-I curves for DMFC with a RuSe_x/C cathode operating with anode feeds of different methanol concentration. Cell performance is almost not influenced by the methanol concentration on the anode side.

Some preliminary tests for the ORR in presence of ethanol showed that the double

layer capacity of RuSe_x/C catalysts gets reduced in the presence of ethanol. But no influence on the ORR reaction kinetics has been found so far.

Anode catalysts for the Ethanol oxidation

Compared to the situation with methanol the current densities achieved in the oxidation of ethanol in PEM type fuel cells are quite low. The highest activity for this reaction is usually found with PtSn/C catalyst with a Pt:Sn ratio in the order of 3:1 [6-8]. PtRu/C catalysts, which have the highest activity in methanol oxidation, don't promote the ethanol oxidation reaction as strongly. It is commonly accepted that the rate determining step of the ethanol oxidation reaction will comprise the scission of the C-C bond. From heterogeneous catalysis it is known that ceria (CeO_2) is a good supporting material for catalysts used in the total oxidation of alcohols like ethanol. However, a direct utilisation of ceria as support of an electrocatalyst will fail most likely, due to the limited electronic conductivity of the material. Therefore, the effect of the addition of a ceria layer onto the standard carbon support, Cabot Vulcan XC-72R, on the activity of a supported Pt catalyst for the ethanol oxidation reaction was studied. To apply the ceria layer onto the Vulcan support, the support was dispersed in a solution of $\text{Ce}(\text{NO}_3)_3$. The pH of this solution was set to 10 by adding ammonium hydroxide solution. Then the $\text{Ce}(\text{III})$ was oxidised to $\text{Ce}(\text{OH})_4$ by adding hydrogen peroxide. Finally the Vulcan support with the precipitated $\text{Ce}(\text{OH})_4$ was filtered-off, dried and calcined at 500°C in air. On this prepared carbon-ceria support platinum nanoparticles were deposited using ethylene glycol reduction method [9,10]. The obtained catalysts were characterised by XRD, SEM (EDX) and TEM (EDX) measurements. The activity towards the ethanol oxidation reaction was studied at a thin film of catalyst applied to a gold electrode immersed into a sulphuric acid solution of ethanol. The TEM and SEM analysis shows that CeO_2 gets deposited as amorphous clusters

onto parts of the carbon surface. Well defined Pt-particles have so far mainly been found in regions where no ceria was present. Nevertheless, a strong increase of activity for the ethanol oxidation was found for the catalyst with ceria compared to a pure Pt/C catalyst.

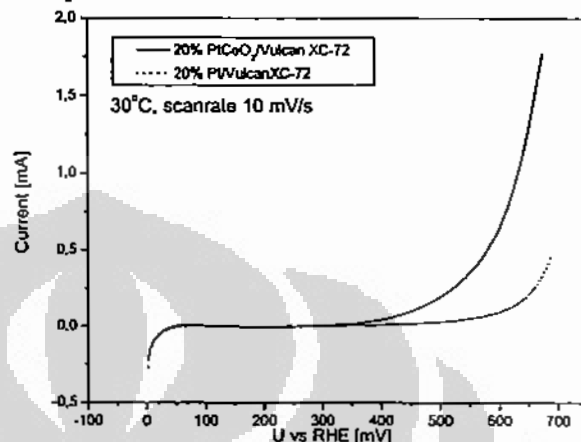


Fig. 2: Linear sweep voltammograms of the ethanol oxidation at thin film electrodes using PtCeO_2/C and Pt/C catalysts, respectively

In CO stripping experiments a second CO oxidation peak was found shifted to lower oxidation potentials, while the peak found at the same position as for pure Pt/C remained. The relative intensity of both peaks correlated with the relative amount of Pt and ceria used in the synthesis. The lower potential peak becomes relatively more important if Pt/ CeO_2 ratio is decreased.

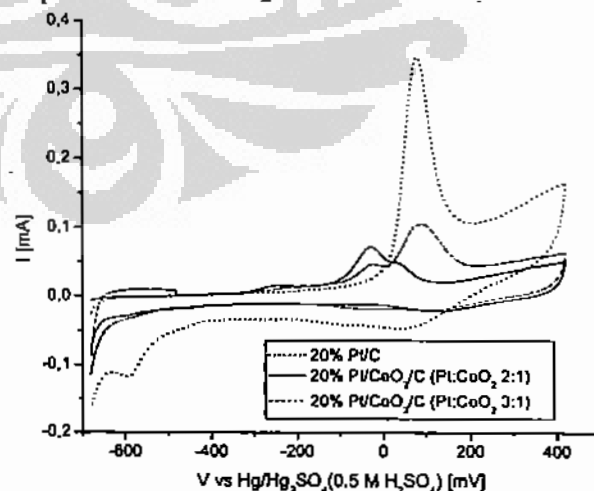


Fig. 3: CO Stripping experiments at supported platinum catalyst with 20 wt% of platinum and different amounts of ceria.

Ethanol oxidation at gas diffusion electrodes

The ethanol oxidation at gas diffusion electrodes was studied by differential electrochemical mass spectroscopy (DEMS). In these studies mainly a commercial 40 % Pt/C-catalyst by E-TEK was employed. Additional tests were made with unsupported Pt black catalyst and a 20 % PtSn/C catalyst provided by the Dalian Institute of Chemical Physics. In the experiments the CO₂ efficiency of the ethanol oxidation was studied as a function of oxidation potential, cell temperature and catalyst loading. As expected the CO₂ efficiency increased with temperature, so that CO₂ efficiencies of more than 90% are achievable for temperatures above 90 °C. CO₂ efficiency also depends on the anode potential. Here the experiments show that CO₂ efficiency strongly decreases if the potential is raised above 0.5 V vs. NHE. But the dominant effect seems to be the catalyst loading. High CO₂ efficiencies could only be realised at high catalyst loadings of about 5 mg/cm². A more detailed description of the results will be given elsewhere [11].

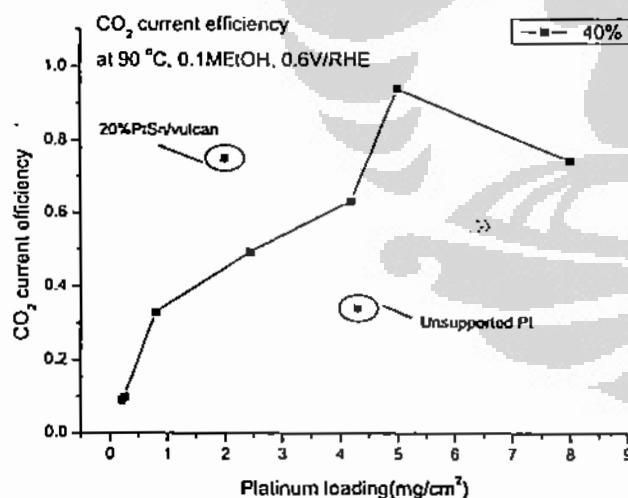


Fig. 4: CO₂ conversion efficiency of the ethanol oxidation as function of the platinum loading. All values, except the both circled ones, were determined for a 40 % Pt/C catalyst by E-TEK

Influence of support materials on the methanol oxidation reaction at gas diffusion electrodes

Using an electro-catalyst in a gas diffusion electrode (GDE) instead of a thin-film electrode, results in a number of additional requirements. So the condition of the three phase boundary, i.e. the simultaneous contact to the ion and electron conducting phases and the reactant room is much more difficult to fulfil than in a thin-film electrode, especially if compared to a situation where the latter is immersed into a liquid electrolyte. To achieve the goal of a high catalyst utilisation, also under the condition of a GDE with a solid electrolyte, the choice of an appropriate support is of high importance.

One of the parameters influencing the catalyst performance is the surface area and structure of the support. In a recent work the influence of the BET surface area S_{BET} of the carbon support on the catalyst activity for the methanol oxidation reaction was studied in a systematic way. Using SibunitTM type of support, provided by the Boreskov institute of catalysis, the S_{BET} of the support could be adjusted without modifying other properties of the support. In that way supported PtRu-catalysts using supports with S_{BET} ranging from 1 to 412 m²/g were tested for the methanol oxidation at gas diffusion electrodes. Thereby it was shown, that the achievable mass activity of the catalyst decreases with increasing surface area of the support [12].

Another approach to increase catalysts utilisation is to use support materials which do exhibit proton conductivity themselves. In this case, problems, related to the incorporation of a solid electrolyte into the electrode structure for the ionic contact to the catalyst particles, are reduced. One potential support of this kind is hydrous ruthenium oxide which was investigated in a recent study. In this study it was shown, that the mass activity for CO stripping can be increased significantly compared to a Vulcan XC-72R supported catalyst using hydrous ruthenium oxide as support instead. At the same time the amount of Nafion binder

Acknowledgements

We like to acknowledge the partially financial support of this work by the following organisations:

- 1 Deutsche Forschungsgemeinschaft (DFG), contracts Sti 74/14-1, Sti 74/16-1 and Sti 74/17-1
- 2 Sino-German Center for Science Promotion Beijing, contracts GZ 210 (101/10), GZ 211 (101/11) and GZ 218 (101/16)
- 3 Deutsches Bundesministerium fuer Bildung und Forschung (BMBF) in the framework of the O2RedNet contract 01SF0302
- 4 Bayerisches Staatsministerium fuer Wirtschaft, Infrastruktur, Verkehr und Technology (BStMWVT), contract 1303/89266/824/02
- 5 Carl von Linde Stiftung
- 6 Deutscher Akademischer Austausch Dienst (DAAD) for the fellowship granted to Hariyanto under contract A/03/41170

- 1 Carsten Cremers, Bavarian Center for Applied Energy Research (ZAE Bayern), Division 1, Walther-Meissner-Str. 6. 85748 Garching, Germany (corresponding author, phone +49-89-32944229, fax +49-89-32944212, email Cremers@muc.zae-bayern.de)
- 2 Hariyanto, Technical University of Munich, Department of Physics E19, James-Frank-Str. 1, 85748 Garching, Germany (email: hyanto@ph.tum.de) and University of Indonesia, Chemical Engineering Study Program, Faculty of Engineering, Jakarta, Indonesia
- 3 Vineet Rao, Technical University of Munich, Department of Physics E19 (email: vrao@ph.tum.de)
- 4 Alexander Racz, Technical University of Munich, Department of Physics E19 (email: aracz@ph.tum.de)
- 5 Werner Seliger, ZAE Bayern, Division 1 (email: Seliger@muc.zae-bayern.de)
- 6 Franz Schweiger, ZAE Bayern, Division 1 (email: Schweiger@muc.zae-bayern.de)
- 7 Ulrich Stimming Technical University of Munich, Department of Physics E19, and ZAE Bayern Division 1 (corresponding author: phone: +49-89-28912532, fax: +49-89-28912530, email: Stimming@ph.tum.de)



PAPER V

**Investigation of the ethanol electro-oxidation in alkaline
membrane electrode assembly by differential
electrochemical mass spectrometry**



Investigation of the Ethanol Electro-Oxidation in Alkaline Membrane Electrode Assembly by Differential Electrochemical Mass Spectrometry

V. Rao^{1*}, Hariyanto¹, C. Cremers^{2a}, and U. Stimming^{1,2}

¹ Department of Physics E19, Technische Universität München (TUM), James-Frank-Str. 1, D-85748 Garching, Germany

² Bavarian Center for Applied Energy Research [ZAE Bayern], Walther-Meißner-Str. 6, D-85748 Garching, Germany

Received May 24, 2007; accepted September 12, 2007

Abstract

The fuel cell differential electrochemical mass spectrometry (FC-DEMS) measurements were performed for studying the ethanol oxidation reaction (EOR), using alkaline membrane electrode assemblies (MEAs) made up of nanoparticle Pt catalyst and alkaline polymeric membranes. The obtained results indicate that in an alkaline medium, ethanol undergoes significantly more complete electro-oxidation to CO₂ than in an acidic MEA using the same Pt anode. The CO₂ current efficiency (CCE) can be compared for acidic and alkaline MEA with similar electrochemical active area on the anode side. The CCE estimated, in case of alkaline MEA with Pt anode, is around 55% at 0.8 V/RHE, 60 °C and 0.1 M ethanol. In comparison, under similar conditions, acidic MEAs using the same anode catalyst show only 2% CCE. This might indicate that the C-C bond scission rates are much higher in alkaline media. However, the mechanism

of ethanol oxidation in alkaline media is not exactly known. CO₂ produced in electrochemical reaction forms soluble carbonates in the presence of aqueous alkaline electrolyte. This makes it difficult to study ethanol oxidation in alkaline media using FTIR or model DEMS systems. The alkaline polymer electrolyte membranes as used in this study for making alkaline MEAs provide an important opportunity to observe CO₂ produced during EOR using FC-DEMS system.

Keywords: Alkaline Anion Exchange Membranes (AAEM), CO₂ Current Efficiency (CCE), Direct Ethanol Fuel Cell (DEFC), Electrocatalysis, Ethanol Electro-Oxidation, Fuel Cell, Fuel Cell Differential Electrochemical Mass Spectrometry (FC-DEMS)

1 Introduction

Acidic proton exchange membranes (PEM) have been used in fuel cells because of their high proton conductivity and mechanical stability. Furthermore, these membrane materials are rather easily available as they are widely used in chlor-alkali electrolysis, which also helped their adoption into fuel cells. By adding the ionomer in the catalyst layer, which provided the necessary proton conductivity, the reaction interface is extended

from the catalyst-membrane interface into the catalyst layer. This made the membrane electrode assembly (MEA) more efficient with respect to current and power density. The completely solid phase MEA, without the need of any liquid electrolyte, is highly desirable as it avoids heavy corrosion problems within the whole fuel cell system. However, despite all the above-mentioned advantages, the acidic membranes are highly disadvantageous with regard to the kinetics of almost all major fuel cell processes. In particular, the oxidation of any organic fuel, e.g. methanol in DMFC, is kinetically much slower in acidic media than in alkaline medium. The over-voltage losses are compara-

[*] Present address: Fraunhofer Institute for Chemical Technology, Division of Applied Electrochemistry, Joseph-von-Fraunhofer-Str. 7, D-76327 Pfaffzettel, Germany.

[*] Corresponding author, vr Rao@ph.tum.de

tively smaller and the poisoning effect of carbonyl species and CO, which are generally stable residues of the electro-oxidation process of every organic molecule, are comparatively weaker in alkaline media. These advantages associated with alkaline medium membranes offer good incentives for their use in fuel cells. Until recently, the unavailability of proper solid alkaline membranes, which are stable under fuel cell conditions, precluded their extensive use; however, recent progress in the field of solid polymeric anion exchange membranes, has provided impetus to the application of these membranes in fuel cells. Several groups have carried out tests on these solid polymeric anion exchange membrane fuel cells [1–4]. Solid alkaline fuel cells are also attractive as they can give reasonable power output with non-noble metal catalysts because of the improved kinetics in alkaline medium and the increased stability of the non-noble metals at higher pH values.

Methanol is, to date, the most preferred liquid fuel for fuel cells because of facile kinetics in comparison to other alcohols. Some disadvantages of methanol are its toxicity and its relatively low boiling point. Ethanol, the next alcohol is considered to be an option as it is less toxic, has a high energy content (ethanol: 8 kWh kg methanol: 6 kWh kg), and is more easily available from renewable resources. The oxidation of ethanol to CO₂, however, is much slower in comparison to methanol, as it requires the scission of a C–C bond. The ethanol electro-oxidation follows a multi-step process during which several intermediates like acetaldehyde and acetic acid get formed which tends to leave the fuel cell as undesired byproducts. The efficiency of ethanol oxidation can be improved by development of catalysts exhibiting faster kinetics and higher selectivity towards CO₂. This requires detailed understanding of the mechanism of ethanol oxidation reaction (EOR). But the mechanism of EOR has been studied mostly in acid medium, either liquid electrolyte or solid PEM. EOR mechanism in alkaline medium is difficult to investigate because the main product CO₂ is highly soluble in aqueous alkaline electrolytes, due to the formation of carbonates and bicarbonates, which renders it difficult to observe with techniques such as FTIR or model differential electrochemical mass spectrometry (DEMS). It is, however, important to gain more understanding of the EOR in alkaline medium, especially since the kinetics of ethanol oxidation is expected to be faster in alkaline medium than acidic medium. Thus, in this study it is our endeavor to shed light on the product distribution of the ethanol electro-oxidation reaction in alkaline media MEAs. In this paper, we applied the DEMS technique to study the mechanism of EOR in alkaline medium MEAs.

2 Preparation of the MEA and its Characterisation

2.1 MEA

A suitably sized (2.5 cm × 2.5 cm) piece of alkaline membrane (Acta Spa, Tokuyama) was cut. The membrane was then hydrated in 1 M KOH solution overnight at room

temperature. Unsupported Pt black (Alpha Aesar) was used as a cathode and anode catalyst. In order to make an MEA, the ionomer solution (Acta Spa, Tokuyama) was applied on both sides of the membrane and catalyst ink (catalyst + water + isopropanol) was dispersed by a paintbrush subsequently. In a semi-dry stage two carbon backing layers (Toray paper from E-Tek, TGPB 060, no wet proofing), were placed one on each side. The completed 'sandwich' was then hot pressed at 100 °C for 5 min with 1 kN cm⁻² pressure. The resultant MEA active area is 1.2 cm².

2.1.1 Experimental Setup

The fuel cell consisted of two stainless steel plates with integrated serpentine medium distribution channels. Six threaded studs and nuts held the two plates together. The fuel cell can be operated in both modes half-cell and full cell. Generally during the investigation of anode it was used as a half-cell. Cathodes with high Pt loading (4 mg cm⁻²) and continuous hydrogen flow were used as counter and reference simultaneously. The potential of the cathode is assumed to be the same as that of a reversible hydrogen electrode (RHE). All potentials are reported in reference to this.

The anode flow system comprised of a tank filled with alcohol solution and a tank filled with Millipore water. These tanks were connected *via* heated tubes with a three-way valve at the fuel cell inlet (cf. Figure 1). The alcohol solution and the Millipore water were always deaerated with argon before measurements. A dosing pump between the cell outlet and exit tank controls the flow of alcohol solution and water through the cell. To avoid gas bubble formation due to high gas production and the partially low solubility of CO₂ at elevated temperature, the anode flow system was pressurised at 3 bars overpressure. The cathode overpressure was kept at 1 bar to limit the crossover of H₂ to the anode side. The permeation of alcohol to the cathode side does not affect the potential of the cathode (which is also the reference electrode). In all cyclic voltammetry measurements, the potential scan rate is kept at 10 mV s.

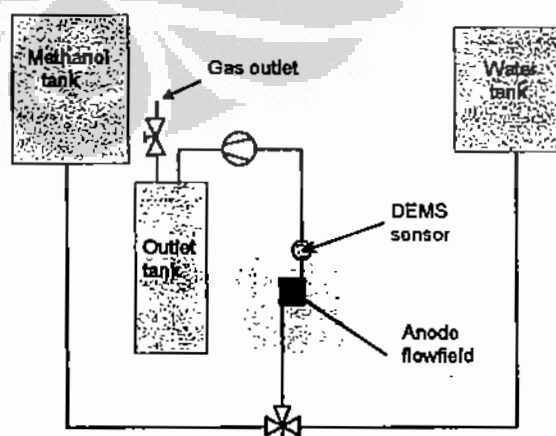


Fig. 1 Schematics of the fuel cell DEMS setup.

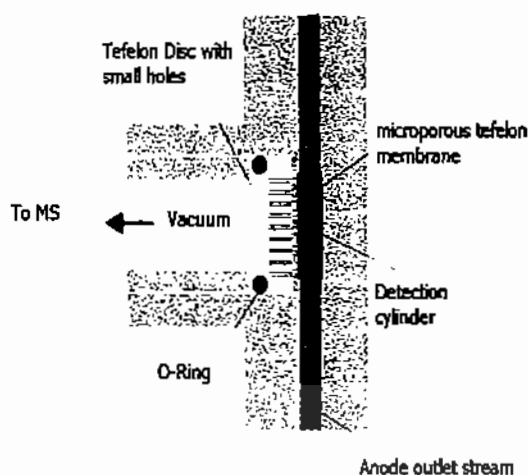


Fig. 2 Design of MS sensor.

The DEMS sensor was positioned at the outlet channel of the anode compartment, it consisted of a cylindrical detection volume with a diameter of 7 mm and a height of 2 mm through which the anode outlet flow passes (cf. Figure 2). This volume was separated from the vacuum system of the mass spectrometer by a Microporous Teflon membrane (Schleicher & Schuell, TE30) with a pore size of 0.02 μm and a thickness of 110 μm. The membrane was supported by a Teflon disc of 2 mm diameter with holes. A Balzer Prisma QMS 200 mass spectrometer and a potentiostat designed by the AGEF were used together with a computerised data acquisition system.

2.1.2 Experimental Strategies

Using our fuel cell DEMS system described above we have investigated the product distribution of the ethanol oxidation with the Pt-based catalysts. It is known that the relevant oxidation products of ethanol are carbon dioxide, acetaldehyde and acetic acid. Of these only the first two are volatile enough to be monitored by DEMS, the problem is that the molecular mass of both CO₂ and CH₃CHO is the same at 44 g mol. Therefore, it was not possible to monitor both together using the m/z = 44 signal, one way of solving this problem would have been to use deuterated ethanol (CD₃CH₂OH), an approach utilised by Fujiwara et al. [5], for determining the product yield ratio between carbon dioxide and acetaldehyde. The high cost of deuterated ethanol precludes its use for extensive experiments. Therefore, an alternative approach consists in monitoring them when their major fragments was used. In this procedure for CO₂ the m/z = 22 signal corresponding to doubly ionised CO₂²⁺ molecular ions can be used, as has been

reported by Wang et al. [6]; similarly for acetaldehyde the most prominent fragment COH⁺ at m/z = 29 can be used.

Accordingly the m/z = 22 and 29 signals were monitored during the ethanol oxidation for CO₂ and CH₃CHO. The calibration of DEMS set-up for CO₂ is performed using the potentiostatic bulk CO oxidation. Figure 3 shows a good signal for m/z = 22, although the signal quality is not as good as for m/z = 44 signal, as the m/z = 22 current is about a factor of 30 smaller.

The calibration constant is calculated using the formula:

$$K_F^2 = 2I_{MS}/I_F \tag{1}$$

where I_{MS} is the steady state ion current for m/z = 22, and I_F is the corresponding Faradaic current.

In order to measure the current efficiency of CO₂ (CCE) formation during ethanol oxidation, we performed potentiostatic oxidation of ethanol at various potentials, temperatures and concentrations of ethanol. Calibration constants were obtained for all temperatures separately. Subsequently, the CCE can be calculated using the formula:

$$CCE(\text{CO}_2 \text{ current efficiency}) = 6I_{MS}/I_F K_F^2 \tag{2}$$

where I_{MS} is the steady state ion current for m/z = 22 for ethanol oxidation, and I_F is the corresponding Faradaic current.

2.1.3 DEMS Measurement in Alkaline Medium

Differential electrochemical mass spectrometry can sense only the volatile products or byproducts of any electrochemical reaction. It means that if any molecule is not volatile enough because of its solubility or because of its boiling point, then DEMS cannot sense that molecule. CO₂ is quite

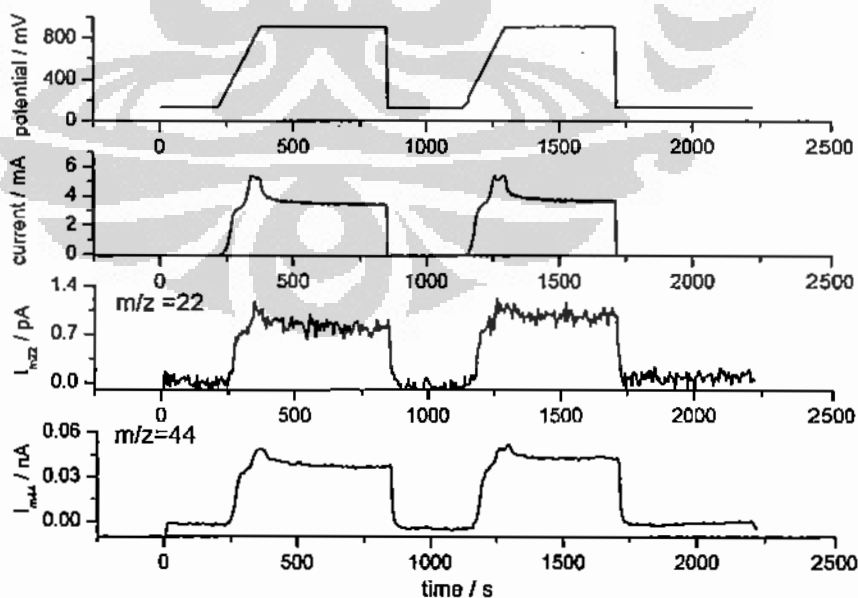


Fig. 3 This figure shows the voltage, bulk CO oxidation current and m/z = 22 and 44 as a function of time.

volatile from the boiling point perspective, but is also very soluble in water. In alkaline solution it will react and form carbonates, so if there is KOH in anolyte then DEMS will not detect any CO_2 signal. Even in the case of less alkaline solutions like 0.5 M Na_2CO_3 (pH = 11.5), no CO_2 signal was seen perhaps because of the formation of bicarbonates. So, for all DEMS measurements the anolyte was kept free of any extra alkaline additive. Although in the presence of alkaline additives like KOH in anolyte stream the membrane ionic resistance is much lower and the ionic contact between the catalyst layer and membrane is better than when it is absent. But for DEMS measurement we depend on the ionic contact between the Pt catalyst layer and solid alkaline membrane interface, for an electrochemical reaction to occur.

Importantly, it must be mentioned that the solid alkaline membranes are prone to carbonation in the presence of aqueous CO_2 . Carbonation is the process of neutralisation of OH^- groups present in the membrane, after reacting with dissolved CO_2 . Carbonation will result in decreased ionic conductivity of the membrane. Carbonation of the alkaline membrane itself was not studied for this paper but proper care was taken in order to exclude its influence on our experimental results. For example, our experiments were performed in steady state conditions of membrane conductivity. The resistance of the MEA measured over a period of several weeks did not change much. Also the current densities of CO oxidation and ethanol oxidation were stable under our experimental conditions for several weeks of experiment time. CO_2 produced during CO and ethanol oxidation can also contribute

to carbonation. But again repeated experiments involving CO_2 formation did not result in change of the membrane resistance. Also it should be considered that our experimental conditions are similar to real fuel cell operational conditions and alkaline membranes in real world fuel cells will be exposed to CO_2 to the same extent as in our experiments.

2.2 Electrochemical Characterisation of MEA

Electrochemical characterisation of the MEA was performed after installing the MEA in a fuel cell. The cyclic voltammogram (CV) obtained with deionised water as anolyte is shown in Figure 4(a1). The CV differs a bit from what is expected for Pt. The hydrogen features are not clearly resolved, although the oxide region is more clearly visible. Figure 4(a) shows the polarisation curve with 0.1 M EtOH as anolyte and 1 bar abs H_2 pressure at cathode which works as both a counter electrode and reference electrode. Figure 4(b1) shows the CV with 0.2 M KOH as anolyte. This CV shows all the standard features of Pt. Figure 4(b) shows the polarisation curve for a half cell with 0.2 M KOH + 0.1 M EtOH as anolyte and H_2 at cathode. The Faradaic current in this case is higher. This might be due to the better ionic contact between the catalyst particles and the membrane and also better due to ionic conductivity of the membrane itself in the presence of KOH. The resistance of MEA is measured by current-interrupt method. It was found that the resistance of the MEA decreased from 7 ohm in the presence of deionised water to 1 ohm in the presence of KOH.

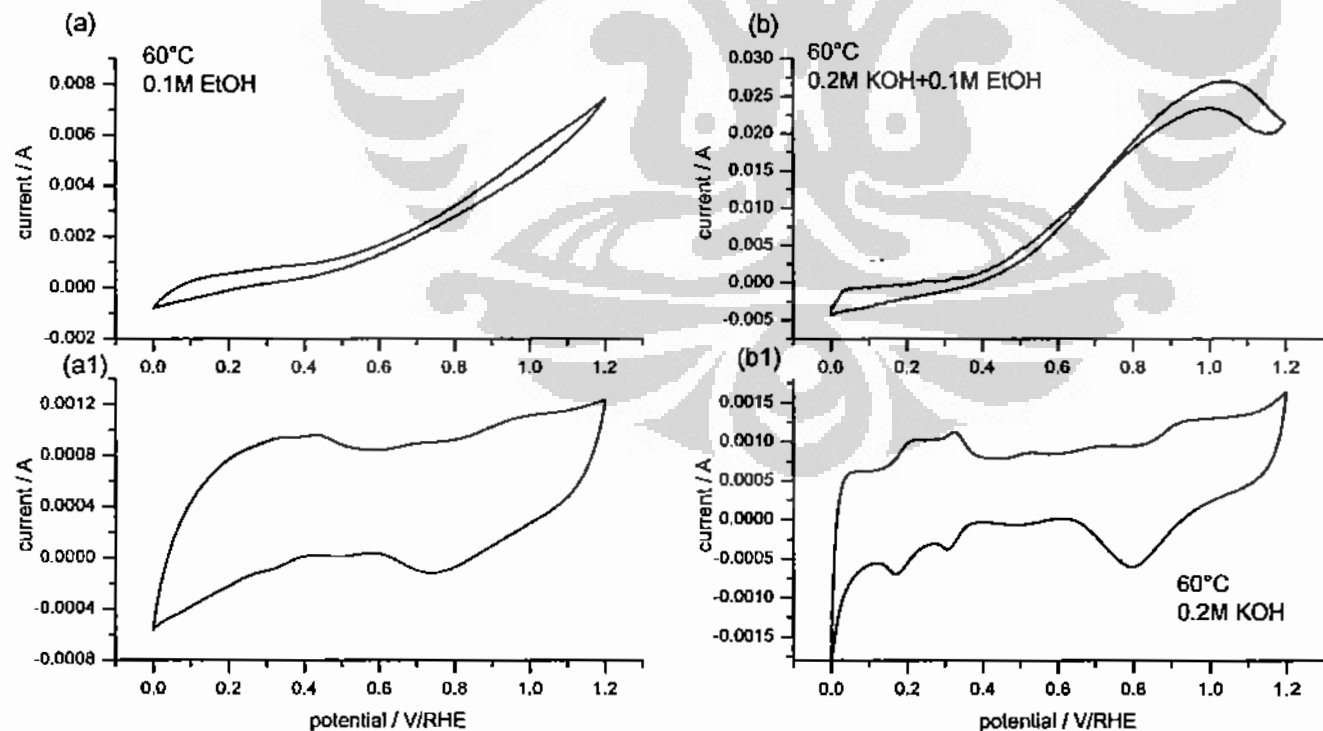


Fig. 4 CV for the alkaline MEA are shown (a1) for only deionised water in anolyte, (a) with 0.1 M EtOH solution, (b1) with KOH in the anolyte and (b) with KOH + 0.1 M EtOH.

2.3 Electrochemical Active Area (ECA) ■ Verify change here. ■ Measurement by CO Stripping

The ECA available in the anode catalyst layer of the MEA is determined with the CO stripping technique. CO is adsorbed on to Pt sites at 0 V vs. RHE, by flowing CO saturated water through the anode. CO is removed from the solution phase by purging the anode with argon-bubbled deionised water and then CO stripping is done. The CO stripping CV performed at 60 °C is shown in Figure 5. It is noticeable that the CO stripping peak for alkaline MEA (cf. Figure 5) is very broad in comparison to a CO stripping peak in an acidic MEA (cf. Figure 6) with Pt anode. Also the onset of CO oxidation in the alkaline MEA is negative-shifted in comparison to an acidic membrane-based MEA with Pt electrode. The CO stripping charge is estimated by integrating the area under the CO stripping peak. CO stripping charge is shown on the CO stripping graphs, which is directly proportional to the real ECA by a conversion factor of 420 $\mu\text{C cm}^{-2}$. It has been

reported earlier that the ECA available in a catalyst layer of the MEA, is the one of the main determinant of the CCE for EOR [7]. Thus in this paper, the CCE for EOR, of two MEAs, acidic and alkaline with platinum as catalyst, with approximately similar ECAs is compared.

2.4 DEMS Measurement with CO Bulk Oxidation and Ethanol Oxidation

The mass spectrometer cyclic voltammograms (MSCV) were measured with the alkaline MEA, with CO saturated water as anolyte, to check for the observability of CO₂ in general and by the $m/z = 22$ signal in particular. As can be seen in Figure 7(a), the $m/z = 22$ signal is prominently observable.

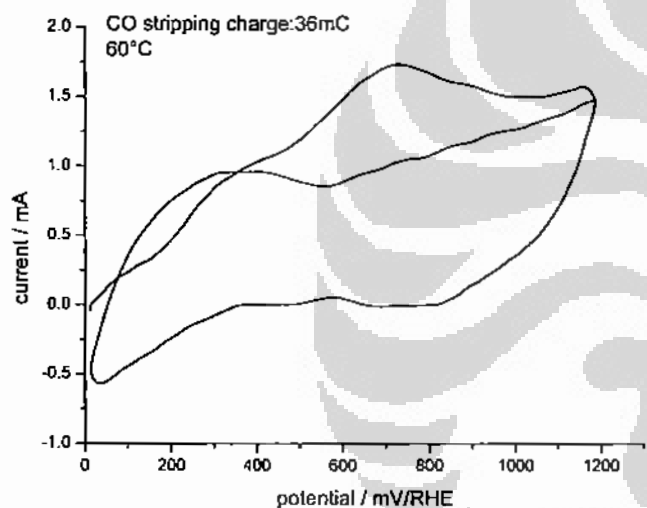


Fig. 5 CO stripping CV for the alkaline MEA.

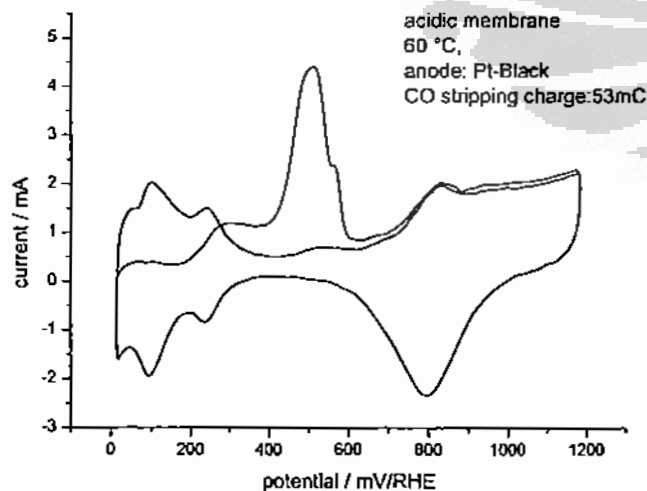


Fig. 6 CO stripping CV for the acidic MEA.

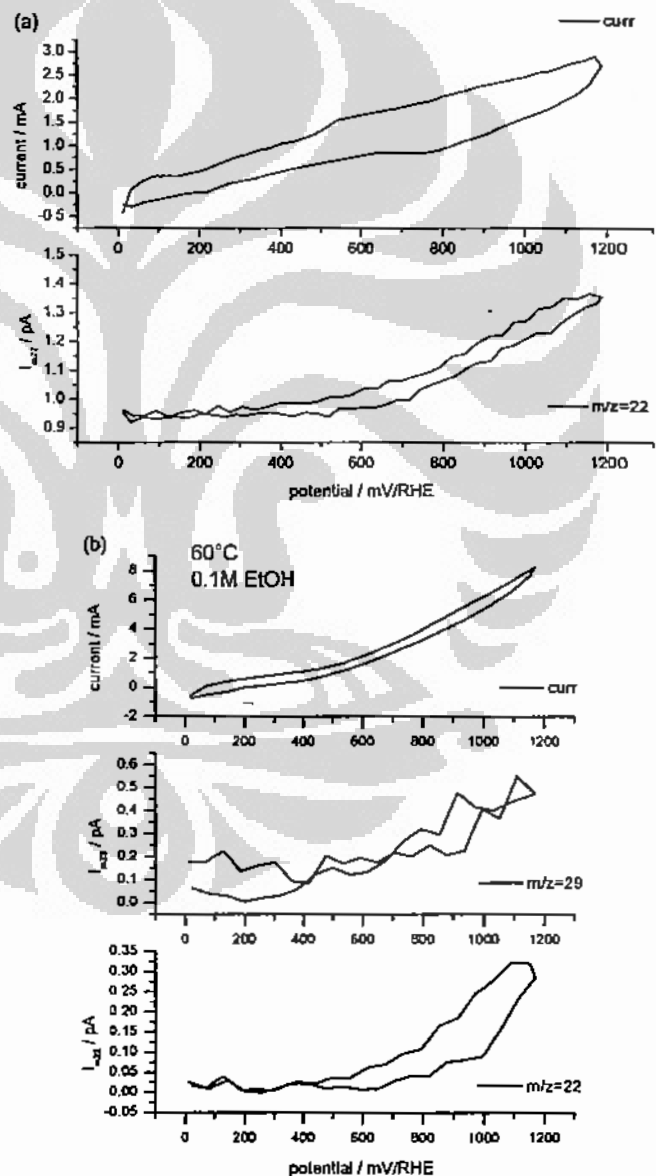


Fig. 7 CV and MSCV for (a) bulk CO oxidation and (b) for ethanol oxidation for the alkaline MEA.

Also the effect of high membrane ionic resistance is visible in the shape of the CV. Figure 7(b) shows the MSCVs with 0.1 M EtOH as anolyte. The volatile byproduct acetaldehyde was observed at $m/z = 29$ and the CO_2 was observed at $m/z = 22$. Both the MSCVs follow the Faradaic current, although the signal of $m/z = 29$ is weak. Quantitative estimation is performed for CO_2 using an appropriate calibration process. The calculation of CCE for EOR in alkaline MEA with Pt anode is presented in the next section.

2.5 CCE for EOR

For CCE estimation, potentiostatic bulk oxidation was performed at different potentials. Figure 8 shows the potential, current and $m/z = 22$ signals as a function of time. The active area in the MEA is small, and the ionic resistance of the membrane is very high. Therefore, the over potential needed for any appreciable current is also high. It is noticeable that the CO_2 signal ($m/z = 22$) is not visible for 0.6 V, since the Faradaic current is small (<2 mA); however, even if CO_2 is formed, it would be below the detection limit of our DEMS-setup. At 0.8 V anode potentials Faradaic currents are higher and the CO_2 signal is strong.

Figure 9 shows CCE at different potentials for an alkaline MEA with Pt anode and an acidic MEA also with Pt anode. The conditions for both MEAs were the same at 60 °C temperature and 0.1 M EtOH as anolyte. The ECA in both MEAs was estimated with the CO stripping technique. For the alkaline MEA Pt anode the ECA was estimated to be 85 cm² (CO stripping charge: 36 mC and conversion factor: 420 $\mu\text{C cm}^{-2}$).

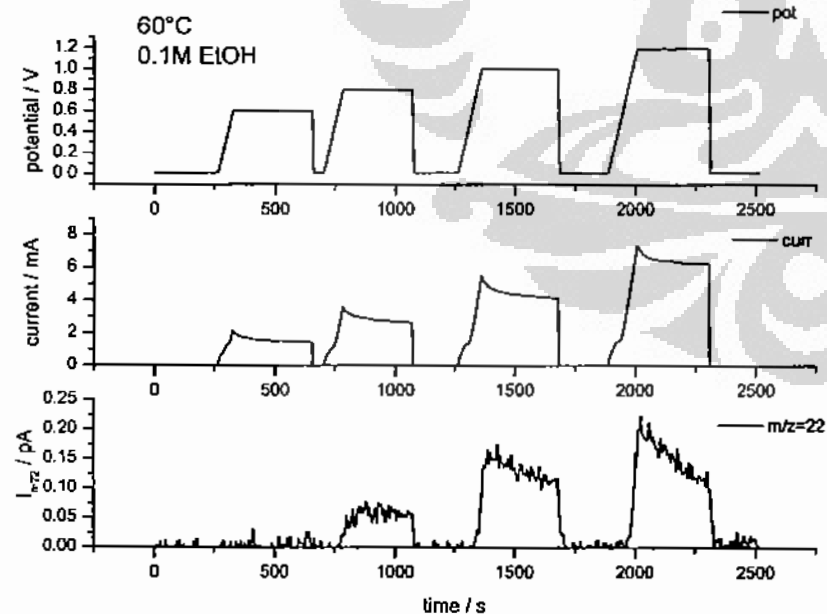


Fig. 8 Potentiostatic bulk oxidation of ethanol at different potentials. The corresponding $m/z = 22$ signal is also shown.

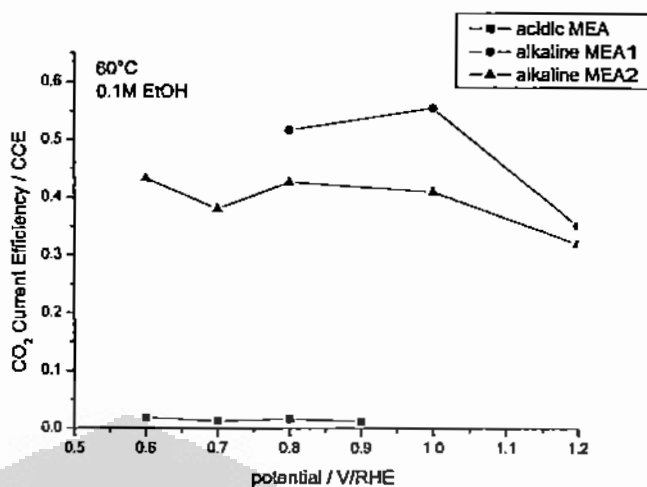


Fig. 9 Comparison between the acidic and alkaline MEAs with Pt as catalyst for CCE at 60 °C.

For the acidic MEA, the ECA in anode side was estimated to be 123 cm² (CO stripping charge: 53 mC and conversion factor: 420 $\mu\text{C cm}^{-2}$). The comparison of these two MEAs with similar ECAs in anode catalyst layer, from a CCE perspective provides interesting insights about the mechanism of ethanol oxidation in alkaline medium membrane.

The CCE in the case of alkaline MEA is very high. For example at 0.8 V, alkaline MEA Pt anode shows a CCE of around 55%, but the acidic MEA Pt anode shows only around 2%. This might be a qualitative indication that the C-C bond scission rates in alkaline media are significantly higher than the acid media. The unoptimised alkaline MEA has low ECA and higher ionic resistance. Because of this the potential range in which we could see a noticeable amount of CO_2 is the high potential range. Although higher ECA and lower ion resistance are easily achievable with the addition of KOH in anolyte as is done in alkaline fuel cells. All solid alkaline fuel cells with alkaline polymer electrolyte membranes and no aqueous alkaline electrolyte have also been demonstrated [3]. In our case also no aqueous alkaline electrolyte was used. The electrochemical reaction takes place at the interface between the Pt catalyst and the solid alkaline electrolyte. So, one can possibly extend the insights obtained from EOR for all solid alkaline MEA to alkaline MEAs with aqueous KOH the at anode side also, as the pH and related conditions in both cases would be similar. Figure 9 shows the CCE data for a second alkaline MEA, depicted as alkaline MEA2. The ECA value for this MEA is not available.

3 Conclusion

The DEMS measurements performed for all solid alkaline MEA indicate that in the case of alkaline media MEA ethanol undergoes significantly more complete electro-oxidation to CO_2 than in the case of acidic MEA with the same Pt anode. The CCE can be compared for acidic and alkaline MEA with similar ECA in the anode catalyst layer. It is important to compare keeping similar ECA, as CCE for EOR increases with increasing ECA available in the catalyst layer. This has been found earlier in the experiment with acidic MEAs [7]. The CCE estimated in the case of alkaline MEA with Pt anode is around 55% at 0.8 V/RHE, 60 °C and 0.1 M EtOH. But in similar conditions acidic MEA shows only 2% CCE. This indicates that the C–C bond scission rates are much higher in alkaline media. But the mechanism of ethanol oxidation in alkaline media is not entirely clear. CCE estimation provides only a partial insight into the EOR mechanism. The fact that CO_2 will form carbonates in the presence of an aqueous alkaline electrolyte makes it difficult to study EOR in FTIR or model DEMS systems. The polymer alkaline electrolyte as

used in this study for making alkaline MEAs provides a valuable opportunity to observe the CO_2 produced during EOR using a DEMS system.

4 References

- [1] C. Coutanceau, L. Demarconnay, C. Lamy, J. M. Leger, *J. Power Sources* 2006, 156, 14.
- [2] J. R. Varcoe, R. C. T. Slade, *Fuel Cells*, 2005, 5, 187.
- [3] J. R. Varcoe, R. C. T. Slade, E. L. H. Yee, *Chem. Commun.* 2006, 1428.
- [4] J. R. Varcoe, R. C. T. Slade, *Electrochem. Commun.* 2006, 8, 839.
- [5] N. Fujiwara, K. A. Friedrich, U. Stimming, *J. Electroanal. Chem.* 1999, 472, 120.
- [6] H. Wang, Z. Jusys, R. J. Behm, *J. Phys. Chem. B* 2004, 108, 19413.
- [7] V. Rao, C. Cremers, U. Stimming, *J. Electrochem. Soc.* 2007, 154, 11.





PAPER VI

**Ethanol electro-oxidation on PtRhCeO₂/C catalyst in
direct oxidation fuel cell**

added to the electrode structure could be reduced from about 30 wt% to 9 wt %. Also the fuel cell performance using methanol as fuel is increased for high current density operation, compared to unsupported PtRu-black catalyst [13].

Intermediate temperature electrolytes

Increasing the operation temperature is also a beneficial approach to increase the power density of direct converting fuel cells. However, temperatures as high as those used with high temperature fuel cells today will lead to heavy material constraints and to operation limitations which render such fuel cells less suitable for a number of interesting applications. Therefore, electrolytes working in an intermediate temperature regime around 200 °C are of high interest. One promising candidate material for such electrolytes is ammonium polyphosphate (APP) [14,15], an inexpensive inorganic polymer which is mass produced today as flame retardant for polymers. In order to become useful for fuel cell applications the stability of the material under the desired fuel cell operation conditions needed to be improved. In particular, hydrolysis of the material in humidified atmospheres at elevated temperatures must be avoided. As was demonstrated, this goal can be achieved by forming composite materials with metal oxides like silicon oxide, titanium oxide or even cer-gadolinium-oxide (CGO). A number of such composites were tested and composites of APP and SiO₂ or TiO₂ in a ratio of 2:1 proved to be the most stable ones [16].

Outlook

Within the ongoing work in our groups a number of issues are addressed which each can help to increase the performance of low to intermediate temperature direct alcohol fuel cells. But to fully profit from these attempts they should be combined and realised in a demonstration stack. This is the only way to give the use of this technology a chance for further spreading. Therefore we would like to join our expertise in a common project and try to realise a demonstration

stack comprising the different technical approaches were possible.

As basis for this development, the design of a DMFC stack which resulted from a prior collaboration of our groups [17] can be provided. A first contact to Indonesia has also been established by the exchange of a PhD student between the University of Indonesia and the Technical University of Munich. Additional contacts to academic groups and enterprises are currently built up. Together with these partners and some additional industrial partners from Germany it should be possible to realise a demonstration stack of direct ethanol fuel cells which implies a number of the innovative concepts proposed above. Thereby the requirements of the Indonesian market will be considered, e.g. by allowing for the use of fuels derived from biomass like bio-ethanol.

REFERENCES

- [1] N. Alonso-Vante, M. Giersig, H. Tributsch, *J. Electrochem. Soc.* 138 (1991), 639;
- [2] N. Alonso-Vante, H. Tributsch, O. Solarza-Feria *Electrochimica Acta* 40 (1995), 567;
- [3] M. Bron, P. Bogdanoff, S. Fiechter, M. Hilgendorff, J. Radnik, I. Dorbandt, H. Schulenburg, H. Tributsch, *J. Electroanalytical Chemistry* 517 (2001), 85;
- [4] F. Dassenoy, W. Vogel, N. Alonso-Vante, *J. Phys. Chem. B*, 106 (2002), 12152;
- [5] M. Neergat, D. Leveratto, U. Stimming, *Fuel Cells* 2 (2002), 25;
- [6] C. Lamy, E.M. Belgsir, J.-M. Léger, *J. Appl. Electrochem.* 31 (2001) 799;
- [7] C. Lamy, A. Lima, V. Le Rhun, F. Delime, C. Coutanceau, J.-M. Léger, *J. Power Sources* 105 (2002) 283;
- [8] C. Lamy, S. Rousseau, E.M. Belgsir, C. Coutanceau, J.-M. Léger, *Electrochimica Acta* 49 (2004) 3901-3908.
- [9] L. Jiang, G. Sun, S. Sun, J. Liu, S. Tang, H. Li, B. Zhou, Q. Xin, *Electrochimica Acta* 50 (2005), 5384 ;
- [10] Z. Zhou, S. Wang, W. Zhou, G. Wang, L. Jing, W. Li, S. Song, J. Liu, G. Sun, Q. Xin, *Chem. Comm.*, 2003, 394 ;
- [11] V. Rao, C. Cremers, U. Stimming, L. Cao, G. Sun, *in preparation*;
- [12] V. Rao, P.A. Simonov, E.R. Savinova, G.V. Plaksin, S.V. Cherepanova, G.N. Kryukova, U. Stimming, *J. Power Sources* 145 (2005), 178;
- [13] F. Scheiba, M. Scholz, C. Lin, C. Cremers, C. Roth, X. Qiu, U. Stimming, H. Fuess, *Fuel Cells*, *accepted for publication*
- [14] T. Kenjo, Y. Ogawa, *Solid State Ionics* 76 (1995), 29;
- [15] M. Cappadonia, O. Niemi, U. Stimming, *Solid State Ionics* 125 (1999), 333;
- [16] L. Liu, H. Tu, C. Cremers, U. Stimming, *Solid State Ionics* (*submitted*)
- [17] C. Cremers, M. Scholz, A. Racz, W. Knechtel, J. Rüttmair, F. Grafwallner, H. Peller, U. Stimming, 3rd European Polymer Electrolyte Fuel Cell Forum, 4-8 July 2005, Lucerne, Switzerland, CD-Rom proceedings, file B116.pdf

ETHANOL ELECTRO-OXIDATION ON Pt-Rh-CeO₂/C CATALYST IN DIRECT OXIDATION FUEL CELLS

Hariyanto^{1,2}, Widodo W. Purwanto¹, Roekmijati W. Soemartojo¹
and U. Stimming³

¹Chemical Engineering Departement - UI
Kampus Baru UI, Depok 16424, Indonesia

²Energy Technology Center - B2TE

Kawasan Puspipetek, Serpong 15314, Tangerang, Indonesia

³Physics Department, Technical University of Munich
Germany

ABSTRACT

ETHANOLELECTRO-OXIDATIONONPt-Rh-CeO₂/CCATALYSTINDIRECTOXIDATIONFUELCELLS. Ethanol is one of an alternative fuels in direct oxidation fuel cell. In this research work, Pt-Rh-CeO₂/C catalyst was performed for ethanol electro-oxidation in electrochemical cell in acid medium (H₂SO₄) and alkaline medium (NaOH). The aim of the present paper is to investigate the activity of carbon supported Pt-Rh-CeO₂ to the activity for ethanol electro-oxidation reaction. Highly dispersed catalysts are obtained by alcohol reduction method, and after careful physical characterization by X-Ray Diffraction (XRD) and Transmission Electron Microscopy (TEM), the catalyst are performed in electrochemical cell (half cell test) to investigate the activity for electro-oxidation reaction (EOR) of ethanol. Electrochemical characterization was carried out by measured of cyclic voltammetry and CO stripping voltammetry on the polycrystalline gold electrode. Physical characterization result of Pt-Rh-CeO₂/C catalyst which synthesized by alcohol reduction methods provide average particle size about 2.9 ± 0.2 nm. Electrochemical characterization shows that PtRhCeO₂/C catalyst improved the activity of ethanol electro-oxidation in comparison to the Pt/C commercial either in acid or alkaline medium especially at lowers potential. Detail result of those will be presented in detail.

Key words : Ethanol electro-oxidation, Pt-Rh-CeO₂/C, electrochemical characterization

INTRODUCTION

Fuel cell is an attractive device to obtain directly electric energy from the chemical energy. Proton exchange membrane fuel cell (PEMFC) hydrogen oxygen fuel cell is low temperature fuel cell which seems able to be applied for a large range of power application. However, hydrogen or hydrogen rich gas utilization for PEMFC in some applications was has a problem related to its storage. The direct uses of organic fuels have been often considered despite of their rather low electrochemical reactivity in comparison to hydrogen. The use of hydrogen carriers like alcohols in direct alcohol fuel cells (DAFCs) appears then advantageous for two main reasons: they are liquids which simplifies the problem of storage and their theoretical mass energy density is rather high 6.1 and 8.0 kWh/kg for methanol and ethanol, respectively.

However, there is the problem that methanol is toxic for human.

It is well known that ethanol is not toxic for human and is easily produced from biomass. This means that carbon dioxide (CO₂) emitted from direct type fuel cell using ethanol can be recycling by planting. In the case of ethanol as the fuel in a DEFC, the problem is again more complicated because ethanol contains two atoms of carbon, and a good electrocatalyst towards the complete oxidation of ethanol to CO₂ must activate the C-C bond breaking.

Electrocatalytic oxidation of ethanol using platinum or platinum alloy catalyst has been investigated [1-8] studied the adsorb behavior of ethanol on a polycrystalline platinum using a differential electrochemical mass spectroscopy (DEMS) and FTIR.

Pure platinum catalyst is reported rapidly poisoned by strongly adsorbed intermediate such as carbon monoxide resulting from the dissociative chemisorption of the molecule. In order to improve the performance of DEFC on Pt-based metal catalyst which is used extensively at present, it is of great importance to look for more active anode catalysts for ethanol electro-oxidation at lower temperatures.

The aim of the present paper is to investigate the activity of carbon supported Pt-Rh-CeO₂ to the activity for ethanol electro-oxidation reaction. Highly dispersed catalysts are obtained from ethylene glycol reduction methods and after careful physical characterization are performed in electrochemical half cell.

EXPERIMENTAL METHOD

Preparation of Pt-Rh-CeO₂/C Catalyst

The research work was initiated by preparation of CeO₂ nano particles by two step precipitation methods [9]. As synthesized CeO₂, H₂PtCl₆·6H₂O and RhCl₃· were used as precursors of PtRhCeO₂/C catalysts. XC-72R carbon black from Cabot and ethylene glycol (EG) was used as a support and reducing agent, respectively. Detailed of ethylene glycol method is presented in elsewhere [8,10]. Following is a brief description of the preparation method: the required amounts of H₂PtCl₆·H₂O and RhCl₃· were added to the mixture of EG and deionized water with stirring to form homogeneous slurry. The slurry was heated to 160 °C and kept at this temperature in an oil bath for 3 h. The slurry was then cooling down to the room temperature while continue stirring. Carbon-XC-72 then added to the slurry and stirring for overnight. Then the black solid sample was filtered, washed and dried at 80 °C for 10 h in a vacuum oven. The nominal loading of Pt in the catalysts was 20 wt.%.

Characterization of Catalysts

X-Ray Diffraction measurement of the catalyst is done used instrumentation of Bruker D8 Advance diffractometer equipped with a Cu anticathode, adjustable divergence slit, graphite

monochromator on the diffracted beam and proportional detector. Data acquired at 2θ range from 20 to 65°, scan step of 0.02° and fixed counting time of 6 s for each step.

SEM measurement was carried out by used instrumentation with Hitachi S-4000. Method of acquisition was amount of catalysts powder was prepared on the carbon tape sample holder 200 kV voltage, magnification till 15000 X. EDX measurement using Windshell software.

TEM measurement was carried out by using instrumentation of JEOL JEM 2000 EX. Sample preparation on holey carbon Cu-grids TEM 120 keV bright field dry preparation on grid data storage 1024x1024, 150 kX magnification.

Electrochemical Characterization

The cyclic voltammetry spectra were recorded using a potentiostat/galvanostat (autolab model PG30). Ten milligram of Pt-based catalyst was suspended in 300 μL of distilled water and 500 μl of 0.1 % Nafion® solution to prepare catalyst ink. Then 13 μL of ink was transferred with an injector to clean gold disk electrode (with area of 0.2826 cm²). After the ethanol volatilization, the electrode was heated at 60 at.%C for 5 min.

For surface area determination, CO stripping voltammetry by CO adsorption method was used. The electrochemical active surface area (S_{co}) was determined as follows:

$$S_{co} = \frac{Q_{co}}{0.420mCcm^{-2}} \dots\dots\dots (1)$$

Where Q_{co} was CO stripping charge (in mC) vetermined after CO adsorption, and 0.420 mC cm⁻² correspond to a monolayer of adsorbed CO.

For acid medium, a mixture solution containing 0.5 M H₂SO₄ and 1.0 M ethanol was used as electrolyte, which was saturated by pure argon in order to expel oxygen in the solution. The scan rate was 10 mV/s, and a Hg/Hg₂SO₄ (0.5 M) was used as reference electrode, and a platinum wire was used as counter electrode.

For alkaline medium, a mixture solution containing 0.1 M NaOH and 1.0 M ethanol was used as electrolyte, which was saturated by pure argon in order to expel oxygen in the solution. The scan rate was 10 mV/s, and a Hg/HgO (0.1 M NaOH) was used as reference electrode, and a platinum wire was used as counter electrode.

RESULTS AND DISCUSSION

Physical Characterization

X-ray diffraction was applied to learn more about the crystalline phases in our catalysts, especially for CeO₂. Figure 1 show X-ray diffraction pattern of ceria and Pt-Rh-CeO₂/C catalysts. From this XRD pattern, the characteristic peaks located at 2θ: 28.5°, 33.1°, 47.5°, 56.3° and 59.01° are corresponding to [1 1 1], [2 0 0], [2 2 0], [3 1 1] and [2 2 2] planes, respectively. These match well with the peaks of cubic fluorite CeO₂ crystal structure in XRD-pattern database.

The first peak at 2θ H^o 23° in Figure 1 originates from the Vulcan XC-72 carbon support. The peaks at 2θ H^o 40.04° are reflections of the face centered cubic [f.c.c] crystal lattice of Pt [111]

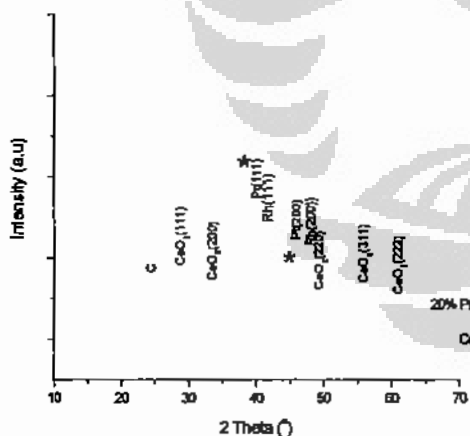


Figure 1. X-Ray diffraction pattern of catalysts

High resolution transmission electron microscopy (HR-TEM) with 500 kX magnification picture for CeO₂ was shown in Figure 2. The particle size of the CeO₂ crystal is about 8-9 nm. As prepared nanoparticle CeO₂ then used as modifier in PtRhCeO₂/C catalyst.



Figure 2. High resolution transmission micrograph of CeO₂

Morphology of the surface catalyst was characterized by scanning electron microscopy (SEM) as shown in Figure 3, while the qualitative element composition of the catalyst was characterized by Energy dispersive of X-Ray (EDX) (Figure 4).

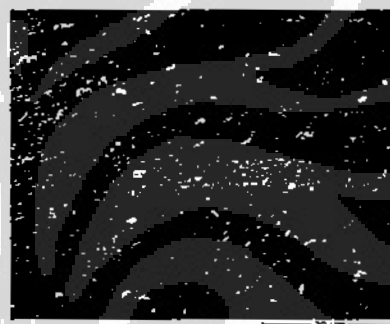


Figure 3. SEM picture of Pt-Rh-CeO₂/C catalyst

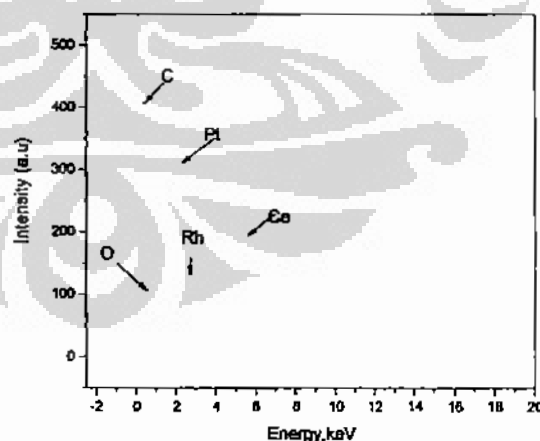


Figure 4. EDX-picture of the catalyst

All of the catalysts element signals (Pt, Rh, Ce, O, C) were existing from the EDX measurement result.

In-set picture show a histogram of particle size distribution which average particle size was about 2.9 ± 0.2 nm. This particle size was well agreement with the XRD result which was determined by Scherer formula.

Electrochemical Characterization

CO stripping charge was determined by integrating of the CO stripping voltammetry peak. Therefore, the electrochemical active surface area was determined by equation (1) which provided value of about 23.8 cm^2 for Pt/C catalyst and 24.1 cm^2 for Pt-Rh-CeO₂/C catalysts respectively. These S_{CO} value was used to normalize faradaic current which is obtained from ethanol electrooxidation reaction (EOR).

EOR on Pt-Rh-CeO₂/C catalyst in acid medium was shown in Figure 6. The on-set oxidation potential was occurred at the potential of about 0.43 V vs. RHE. Meanwhile, over Pt/C catalyst the on-set potential was occurred at 0.5 V vs.RHE. These activity of the EOR was slower than which happened in direct methanol fuel cell (DMFC) at 0.4 V vs. RHE over Pt/C catalyst.

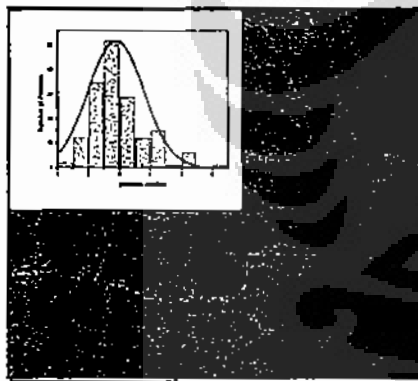


Figure 5. TEM of Pt-Rh-CeO₂/C catalyst

The low activity in ethanol fuel cell was due to difficulty to break C-C bond in ethanol. However, over Pt-Rh-CeO₂/C catalyst had increased the activity of the catalyst compared to the reference catalyst of Pt/C. The Faradaic current over Pt-Rh-CeO₂/C was increase by factor of 2 at potential 0.6 V vs RHE in comparison to the reference catalyst.

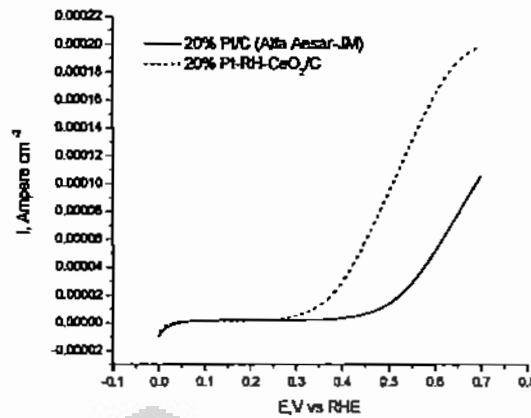


Figure 7. EOR on Pt-Rh-CeO₂/C in alkaline medium.

It is well known that in alkaline medium EOR over Pt catalyst was more active than in acid medium. However, increasing of performance of Pt-Rh-CeO₂/C catalyst in alkaline medium was higher than in acid medium. It was shown by the onset oxidation potential which shifted to more negative potential in alkaline medium. Over Pt-Rh-CeO₂/C catalyst, the onset oxidation potential was about 0.3 V vs.RHE, while over Pt/C catalyst was about 0.44 V vs RHE. Increasing Faradaic current over Pt-Rh-CeO₂/C at potential 0.6 V vs. RHE was about factor of 3 compared to the reference catalyst. The higher activity in alkaline medium probably due to the C-C bond breaking could easily happen in this medium. In order to further study of the reaction product of EOR, in the next will be carried out experiment by in-situ differential electrochemical mass spectrometry.

CONCLUSIONS

Electro-oxidation of ethanol is a very complex reaction because several reaction products and intermediates may be formed. Electro-oxidation of ethanol on PtRhCeO₂/C either in acid medium or in alkaline medium could increase the activity of the catalyst in comparison to the Pt/C reference catalyst.

The increase performance at potential 0.6 V vs RHE over Pt-Rh-CeO₂/C catalyst was about factor of 2 in acid medium and factor 3 in alkaline medium compared to the reference Pt/C commercial catalyst.

ACKNOWLEDGMENTS

We are indebted to the Chair-E-19, Department of Physics, and Technical University of Munich for the research facilities. We thank to Dr. Cristina Tealdi (Univ. Pavia Italy) for X-ray Diffraction measurement and Petra Belle for TEM measurement and discussion. Financial support by DAAD under contract A/03/41170 was also acknowledged.

REFERENCES

- [1]. G.A. CAMARA, T.IWASITA, *Journal of Electroanalytical Chemistry*, **578** (2005) 315-321
- [2]. G.A. CAMARA, R.B. DE LIMA, T. IWASITA, *Electrochemistry Communications*, **6** (2004) 812-815
- [3]. J.-M. L'ÉGER, *Electrochimica Acta*, **50** (2005) 3123-3129
- [4]. J.-M. LEGER, S. ROUSSEAU, C. COUTANCEAU, F. HAHN, C. LAMY, *Electrochimica Acta*, **50** (2005) 5118-5125
- [5]. T. IWASITA and E. PASTOR, *Electrochim. Acta*, **39** (1994) 531
- [6]. C. LAMY, S. ROUSSEAU, E.M. BELGSIR, C. COUTANCEAU, J.-M. LÉGER, *Electrochimica Acta*, **49** (2004) 3901-3908
- [7]. CARSTEN CREMERS, HARIYANTO, V. RAO, A. RACS, Direct Ethanol Fuel Cells, *Proceeding Workshop of TFI*, Duisburg Germany, (2006)
- [8]. HARIYANTO, W. PURWANTO, Ethanol ElectroOxidation on Pt-based Catalyst, *Seminar Nasional Teknik Kimia*, UNSRI, Palembang, (2006)
- [9]. BORO DJURICIC and STEPHEN PICKERING, *Journal of the European Ceramic Society*, **19** (1999) 1925-1934
- [10]. CHRISTINA BOCK, CHANTAL PAQUET, MARTIN COUILLARD, GIANLUIGIA. BOTTON, and BARRY R. MACDOUGALL, *J. AM. Chem. Soc.*, **126** (2004) 8028-8037